Fall 2021

Quantification of Marine Acoustic Environments

Dylan Charles Wilford
University of New Hampshire, Durham

Quantification of Marine Acoustic Environments

By

Dylan Charles Wilford
B.Sc. Facilities Engineering, Massachusetts Maritime Academy
2014

Submitted to the University of New Hampshire
In Partial Fulfillment of
The Requirements for the Degree of

Master of Science
in
Oceanography

September 2021

This thesis was examined and approved in partial fulfillment of the requirements for the degree of M.Sc. in Oceanography by:

Jennifer Miksis-Olds, PhD
Research Professor
Thesis Advisor

Anthony Lyons, PhD
Research Professor

Daniel Howard, PhD
Assistant Professor

Kim Lowell, PhD
Research Scientist

Bruce Martin, PhD
Applied Sciences Manager (JASCO, Applied Sciences)

On 7/30/2021

Approval signatures are on file with the University of New Hampshire Graduate School.

Table of Contents

List of Tables v
List of Figures vi
Abstract x
CHAPTER 1: Introduction 1
Underwater Sound Sources 1
Soundscapes and ocean sound 6
Challenges in Marine Soundscape Studies 9
Proposed Soundscape Code 13
Amplitude 15
Impulsiveness 16
Periodicity 18
Uniformity 20
Research Goal and Objectives 24
CHAPTER 2: The Soundscape Code 25
Methodologies 25
Soundscape Code Data Sets 25
Data processing 27
Metric response analysis 29
Soundscape Code results 32
Impulsiveness 32
Periodicity 38
Uniformity 43
Statistical Groupings of Metric Values 47
Soundscape Code Discussion 50
CHAPTER 3: Soundscape comparison using the proposed methodology 55
Introduction 55
Methodologies 58
Results 60
Soundscape Code comparison discussion 67
CHAPTER 4: Discussion 71
List of References 76

List of Tables

TABLE 1 SELECTED LITERATURE OF SOUNDSCAPE COMPARISON METRICS. 11
TABLE 2 SOUNDSCAPE PROPERTIES AND CORRESPONDING METRICS, STATISTICAL MEASURES, AND INDICES 14
TABLE 3: SOUNDSCAPE CODE DATA SET INFORMATION 25
TABLE 4 QUALITATIVE COMPARISONS OF SOUNDSCAPE CODE PROPERTY METRICS AND SUMMARY OF RESULTS. 31
TABLE 5 LONG-TERM DATASET INFORMATION AND DATA COLLECTION PARAMETERS 59

List of Figures

FIGURE 1. VISUAL REPRESENTATION OF THE THREE TYPES OF SOUNDS THAT OCCUR IN THE OCEAN: 1) NATURAL-ABIOTIC (GREEN); 2) NATURAL-BIOTIC SOUND SOURCES (WHITE); AND 3) ANTHROPOGENIC SOUND SOURCES (ORANGE). FROM NOAA'S OCEAN NOISE STRATEGY. AVAILABLE AT HTTP://ACOUSTICSTODAY.ORG/NEFSC. 2
FIGURE 2. WENZ CURVES AND OCEAN SOUND SOURCES (WENZ, 1962). FROM HTTPS://DOSITS.ORG. 3
FIGURE 3 WMO EGG CODE (WMO 2004). CONTAINED IN THE SIMPLE OVAL ARE DATA REGARDING CONCENTRATIONS, STAGES OF DEVELOPMENT, AND FORM OF ICE. CODE CONFORMS TO AN INTERNATIONAL CONVENTION. 13
FIGURE 4 SIGNALS DETECTED AT DESIGNATED SOUNDSCAPE CODE DATASET SITES A) ICE SOUNDS, B) SEISMIC SURVEY, C) HUMPBACK AND FIN WHALE VOCALIZATION, D) IMPACT PILE DRIVING, E) NORTHERN BOTTLENOSE WHALE AND COMMON DOLPHIN VOCALIZATIONS IN QUIET SOUNDSCAPE, F) FIN WHALE VOCALIZATIONS, G) REEF SOUNDS. 27
FIGURE 5 A PRIORI METRIC RESPONSE EXPECTATIONS FOR EACH DATA SET. EXPECTATIONS FORMED CRITERIA TO COMPARE METRICS AND INFORM THE METRIC SELECTION. GREEN-YELLOW-RED COLORATION REPRESENTS RELATIVE EXPECTED METRIC RESPONSE LEVEL WHERE GREEN INDICATES A LOW PROPERTY LEVEL, YELLOW INDICATES A MID-LEVEL, AND RED INDICATES HIGH-LEVEL RESPONSES. LOW-LEVEL RESPONSES FOR THE UNIFORMITY CATEGORY INDICATE A HIGHLY UNIFORM ACOUSTIC ENVIRONMENT, AND HIGH LEVEL RESPONSES INDICATE A LACK OF UNIFORMITY. CORRESPONDING SOUNDSCAPE CODE FREQUENCY BAND IS INDICATED BY BB, L, M, H, UH. 30
FIGURE 6 IMPULSIVENESS COMPARISON 1 (I1) RESULTS. WHEREIN THE BOXPLOTS RED HORIZONTAL LINE INDICATES MEDIAN VALUE, OUTER EDGES OF BOXES REPRESENT 25TH AND 75TH PERCENTILES, WHISKERS MARK BOUNDARY THAT CONTAINS APPROXIMATELY 99% OF DATA VALUES, AND THE RED POINTS ARE OUTLIERS. 33
FIGURE 7 IMPULSIVENESS COMPARISON I2 RESULTS. 1-SECOND SPL_{PK} PLOT SHOWS PULSED NATURE OF THE FIN WHALE VOCALIZATIONS AND THE 1-MINUTE METRIC TIME SERIES REPORT THE RESPONSE OF KURTOSIS AND CREST FACTOR METRICS. HORIZONTAL RED LINE SHOWS THE IMPULSIVENESS THRESHOLD FOR EACH IMPULSE METRIC. VALUES ABOVE THIS THRESHOLD INDICATE THE PRESENCE OF IMPULSIVE SIGNALS. 35
FIGURE 8 BOXPLOTS OF KURTOSIS (LEFT) AND CREST FACTOR (RIGHT) VALUES AT GB4V35. EACH BOX REPRESENTS THE RANGE OF METRIC VALUES IN A 10-MINUTE TIME WINDOW COMPRISED OF METRICS CALCULATED OVER 1-MINUTE TIME WINDOWS (EACH BOXPLOT CONTAINS 10 METRICS VALUES). CIRCLED DOTS INTERSECTING BOXES INDICATE MEDIAN VALUES, THICK BOXES INDICATE 25TH AND 75TH PERCENTILE RANGE, SKINNY LINES INDICATE RANGE OF 99% OF DATA, AND BLUE CIRCLES INDICATE OUTLIERS. 36
FIGURE 9 IMPULSIVENESS COMPARISON 3 (I3) RESULTS. 1-SECOND SPL_{PK} PLOT SHOWS PULSED ACOUSTIC SIGNATURE OF THE SEISMIC SURVEY AND THE 1-MINUTE METRIC TIME SERIES REPORT THE RESPONSE OF KURTOSIS AND CREST FACTOR METRICS. HORIZONTAL RED LINE SHOWS THE IMPULSIVENESS THRESHOLD FOR EACH IMPULSE METRIC. VALUES ABOVE THIS THRESHOLD INDICATE THE PRESENCE OF IMPULSIVE SIGNALS. 37
FIGURE 10 BOXPLOTS OF KURTOSIS (LEFT) AND CREST FACTOR (RIGHT) VALUES AT GB4V0. EACH BOX REPRESENTS THE RANGE OF METRIC VALUES IN A 10-MINUTE TIME WINDOW COMPRISED OF METRICS CALCULATED OVER 1-MINUTE TIME WINDOWS (EACH BOXPLOT CONTAINS 10 METRICS VALUES). CIRCLED DOTS INTERSECTING BOXES INDICATE MEDIAN VALUES, THICK BOXES INDICATE 25TH AND 75TH PERCENTILE RANGE, SKINNY LINES INDICATE RANGE OF 99% OF DATA, AND BLUE CIRCLES INDICATE OUTLIERS. 38
FIGURE 11 BROADBAND PERIODICITY METRIC CANDIDATE RESULTS FOR ALL SOUNDSCAPE CODE DATASETS. VALUES REPRESENT PEAKS-PER-MINUTE AS REPORTED BY PERIODICITY METRICS. RED HORIZONTAL LINE INDICATES MEDIAN VALUE, OUTER EDGES OF BOXES

REPRESENT 25TH AND 75TH PERCENTILES, WHISKERS MARK BOUNDARY THAT CONTAINS APPROXIMATELY 99% OF DATA VALUES, AND THE RED POINTS ARE OUTLIERS.....39
FIGURE 12 QUALITATIVE COMPARISON (P1) RESULTS. FREQUENCY FILTERED 1-SECOND SPL_{PK} FOR TIME WINDOW 1 (LEFT) AND TIME WINDOW 2 (RIGHT). RANGE OF PERIODICITY CANDIDATE METRIC VALUES (PPM) CORRESPONDING TO THE TWO TIME WINDOWS FOR CEPSTRUM, ACORR2, AND ACORR3. RED HORIZONTAL LINE INDICATES MEDIAN VALUE, OUTER EDGES OF BOXES REPRESENT 25TH AND 75TH PERCENTILES, WHISKERS MARK BOUNDARY THAT CONTAINS APPROXIMATELY 99% OF DATA VALUES, AND THE RED POINTS ARE OUTLIERS...40
FIGURE 13 BOXPLOTS OF CEPSTRUM (LEFT), ACORR2 (MIDDLE), AND ACORR3 (RIGHT) VALUES AT GB4V35. EACH BOX REPRESENTS THE RANGE OF METRIC VALUES IN A 10-MINUTE TIME WINDOW COMPRISED OF METRICS CALCULATED OVER 1-MINUTE TIME WINDOWS (EACH BOXPLOT CONTAINS 10 METRICS VALUES). CIRCLED DOTS INTERSECTING BOXES INDICATE MEDIAN VALUES, THICK BOXES INDICATE 25TH AND 75TH PERCENTILE RANGE, SKINNY LINES INDICATE RANGE OF 99% OF DATA, AND BLUE CIRCLES INDICATE OUTLIERS. 41
FIGURE 14 QUALITATIVE COMPARISON P2 FREQUENCY FILTERED 1-SECOND SPL_{PK} FOR TIME WINDOW 1 (LEFT) AND TIME WINDOW 2 (RIGHT). RANGE OF PERIODICITY CANDIDATE METRIC VALUES (PPM) CORRESPONDING TO THE TWO TIME WINDOWS FOR CEPSTRUM, ACORR2, AND ACORR3. RED HORIZONTAL LINE INDICATES MEDIAN VALUE, OUTER EDGES OF BOXES REPRESENT 25TH AND 75TH PERCENTILES, WHISKERS MARK BOUNDARY THAT CONTAINS APPROXIMATELY 99% OF DATA VALUES, AND THE RED POINTS ARE OUTLIERS...42
FIGURE 15 QUALITATIVE COMPARISON (P3) RESULTS. FREQUENCY FILTERED 1-SECOND SPL_{PK} FOR TIME WINDOW 1 (LEFT) AND TIME WINDOW 2 (RIGHT). RANGE OF PERIODICITY CANDIDATE METRIC VALUES (PPM) CORRESPONDING TO THE TWO TIME WINDOWS FOR CEPSTRUM, ACORR2, AND ACORR3. RED HORIZONTAL LINE INDICATES MEDIAN VALUE, OUTER EDGES OF BOXES REPRESENT 25TH AND 75TH PERCENTILES, WHISKERS MARK BOUNDARY THAT CONTAINS APPROXIMATELY 99% OF DATA VALUES, AND THE RED POINTS ARE OUTLIERS...43
FIGURE 16 BROADBAND UNIFORMITY METRIC VALUES. RED HORIZONTAL LINE INDICATES MEDIAN VALUE, OUTER EDGES OF BOXES REPRESENT 25TH AND 75TH PERCENTILES, WHISKERS MARK BOUNDARY THAT CONTAINS APPROXIMATELY 99% OF DATA VALUES, AND THE RED POINTS ARE OUTLIERS. 44
FIGURE 17 QUALITATIVE COMPARISON (U1) RESULTS SHOWING THE H-INDEX VALUES FOR BGE AND MB SITES AND D-INDEX VALUES FOR BGE AND MB SITES WHEREIN THE BOXPLOTS RED HORIZONTAL LINE INDICATES MEDIAN VALUE, OUTER EDGES OF BOXES REPRESENT 25TH AND 75TH PERCENTILES, WHISKERS MARK BOUNDARY THAT CONTAINS APPROXIMATELY 99% OF DATA VALUES, AND THE RED POINTS ARE OUTLIERS. 45
FIGURE 18 UNIFORMITY COMPARISON (U2) RESULTS SHOWING THE H-INDEX AND D-INDEX VALUES FOR OR AND GBR SITES WHEREIN THE BOXPLOTS RED HORIZONTAL LINE INDICATES MEDIAN VALUE, OUTER EDGES OF BOXES REPRESENT 25TH AND 75TH PERCENTILES, WHISKERS MARK BOUNDARY THAT CONTAINS APPROXIMATELY 99% OF DATA VALUES, AND THE RED POINTS ARE OUTLIERS. 46
FIGURE 19 BOXPLOTS OF D-INDEX (LEFT) AND H-INDEX (RIGHT) VALUES AT OR. EACH BOX REPRESENTS THE RANGE OF METRIC VALUES IN A 10-MINUTE TIME WINDOW COMPRISED OF METRICS CALCULATED OVER 1-MINUTE TIME WINDOWS (EACH BOXPLOT CONTAINS 10 METRICS VALUES). CIRCLED DOTS INTERSECTING BOXES INDICATE MEDIAN VALUES, THICK BOXES INDICATE 25TH AND 75TH PERCENTILE RANGE, SKINNY LINES INDICATE RANGE OF 99% OF DATA, AND BLUE CIRCLES INDICATE OUTLIERS. 47
FIGURE 20 MCT RESULTS FOR (TOP) KURTOSIS AND (BOTTOM) CREST FACTOR. SITE DESIGNATIONS APPEAR IN A COLUMN ON THE LEFT OF EACH PANEL. IDENTICAL LETTERS INDICATE CORRESPONDING SITES HAVE METRIC VALUES THAT ARE NOT SIGNIFICANTLY DIFFERENT. MCTS WERE PERFORMED ON 1-MINUTE METRIC VALUES OBSERVING THE SOUNDSCAPE CODE FREQUENCY BANDS. COLOR BARS REPRESENT A PRIORI EXPECTATIONS

FOR METRIC LEVELS WHERE RED REPRESENTS A HIGH-LEVEL, YELLOW REPRESENTS A MID-LEVEL, AND GREEN REPRESENTS A LOW-LEVEL RESPONSE. 48
FIGURE 21 MCT RESULTS FOR (TOP) CEPSTRUM, (MIDDLE) ACORR2, AND (BOTTOM) ACORR3. SITE DESIGNATIONS APPEAR IN A COLUMN ON THE LEFT OF EACH PANEL. IDENTICAL LETTERS INDICATE CORRESPONDING SITES HAVE METRIC VALUES THAT ARE NOT SIGNIFICANTLY DIFFERENT. MCTS WERE PERFORMED ON 1-MINUTE METRIC VALUES OBSERVING THE SOUNDSCAPE CODE FREQUENCY BANDS. COLOR BARS REPRESENT A PRIORI EXPECTATIONS FOR METRIC LEVELS WHERE RED REPRESENTS A HIGH-LEVEL, YELLOW REPRESENTS A MID-LEVEL, AND GREEN REPRESENTS A LOW-LEVEL RESPONSE. 49
FIGURE 22 MCT RESULTS FOR (TOP) H-INDEX AND (BOTTOM) D-INDEX. SITE DESIGNATIONS APPEAR IN A COLUMN ON THE LEFT OF EACH PANEL. IDENTICAL LETTERS INDICATE CORRESPONDING SITES HAVE METRIC VALUES THAT ARE NOT SIGNIFICANTLY DIFFERENT. MCTS WERE PERFORMED ON 1-MINUTE METRIC VALUES OBSERVING THE SOUNDSCAPE CODE FREQUENCY BANDS. COLOR BARS REPRESENT A PRIORI EXPECTATIONS FOR METRIC LEVELS WHERE RED REPRESENTS A HIGH-LEVEL, YELLOW REPRESENTS A MID-LEVEL, AND GREEN REPRESENTS A LOW-LEVEL RESPONSE. 50
FIGURE 23 SOUNDSCAPE CODE RESULTS FOR THE SEVEN SOUNDSCAPE CODE DATASETS: (A) MB, (B) OR, (C) BGE, (D) GBR, (E) GB4V35, (F) GB4V0, (G) GB5. COLUMNS INDICATE THE FREQUENCY BAND, AND FOR EACH BAND THE MEDIAN (MED) AND 95% CONFIDENCE INTERVALS (C95) ARE REPORTED. PANEL (H) REPORTS THE MINIMUM AND MAXIMUM SOUNDSCAPE CODE MEDIAN VALUES OBSERVED ACROSS ALL SITES IN CORRESPONDING FREQUENCY BANDS. METRICS REPRESENTED IN EACH ROW OF THE SOUNDSCAPE CODES ARE FROM TOP TO BOTTOM: SPL_{RMS}, SPL_{PK}, KURTOSIS, D-INDEX INDEX, ACORR3. THE TOTAL RANGE OF THE SOUNDSCAPE CODE MEDIANS AND C95S PRESENTED IN PANEL H WAS DIVIDED INTO QUARTILES (RESPECTIVELY), AND THE CELL COLORS CORRESPOND TO WHICH QUARTILE THE VALUE FALLS INTO FROM LOW (1/4) TO HIGH (4/4): BLUE (1/4), GREEN (2/4), YELLOW (3/4), RED (4/4). 51
FIGURE 24 ADEON LANDER LOCATIONS AND BATHYMETRY FOR (A) WIL, (B) SAV AND (C) BLE. RH LANDER LOCATION IN CLOSE PROXIMITY TO THE SAV LANDER, BUT IS NOT INDICATED ON THIS FIGURE. 57
FIGURE 25 ADEON LANDER LOCATIONS AND SITE IMAGES CAPTURED BY ROVS ON RESEARCH DIVES TO (A) WILMINGTON, (B) SAVANNAH DEEP AND (C) BLAKE ESCARPMENT. 58
FIGURE 26 EXAMPLE OF PROCESS BY WHICH CHANGE IN SSC INTERPRETATION WAS QUANTIFIED SHOWN FOR BLE BB AMPLITUDE METRICS ONLY. BLACK ARROWS INDICATE THE FLOW OF THE PROCEDURE. UPPER LEFT BOX SHOWS CONDENSED SSC COLOR CODE INFORMATION WHERE M, W, AND D REPRESENT THE MONTH, WEEK, AND DAY SSCS AND THE COLOR SHOWS WHICH QUARTILE THE CORRESPONDING METRIC FELL INTO. UPPER RIGHT BOX SHOWS HOW THE QUARTILES WERE QUANTIFIED. LOWER LEFT SHOWS THE DIFFERENCE VALUE FOUND BY SUMMING THE DIFFERENCES BETWEEN THE MONTH AND WEEK, MONTH AND DAY, AND WEEK AND DAY QUARTILE VALUES. LOWER LEFT SHOWS THE BB DIFFERENCE VALUES AND TOTALS FOR BLE AMPLITUDE METRICS. TOTALS CALCULATED BY SUMMING DIFFERENCES ACROSS FREQUENCY BANDS FOR EACH METRIC. 60
FIGURE 27 NUMERICAL DIFFERENCES IN SSC METRIC QUARTILES ACROSS MONTH, WEEK, AND DAY ANALYSIS PERIODS. METRIC DIFFERENCES ARE CALCULATED FOR THE MEDIAN AND C95S, AND THEN SUMMED ACROSS FREQUENCY BANDS. TOTAL DIFFERENCE VALUES ARE SHOWN IN FAR RIGHT COLUMN OF EACH BOX. 61
FIGURE 28 ONE-MONTH SOUNDSCAPE CODES FOR THE DEEP/SHALLOW, CORAL/SANDY BOTTOM SITES ANALYZED. THE RANGES REPORTED IN THE LOWER RIGHT PANEL INDICATE THE RANGE OF 1-MONTH SSC MEDIANS. THE TOTAL RANGE OF THE SSC MEDIANS AND C95S WAS DIVIDED INTO QUARTILES, AND THE CELL COLORS CORRESPOND TO WHICH QUARTILE THE VALUE FALLS INTO FROM LOW TO HIGH: BLUE, GREEN, YELLOW, RED. 62

FIGURE 29 ONE-WEEK SOUNDSCAPE CODES FOR THE DEEP/SHALLOW, CORAL/SANDY BOTTOM SITES ANALYZED. THE RANGES REPORTED IN THE LOWER RIGHT PANEL INDICATE THE RANGE OF 1-MONTH SSC MEDIANS. THE TOTAL RANGE OF THE SSC MEDIANS AND C95S WAS DIVIDED INTO QUADRANTS, AND THE CELL COLORS CORRESPOND TO WHICH QUADRANT THE VALUE FALLS INTO FROM LOW TO HIGH: BLUE, GREEN, YELLOW, RED. 63
FIGURE 30 ONE-DAY SOUNDSCAPE CODES FOR THE DEEP/SHALLOW, CORAL/SANDY BOTTOM SITES ANALYZED. THE RANGES REPORTED IN THE LOWER RIGHT PANEL INDICATE THE RANGE OF 1-MONTH SSC MEDIANS. THE TOTAL RANGE OF THE SSC MEDIANS AND C95S WAS DIVIDED INTO QUADRANTS, AND THE CELL COLORS CORRESPOND TO WHICH QUADRANT THE VALUE FALLS INTO FROM LOW TO HIGH: BLUE, GREEN, YELLOW, RED. 64

Abstract

The soundscape is an acoustic environment made up of all sounds arriving at a receiver. A methodology for the analysis of soundscapes was developed in an attempt to facilitate efficient and accurate soundscape comparisons across time and space. The methodology included generating and combining results from a collection of traditional soundscape metrics, statistical measures, and acoustic indices that were selected to quantify several salient properties of marine soundscapes: amplitude, impulsiveness, periodicity, and uniformity. The metrics were calculated using approximately 30 hours using semi-continuous passive acoustic data gathered in seven unique acoustic environments. The calculated values for each candidate metric were compared to *a priori* soundscape descriptions and cross-examined statistically to determine which combination of metrics most effectively captured the characteristics of the representative soundscapes. The selected measures of were SPL_{rms} and SPL_{pk} for amplitude, kurtosis for impulsiveness, an autocorrelation-based metric for periodicity, and the dissimilarity index for uniformity. The metrics were combined to develop a proposed soundscape code, which enables rapid multidimensional and direct comparisons of salient soundscape properties across time and space. The proposed soundscape code was applied to a series of soundscapes that were recorded at several deep ocean environments along the US outer continental shelf (OCS) and the Great Barrier Reef. The soundscape code clearly distinguished between the deep OCS soundscapes and the shallow Great Barrier Reef soundscape in terms of amplitude, impulsiveness, and periodicity. Nuanced differences in deep OCS soundscape codes in terms of periodicity, impulsiveness, and the frequency of dominant signals suggest a connection between the respective soundscapes and bottom type or habitat. The combination of metrics that make up the soundscape code provided a first assessment to establish baseline acoustic properties for the deep ocean OCS sites. This initial soundscape characterization will aid in directing further analyses and guiding subsequent assessments used in understanding soundscape dynamics.

CHAPTER 1: Introduction

The oceans are filled with sounds and contain a wealth of information owing to the highly efficient manner in which acoustic energy travels through water. Many aquatic species utilize sound cues in local environments for a variety of activities: foraging, navigation, habitat selection, predator detection, migration, and breeding (Wartzok & Ketten, 1999; Richardson et al., 1995; Tyack, 1998; Bass et al. 2003; Au, 2012). Consequently, by studying the ambient sound field, it is possible for researchers to learn about an environment based on the sounds recorded in that environment. In the 1950s, a series of 20 Hz pulses confounded researchers "listening" on navy surveillance systems; in 1963, these pulses were attributed to finback whale courtship displays (Schevill et al., 1964). Prior to WWII, little research attention was given to ambient ocean sounds, but wartime technology like the acoustic mine (which relied on ambient noise measurements for the firing mechanism) incentivized research into ocean ambient noise. In the 1960s, a surge in ambient ocean sound research was due in a large part to a "belated" interest by the Navy in passive sonar systems like towed line arrays and submarine sonars for long range detection and surveillance (Urick, 1984). Since then, the number of ocean sound studies has increased, with the scope and intent of the research greatly expanding.

Underwater Sound Sources

All ocean sounds can be classified into three groups: 1) abiotic sounds generated from natural processes such as seismic events, wind, waves, and weather; 2) biotic sounds produced by marine life; and 3) human generated sounds (*Figure 1*).

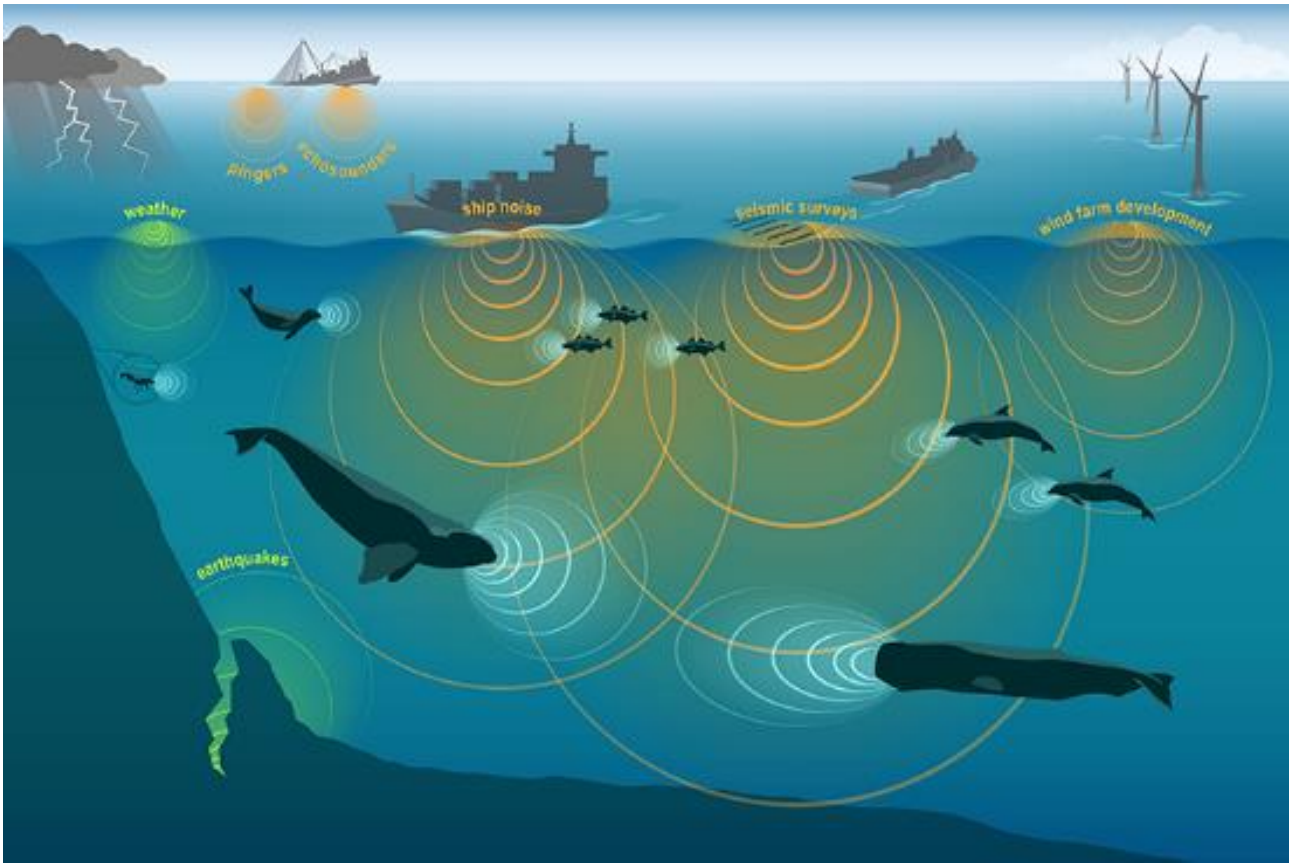

Figure 1. Visual representation of the three types of sounds that occur in the ocean: 1) natural-abiotic (green); 2) natural-biotic sound sources (white); and 3) anthropogenic sound sources (orange). From NOAA's Ocean Noise Strategy. Available at http://acousticstoday.org/nefsc.

Prior to the industrial revolution and the invention of motorized propulsion for ships, ocean sounds were generated predominantly by the two types of naturally occurring sources: biotic and abiotic. Many of these natural processes have unique acoustic signatures underwater (*Figure 2*), which allow researchers to study a wide range of events like rainfall, waves, tsunamis, and ice dynamics (Wenz 1962; Nystuen et al. 1986; Pettit et al. 2012; Bradley et al. 2015).

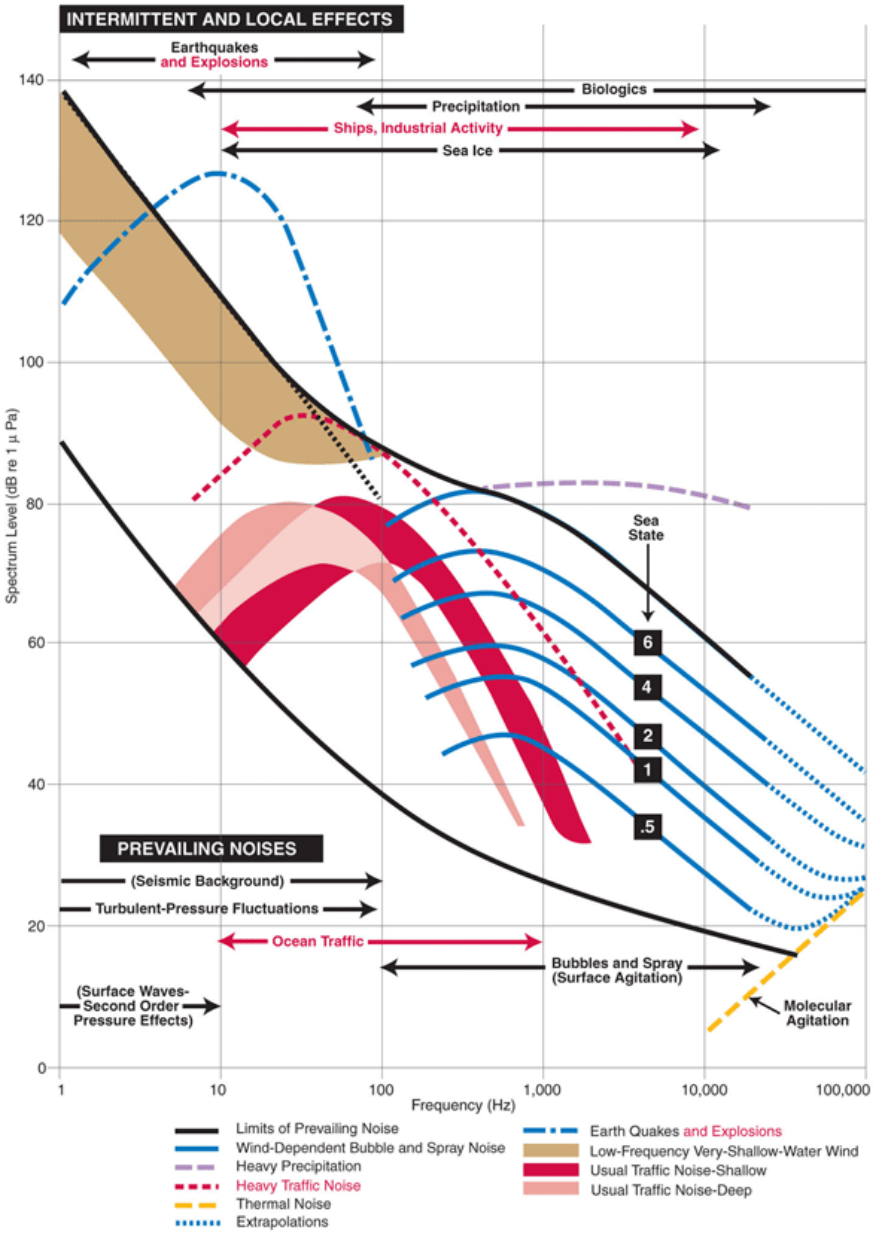

Figure 2. Wenz curves and ocean sound sources (Wenz, 1962). From https://dosits.org.

Sound from rain, which at certain droplet sizes is dependent on wind conditions, dominates ocean noise from 1-15 kHz when present (Wenz, 1962; Nystuen, 1986). Infrasonic frequencies from 5 – 20 Hz correlate strongly with wind speed (Nichols 1987), and wind shows further dominance at higher frequencies as well (400 Hz – 20 kHz; Medwin and Beaky, 1989). Natural,

seismic events transmit significant amounts of energy into the ocean that propagate as T-waves even when the source is far from the ocean boundary (Wenz 1962). Microseisms and wave-to-wave interactions dominate the frequency band below 20 Hz; earthquakes and explosions also occupy the infrasound band (Kibblewhite and Wu, 1989). Each phase of an ice calving event has unique acoustic characteristics including: an infrasonic rumble at the beginning of a calving event, sharp cracks as ice fractures (20 – 100 Hz), ice impacting the water (200 – 600 Hz), and high frequency (> 10 kHz) noise from the oscillation of the fractured ice (Pettit, 2012).

Sound is a critical component in the lives of marine organisms, which rely on it for a number of different life functions. While we know much about how marine mammals interact acoustically with their environment, we know far less about how the more numerous fish and invertebrate species perceive and generate sound. Coral reefs have unique acoustic signatures (Bertucci et al. 2015), and these signatures are utilized by a variety of marine animals in selecting an appropriate habitat or substrate for settlement (Parmentier et al. 2015). Clearly, marine animals have evolved to use and rely on ocean sounds, and up until the industrial revolution, the only sounds they were subjected to were natural biotic and abiotic sounds. In the post-industrial revolution period, however, a new type of sound was introduced in the marine acoustic environment: human-generated sounds.

Anthropogenic sound in the ocean occurs as both a byproduct and as intentionally created noise. Sources that produce noise as a byproduct include shipping and industrial activities. Sounds created intentionally include seismic surveys and sounds from different types of sonar systems. Seismic surveys are conducted by towing air-gun arrays from marine vessels, and while acoustic energy from this type of source is predominantly in the 5 – 300 Hz range, energy up to 30 kHz has been reported in controlled experiments (Martin et al., 2017). In the early 2000s there were over

90 vessels available for this type of operation worldwide, and at a given time, about 20% of these were conducting field operations (Schmidt 2004; Tolstoy et al. 2004).

A variety of sonar devices used for military, commercial, research, and recreational purposes make contributions to ocean sound in different frequency bands depending on the application. Low-frequency active (LFA) sonars are used by the military in large-scale surveillance. These LFA sonars "provide the sound source over scales of 100s of kilometers" for listening platforms in the detection of submarines. LFA sonars operate in the frequency range of 100 – 500 Hz (Anonymous, 2007; Hildebrand, 2009). For submarine detection in the mid-frequency range of <10 kHz, sonar systems use Mid Frequency Active Sonar (MFAS; 1 – 5 kHz) and high source levels (Watts, 2003). Multibeam echo sounders (MBES) are typically used to map the bathymetry and record backscatter of the seafloor and water column for a variety of purposes including fisheries research, detection and classification of underwater targets (e.g., ocean floor, fish, navigational obstructions), and geophysical research, among other tasks. Present-day MBES systems range in frequency from 12 kHz- 700 kHz depending on the usage (Hildebrand, 2009). Recreational and commercial sonars used for detection and classification of underwater targets produce sound at much lower source levels than military sonars, but are far more ubiquitous (NRC, 2003; Hildebrand, 2009).

The propulsion systems of commercial ships are the dominant source of radiated underwater noise at frequencies below 200 Hz (Ross, 1976). Noise from distant shipping can be detected in many parts of the ocean due to the highly efficient manner at which sound propagates at low frequencies. Cavitation at the propeller blades produces noise that is more broadband in nature, but high frequency components do not propagate far. Small boats equipped with outboard motors generally produce sound in the MFAS (1 – 5 kHz) range and have moderate source levels (Erbe,

2002; Kipple et al., 2004). Industrial activities, like marine construction and pile driving, and oil drilling, typically have their highest acoustic energies in the lower frequencies (20 – 1000 Hz; Greene, 1987). Monitoring soundscapes can help foster a better understanding of the magnitude and prevalence of anthropogenic sound, and how it changes over time. In the context of this research, the proposed technique for characterizing, monitoring, and reporting soundscapes will help to inform science-based decisions related to the management and mitigation of noise impacts.

By utilizing the information presented by sound source studies, and by considering the salient acoustic properties of different acoustic events, we can begin to see how different types of sounds contribute to an acoustic environment. These sound sources and their contributions are an important factor in how we define and describe a marine environment in terms of its acoustic properties. It may be relatively easy to describe an acoustic environment in terms of its individual sound sources, but what if the sources are unknown? The soundscape is connected to acoustic events occurring locally and distantly and understanding how different sound sources influence a soundscape will help understand what types of events are occurring even if we know nothing about what sources are present.

Soundscapes and ocean sound

The study of ambient sound and acoustic environments led to the development of the concept of the soundscape, where the soundscape is an acoustic environment tied to the function of a given location, and is made up of all sounds that arrive at a receiving animal or acoustic recorder (Pijanowski et al., 2011). The soundscape was formally defined by IOS 18405 characterization of the ambient sound in terms of its spatial, temporal, frequency attributes, and the types of sources contributing to the sound field (ISO, 2017). By utilizing soundscape information, researchers can better understand environmental impacts on ocean dynamics (Radford et al., 2010; McWilliams

and Hawkins, 2013; Miksis-Olds et al., 2013; Staaterman et al., 2014), biodiversity and ecosystem health (Parks et al., 2014; Staaterman et al., 2014), and the risk of anthropogenic impacts on marine life. Today, while we have a much better understanding of the importance and ubiquity of ocean sound, there is still much work to be done. Researchers still struggle to accurately report and compare important aspects of ocean sound. Ocean sound studies are not trivial endeavors and the complexity of ocean sound dynamics combined with a lack of formal standards, guidelines, and consistent methods can make soundscape analyses difficult. To accurately compare and report important soundscape information across time, space, and studies, efforts must be made to standardize the way in which researchers quantify marine acoustic environments.

Defining and characterizing the soundscape is an important step in the task of assessing, monitoring, and comparing global acoustic environments. In recognition of its inherent value, ocean sound has been recently accepted as an Essential Ocean Variable (EOV) by the Global Ocean Observing System (GOOS) Biology and Ecosystem Panel (Tyack, 2018). EOVs are approved based on three considerations: 1) relevance in helping solve scientific questions and addressing societal needs, 2) contributions to improving marine resource management, and 3) feasibility for global observation regarding cost effectiveness, technology, and human capabilities (https://goosocean.org/index). Once EOVs are approved, an implementation team creates and disseminates recommendations pertaining to data collection and management, which benefit the scientific community tremendously. Specification sheets linked to each EOV detail these recommendations and form guidelines for scientific use of the EOV. Consideration of ocean sound as an EOV will advance the understanding of ocean sound, anthropogenic impacts on ambient ocean sound, effects of anthropogenic sound on marine life, and how passive acoustic monitoring (PAM) can be used to assess biodiversity and ecosystem health (Tyack, 2018; Howe *et al.*, 2019).

Recommendations will help to guide scientific endeavors, while processing guidelines will ensure consistency and easy comparisons in ocean sound studies.

Traditionally, sound is analyzed by measuring the sound pressure level (SPL) as a function of frequency, and other source and amplitude-related parameters such as the number of sources detected, source classification, localization of detectable sources, or sound exposure level (SEL) (Martin et al., 2019). Recently, researchers have developed and applied metrics mathematically summarizing acoustic properties and comparing them with independent ecological data to understand the types of sources present in a soundscape, referred to generally as Acoustic Indices. For example, the Acoustic Complexity Index (ACI) was proposed as a proxy for biodiversity (Pieretti et al., 2011), and Sueur et al. (2008) demonstrated the efficacy of the Entropy Index (H) and the Dissimilarity Index (D) at highlighting biodiversity of a terrestrial environment. In the case of biodiversity measures, traditional visual methods of quantifying biodiversity are time consuming, expensive, and can be invasive (Sueur et al., 2008; Harris et al., 2016). Surveying biodiversity acoustically eases many of these constraints, but processing high volumes of acoustic data, which are generated quickly, is still time consuming. Further distillation and quantification of acoustic data into acoustic metrics helps to alleviate processing time. It also allows for direct comparisons among acoustic environments. Application of acoustic biodiversity indices in a marine environment have yielded mixed results (Bohnenstiehl et al., 2018; Bolgan et al., 2018; Parks et al., 2014; Staaterman et al., 2017). Further investigation into the utility of acoustic indices in marine applications is needed to assess their efficacy.

Challenges in Marine Soundscape Studies

Even though ocean ambient sound and soundscape research has been conducted for decades, the ocean community has still not reached a consensus on how to accurately report and compare important aspects of ocean sound. The methodologies utilized by researchers are often tailored to a specific study, which focuses on answering the question at hand, but contributes little to the understanding of soundscape dynamics on a large regional or global scale if the results cannot be easily interpreted, integrated, or compared to data from other areas. Studies often fail to clearly report metric input parameters critical to the determination of the final metric value; ambiguities in reporting can make replicating study methodologies difficult, and it can lead to erroneous comparisons (Hawkins et al., 2014). Some methodology descriptions are so vague it is nearly impossible to determine averaging times, integration windows, and exactly which metric is being calculated. To accurately report important soundscape information, efforts must be made to standardize the way in which researchers acquire, process, analyze, and report acoustic metrics.

The measures available to researchers for assessing or characterizing marine soundscapes are numerous. While studies comparing soundscapes often use similar methods of statistical analysis, the general disparity in hardware, measurements, processing, and reporting across studies makes it difficult to compare the soundscapes being measured. Presenting the metrics utilized by previous studies highlights the general disparity in analysis methods found across soundscape studies (Table *1*). While measurements like power spectral density (PSD), sound intensity, and SPL are common amplitude metrics used across studies, researchers often apply or report the metrics differently. For example, two studies comparing the soundscapes of proximal reef habitats both calculate mean intensity (Bertucci et al., 2015; Radford et al., 2014), but Bertucci *et al.* (2015) averaged acoustic intensity in linear units, while Radford *et al.* (2014) averaged in the dB-domain. These two different methods of averaging have yielded differences in final metric results of over

10 dB in previous works (Merchant et al., 2012). If direct comparisons are made between the mean intensity results of these two studies utilizing different averaging techniques, inaccurate conclusions could potentially be drawn.

Table 1 Selected literature of soundscape comparison metrics.

Topic	Metrics	Soundscape code Property	Reference
Comparison of reef sound signatures – spatial comparison	▪ Max/min sound intensity and corresponding frequency (day, dusk, dawn) ▪ Mean sound intensity	Amplitude	Bertucci *et al.*, 2015
Comparison of reef sound signatures – spatial comparison	▪ PSD (smoothed) ▪ Mean sound intensity	Amplitude	Radford *et al.*, 2014
Soundscape of the shallow waters of a Mediterranean marine protected area – temporal comparison	▪ Monthly median root-mean-square level of the sound pressure (SPLrms) (per octave band/bb) ▪ Day/night median SPL_{rms} (per octave band/bb) ▪ Day/night median PSD ▪ Filtered Acoustic Complexity Index (ACI; removal of snapping shrimp sounds)	Amplitude Uniformity Impulsiveness	Buscaino *et al.*, 2016
A comparison of inshore marine soundscapes – spatial comparison	▪ ACI ▪ Acoustic Diversity Index (ADI) ▪ PSD	Amplitude Uniformity	McWilliam *et al.*, 2013
The not so silent world: measuring arctic, equatorial, and Antarctic soundscapes in the Atlantic ocean – spatial comparison	▪ Daily median sound levels ▪ Long term spectral averages (LTSA)	Amplitude	Haver *et al.*, 2017
Evaluating changes in the marine soundscape of an offshore wind farm – temporal comparison	▪ 3-5 month spectrograms ▪ Median/mean PSD	Amplitude	Lin *et al.*, 2019
Soundscapes from a tropical Eastern Pacific reef and Caribbean sea reef – spatial comparison	▪ Mean PSD over recording period plotted in 100Hz bins and color mapped	Amplitude, Periodicity	Staaterman *et al.*, 2013
Localized coastal habitats have distinct	▪ Sound intensity over 4 freq bands: 100 - 800 Hz,	Amplitude	Radford *et al.*, 2010

underwater sound signatures – spatial comparison	800 Hz – 2.5 kHz, 2.5 – 20 kHz, 20k – 24 kHz ▪ Proportion of sound intensity (per frequency bands outlined previously) ▪ Dusk/noon PSD		
Assessing marine ecosystem acoustic diversity across ocean basins – spatial comparison	▪ H-index	Uniformity	Parks *et al.*, 2014
Marine soundscape as an additional biodiversity monitoring tool: a case study from the Adriatic Sea	▪ ACI ▪ PSD	Amplitude Uniformity Periodicity	Pieretti *et al.*, 2017
Investigating the utility of ecoacoustic metrics in marine soundscapes	▪ ACI ▪ H-index	Impulsiveness	Bohnenstiehl *et al.*, 2018
Basin-Wide contributions to the underwater soundscape by multiple seismic surveys with implications for marine mammals in Baffin bay	▪ 1/3 octave levels ▪ Mean instantaneous pressure level ▪ Sound exposure level (SEL)	Impulsiveness	Kyhn *et al.*, 2019
Sound exposure level as a metric for analyzing and managing underwater soundscapes – temporal comparison	▪ Sound exposure level ▪ Autocorrelation of sound exposure level	Amplitude	Martin *et al.*, 2019

Many analysis methods produce graphical outputs, which are assessed visually but can become cumbersome when quantitative comparisons are required across time or space. Graphical information, supplemented with standardized quantitative analysis of the multidimensional soundscape within an accepted framework would produce thorough, accurate, and easily comparable results for acoustic recordings.

Proposed Soundscape Code

The World Meteorology Organization (WMO) utilizes a system for sea ice symbology that is commonly referred to as the "egg code" (*Figure 3*)(JCOMM Expert Team on Sea Ice, 2004).

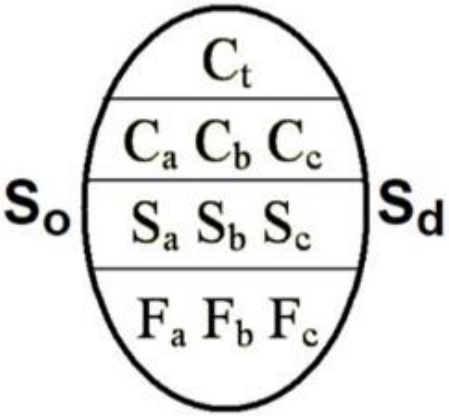

C_t - Total concentration of ice in area, reported in tenths. May be expressed as a single number or as a range, not to exceed two tenths (3-5, 5-7 etc.)

C_a C_b C_c - Partial concentrations (C_a, C_b, C_c) are reported in tenths, as a single digit. These are reported in order of decreasing thickness. C_a is the concentration of the thickest ice and C_c is the concentration of the thinnest ice.

S_a S_b S_c - Stages of development. These codes correspond directly with the partial concentrations above. C_a is the concentration of stage S_a, C_b is the concentration of stage S_b, and C_c is the concentration of S_c.

S_o S_d - Development stage (age) of remaining ice types. S_o if reported is a trace of ice type thicker/older than S_a. S_d is a thinner ice type which is reported when there are four or more ice thickness types.

F_a F_b F_c - Predominant form of ice (floe size) corresponding to S_a, S_b and S_c respectively.

Figure 3 WMO egg code (JCOMM Expert Team on Sea Ice, 2004). Contained in the simple oval are data regarding concentrations, stages of development, and form of ice. Code conforms to an international convention.

This egg code presents standard ice data in a clear and succinct manner. It includes basic details about ice coverage in a way that allows for easy comparison across environments. Furthermore, the multidimensional nature of the egg code reports a variety of relevant ice properties; "one size fits all" measures are rarely adequate in describing dynamic environments. The idea of a measure that captures and reports salient information about an environment is the inspiration for the proposed soundscape code in this thesis. While the egg code reports multiple dimensions of the environmental feature ice, the soundscape code reports multiple dimensions of the environmental feature, ocean sound. By identifying distinguishing properties observed in

marine acoustic environments, a collection of metrics and indices that quantify these characteristics can be compiled in the form of a soundscape code.

Amplitude, variability, impulsiveness, and uniformity are examples of physical soundscape properties that are important to understanding soundscapes and the distribution of sound energy across time, space, and frequency (Table *1)*. The objective of this study was to identify the optimal suite of metrics across some generalized soundscape properties (amplitude, impulsiveness, periodicity, and uniformity; *Table 2*) to create a soundscape code infrastructure for comparing soundscapes. Multiple metrics within each soundscape property were selected and applied to a diverse set of soundscapes to identify the metric that best captured the salient aspects of the acoustic recordings. Comparing the acoustic properties of soundscapes is not meant to be an exhaustive assessment, but rather an initial analysis to understand some of the dynamics of acoustic environments and guide subsequent analysis for more targeted assessments. The resulting product forms the proposed soundscape code, which provides a framework for comparing soundscape properties across space and time utilizing metrics that capture spectral and temporal properties of acoustic environments; characterizing acoustic environments in terms of spatial, spectral, and temporal acoustic properties directly relates to the ISO 18405 definition of a soundscape.

Table 2 Soundscape properties and corresponding metrics, statistical measures, and indices

Soundscape Property	Description	Quantifying Measure
Amplitude	Can be conceptualized as the "loudness" of an environment. Describes the effective sound pressure levels across time.	SPLrms, SPLpk
Impulsiveness	Impulses are characterized as being broadband, short duration, high peak sound pressure, and rapid rise times. Impulsiveness of a soundscape would describe the presence and magnitude of signals that can be characterized as impulsive.	Kurtosis, Crest Factor

Periodicity	Describes the repetitive nature of sounds in the soundscape. The timescale of the periodic activity is an important factor here; pulsed signals with short inter-pulse-intervals like seismic surveys, pile driving, and pulsed minke whale vocalizations are periodic; repeating acoustic events like dawn or evening chorus are also periodic, but on much larger time scales.	Time lagged autocorrelation, Cepstrum
Uniformity	Describes the diversity of a system. In an acoustic context: to what degree are all the sounds similar or different across time?	Entropy Index (H), Dissimilarity Index (D)

Amplitude

Acoustics has been described as the science behind the generation, transmission, and reception of vibrational energy waves in matter. An elastic restoring force that results from a displacement of molecules of a medium enables matter to move in oscillatory vibrations, which thereby generate and transmit acoustic waves (Kinsler et al., 1999). These acoustic waves propagate through compressible mediums like air or water, and can be measured by considering the increase or decrease in pressure observed as the soundwave moves through the medium. To characterize sound, the amplitude of corresponding sound waves is considered. Amplitudes of sound waves represented by the sound pressure are relevant in all ocean sound studies and are the closest link to raw data utilized by researchers. The sound pressure level (SPL), reported in logarithmic decibel (dB) units relative to a reference pressure of 1 μPa, is the most common amplitude metric reported in ocean sound studies. The root-mean-square (rms) SPL captures the average pressure level of the corresponding environment over a specified time period (SPL_{rms}). While still susceptible to upward bias from loud, intermittent sounds, SPL_{rms} is the most ubiquitous acoustic metric (Merchant et al., 2015) (Equation 1)

$$SPL_{rms} = 20\,log_{10}\left(\sqrt{\frac{1}{T}\int_0^T \frac{p^2(t)}{p_{ref}^2}\,dt}\right) \quad (1)$$

where P_{ref} is reference pressure, $p(t)$ is the instantaneous pressure at time (t), and T is the analysis window duration (Madsen 2005, Thompson et al. 2013, Merchant et al. 2015). SPL_{rms}, however, does not capture all the important amplitude information of a soundscape such as maximum sound pressure levels (SPL_{pk}), the sound floor (quietest periods in a soundscape), or sound exposure level (SEL), which quantifies a receiver's exposure to acoustic energy. The SPL_{pk} has added value as an amplitude metric, as it is also a relevant measure in determining the risk of physical damage in auditory systems (Coles et al., 1968) (Equation 2).

$$SPL_{pk} = 10\,log_{10}\left(\frac{p_{max}^2(t)}{p_{ref}^2}\right) \quad (2)$$

Because the SPL_{pk} and SPL_{rms} metrics were identified from previously published work as well-established and effective measures of the amplitude of sound pressure, they were selected for use in the soundscape code without further analysis (Madsen, 2005; Merchant et al., 2015; Thompson et al., 2013). SEL was initially considered for use in the soundscape code, but because SEL typically relates to sound exposure in terms of acoustic impact, which was not a focus of this work, it was not pursued as a candidate metric.

Impulsiveness

Impulsive signals are defined qualitatively as signals that are short duration, have rapid rise times, and high sound levels (NIOSH, 1998; NMFS 2018). Impulsiveness of a soundscape describes the content of impulsive signals in a soundscape and is an important soundscape property

to consider for many reasons. A plethora of sound sources including fin whales (*Balaenoptera physalus*) and seismic surveys produce pulsed acoustic signatures which means it is possible the impulsiveness of a soundscape could be used as an indication of presence of pulsed acoustic sources. Impulsive sounds can potentially have physiological impacts on fish (Casper, Halvorsen, et al., 2013; Casper, Smith, et al., 2013; Halvorsen, Casper, Matthews, et al., 2012; Halvorsen, Casper, Woodley, et al., 2012), and marine mammals (Kastelein et al., 2015; Lucke et al., 2009; Southall et al., 2019), so it is also a valuable property to consider from a regulatory perspective as well as a physical characteristic. Although regulations lack quantitative definitions regarding the difference between impulsive and non-impulsive sounds, several metrics for quantifying impulsiveness have been suggested including kurtosis, crest factor and Harris impulse factor (Erdreich, 1986; Kastelein et al., 2017; Starck & Pekkarinen, 1987, Southall et al., 2007). All three were initially considered candidate metrics to represent impulsiveness in the soundscape code, but Harris impulse factor was removed from consideration due to constraints in the narrow range of the metric and the resulting implications for future use in comparative analysis. Furthermore, Harris impulsive factor is insensitive to the repetition rate of impulsive signals (Martin et al., 2020), which is an important property that needs to be considered when analyzing the impulsiveness of a soundscape.

The crest factor is defined as the difference, in dB, between the SPL_{pk} and the time averaged sound pressure level. It describes the ratio of the SPL_{pk} relative to the effective pressure level (Equation 3):

$$CF = SPL_{pk} - SPL_{rms} \qquad (3)$$

This metric has been used in predicting auditory injury in industrial workers by utilizing A-weighted sound levels where a crest factor value of 15 dB or greater indicated dangerous

impulse noises (Starck & Pekkarinen, 1987). The crest factor using a 10 minute analysis window of a 1-minue long sinusoidal signal in Gaussian noise 12 dB above the noise is also 15 (Martin et al., 2020), so this threshold is clearly not adequate for use in assessing impulses in ocean sound

Kurtosis describes the shape of a probability distribution and is a measure of the weight of the tails of the probability distribution of a real valued random variable. Kurtosis is defined below for the pressure time series $p(t)$ as (Equations 4-6):

$$Kurtosis = \frac{\mu_4}{\mu_2^2} \qquad (4)$$

$$\mu_2 = \frac{1}{t_2 - t_1} \int_{t_1}^{t_2} [\, p(t) - \bar{p}\,]^2 \qquad (5)$$

$$\mu_4 = \frac{1}{t_2 - t_1} \int_{t_1}^{t_2} [\, p(t) - \bar{p}\,]^4 \qquad (6)$$

where $\bar{p}$ is the mean pressure. Proposed as an indicator of the impulsiveness of sounds by Erdreich (1986) for noise exposures with equal spectral energy, permanent threshold shift (PTS) was found to increase with kurtosis up to a value of 40 (Qiu et al., 2013); this value of 40 now represents the threshold above which signals are considered impulsive. In comparison, Gaussian-distributed random noise produces kurtosis values of 3. Time series with strong sinusoidal signals have a kurtosis in the range of 0-3, and time series with transients produce kurtosis values above 3 (Martin et al., 2020).

Periodicity

In acoustics, periodicities typically refer to repetitive temporal variation in acoustic events, like the diel trends of chorusing fish. The term periodicity is inherently general; periodicity can refer to a pattern that repeats over the course of a year, month, day, hour, or second. Seismic airgun signals (Greene and Richardson 1988; Richardson 2013), echolocation clicks (Clarke et al.,

2019), pulsed fish or whale vocalizations, and even the rhythmic rasping of the California spiny lobster (Patek et al., 2009) are examples of real-world signals that are periodic. Because much of this rhythmic acoustic variability observed in a soundscape can be attributed to some natural or human acoustic event, most studies refer to some type of important or revealing periodicity. Sounds characterized by diverse frequency ranges and pulse repetition rates (periodicities) were used to suggest the presence of multiple acoustically active fish species at two shallow hard-bottom sites in the Adriatic Sea (Pieretti et al., 2017). Studies have shown that some pelagic post-larval reef fishes and crustaceans use underwater sound as an orientation cue (Tolimieri et al., 2000; Leis et al., 2002); characterizing temporal patterns in marine soundscapes is critical in developing the understanding of a variety of events, including acoustic cues available to pelagic larvae (Staaterman et al., 2014; Bertucci et al., 2015). The proposed soundscape code focuses on periodicities that 1) impose physical characteristics to a soundscape over short time periods, 2) occur on time scales of less than a minute, and 3) can be captured by metrics calculated over a single minute of acoustic data. A metric for capturing larger scale periodicity related to diel, season, or annual cycles was not explored in this project but could be assessed using a time series of the individual soundscape code parameters. To my knowledge no metric designed specifically for quantifying the content of periodic signals in an acoustic environment exists, so metrics from other fields were repurposed as candidates to represent the periodicity property in the soundscape code.

Cepstrum was first proposed as a tool for analyzing periodic seismological data (Bogert et al., 1963), where the arrival of various waves and phases could be considered as distorted echoes. Cepstrum is not widely used in marine soundscape studies, but has been used with efficacy in a variety of mechanical analyses, and is considered underutilized by those that use it (Randall, 2017).

Cepstrum treats the log spectrum of a time series as a waveform, and the spectrum of this log spectrum produces peaks when the original waveform contains echoes, or periodic components (Oppenheim & Schafer, 2004). Cepstrum is calculated by taking the real part of the inverse discrete Fourier transform (DFT) of the logarithm of the magnitude of the DFT of the signal (Equation 7):

$$Cepstrum = real\big(IFFT(log|FFT(p(t))|)\big) \qquad (7)$$

where p_{ts} is the pressure time series.

Inspired by Martin *et al.* (2019), time lagged autocorrelation used to highlight periodicities in acoustic data was considered as a periodicity metric candidate within the present study. Using an averaged pressure time series, the peaks above a selected threshold in autocorrelation plots can be counted and used as proxies for periodicity in a soundscape. Two averaging windows were assessed within this study to determine the best fit for the soundscape code: 1.0 second mean square (MS) sound pressure averages, and 0.1 second MS sound pressure averages. These nuanced autocorrelation metrics are referred to as "acorr2" (1.0 second average), and "acorr3" (0.1 second average). For all periodicity metrics, the number of peaks in respective outputs that surpass the periodicity threshold are referred to in this study as "peaks-per-minute" (ppm).

Uniformity

Soundscape uniformity is the degree to which the signals change over time in terms of temporal and frequency attributes of the soundscape. It answers the question "to what degree are the soundscapes similar or different?" and describes the dynamic nature of a given soundscape. The inclusion of the uniformity property in the soundscape code was motivated by the widespread

interest in biodiversity, and the use of passive acoustic monitoring techniques to study biodiversity remotely (Peet, 1974; Pimm & Lawton, 1998; Sueur et al., 2014). A suite of quantitative indices has been developed and geared towards quantifying different properties of acoustic environments: Acoustic Complexity Index (ACI), Acoustic Entropy Index (H), Acoustic Dissimilarity Index (D), and Acoustic Richness (AR). These indices have been widely used in terrestrial acoustic studies to measure biodiversity and species richness (Pieretti et al., 2011, 2017; Sueur et al., 2008, 2014). Because the acoustic biodiversity indices quantify biodiversity by considering pressure fluctuations in time and frequency domains (Sueur et al., 2008), they were repurposed as measures of acoustic uniformity. By including a measure that can potentially reflect biodiversity as well as general acoustic diversity or variability, the uniformity property becomes a valuable component of the soundscape code.

For the Acoustic Dissimilarity Index (D), Sueur et al. (2008) utilized a measure that estimated the compositional dissimilarity between two communities. Within this thesis, it is applied to two consecutive acoustic recording periods in an effort to capture the acoustic differences and measure the acoustic uniformity. The amplitude envelope is given by the absolute value of the analytic signal ζ(t), which is defined as (Equation 8)

$$\zeta(t) = p(t) + ip_H(t) \qquad (8)$$

where: $i = \sqrt{-1}$, and $p_H(t)$ is the Hilbert transform of the real valued signal *p(t)*. Probability mass functions (PMF) give the probability that a discrete, random variable is exactly equal to some value, and the PMF of the amplitude envelope *A(t)* and PMF of the mean spectrum *S(f)* is given by (Equation 9 & Equation 10):

$$A(t) = \frac{|\zeta(t)|}{\sum_{t=1}^{n}|\zeta(t)|} \qquad (9)$$

$$S(f) = \frac{|\overline{s(f)}|}{\sum_{t=1}^{n}|\overline{s(f}|} \qquad (10)$$

and is used to quantify envelope dissimilarity where $\overline{s(f)}$ is the mean spectrum. Envelope dissimilarity is estimated between two signals by computing the difference between their envelope PMFs. (Equations 11 & 12):

$$D_t = \frac{1}{2}\sum_{t=1}^{n} |\, A_1(t) - \, A_2(t)| \qquad (11)$$

$$D_f = \frac{1}{2}\sum_{t=1}^{n} |S_1(f) - \, S_2(f)| \qquad (12)$$

where *A(t)* is the PMF of the amplitude envelope and S(f) is PMF of the mean spectrum. Dissimilarity Index (D) is the product of the temporal dissimilarity (D_t) and spectral dissimilarity(D_f):

$$D = \, D_t \times \, D_f \qquad (13)$$

The D index is a between-group (β) index originally developed to measure differences among communities. In the context of this study, the D index will be used to quantify differences in the soundscape across time by calculating it over consecutive acoustic recording periods.

The Entropy Index (H) has been used as a proxy for biodiversity in the marine environment with mixed results (Harris et al., 2016; Parks et al., 2014). Harris et al. (2016) found that H values exhibited a dependence on the size of the FFT window, and at a FFT window length of 512 points

showed little correlation to typical diversity measures, but correlation increased with spectral resolution. Parks *et al.* (2014) had to remove noise from a seismic survey before finding a significant connection between the H index and sampled biodiversity. H-index (Equation 16) is the product of the spectral (H_f) and temporal (H_t) entropies (Equations 14 & 15):

$$H_t = -\sum_{t=1}^{n} A(t) \times log_2\big(A(t)\big) \times log_2(n)^{-1}, with\ H_t \epsilon [0,1] \quad (14)$$

$$H_f = -\sum_{t=1}^{n} S(f) \times log_2(S(f)) \times log_2(N)^{-1}, with\ H_f \epsilon [0,1] \quad (15)$$

$$H = H_t \times H_f \quad (16)$$

where *A(t)* is the PMF of the amplitude envelope, and *S(f)* is the PMF of the mean spectrum. H is 0 for a single pure tone, increases with frequency bands and amplitude modulations, and approaches 1 for random noise. Because H-index was designed to increase with signal diversity in time and frequency, it was repurposed in this study to represent acoustic uniformity, which shares similarities with the principle of acoustic diversity that the metric was built on.

Research Goal and Objectives

This project was broken into two phases: 1) development of the soundscape code and 2) application of the soundscape code to novel soundscape analysis. In the first phase, data from seven unique soundscapes were used as a training dataset to determine which metric best represented the corresponding soundscape code property (Chapter 2). In the second phase of the project, the soundscape code, having been populated with optimal metrics, was applied to four deep sea environments located offshore of several US southeastern states, and one shallow, tropical coral reef environment (Chapter 3).

Goal:

Develop and apply a quantitative method of analyzing, visualizing, and comparing underwater acoustic environments across habitat types.

Objectives:

1) Determine the optimal suite of metrics that comprehensively capture the salient properties of a marine soundscape
2) Compare and contrast five soundscapes corresponding to habitats varying in depth and coral content

The developed soundscape code was applied to datasets collected from two deep sea coral sites, two deep sea sites featuring sandy bottoms, and one tropical, shallow reef environment. Deep sea soundscapes are relatively unexplored, and this research offers valuable contributions to scientists seeking to understand the nature of marine life, and overall marine dynamics in deep sea ecosystems.

CHAPTER 2: The Soundscape Code

Development of the soundscape code relied on literature to identify candidate metrics for consideration. Seven previously analyzed passive acoustic datasets that contained known signals were used to test the performance of the candidate metrics. An optimal combination of metrics is one that most accurately and succinctly captures salient soundscape properties and allows for comparisons and monitoring. Once metric responses to the seven unique soundscapes were analyzed, and optimal metrics were identified, soundscape codes for each of the seven datasets were generated to demonstrate how the optimal metrics could be used to assess the respective soundscapes (Wilford et al., 2021).

Methodologies

The datasets used to assess the performance of the candidate metrics for use in the soundscape code were selected from a pool of passive acoustic data that had already been analyzed, and in some cases, used in publications (Martin et al. 2017; Martin et al. 2019; Martin and Barclay, 2019; Martin et al. 2020). Soundscape code datasets were picked based on previous knowledge of activity in the soundscape region. Passive acoustic recordings were converted to pressure, and then metrics were calculated over each pressure time series.

Soundscape Code Data Sets

Each soundscape code dataset was collected using Autonomous Multi-channel Acoustic Recorders (AMAR, JASCO Applied Sciences) that sampled at a variety of sample rates and durations (*Table 3*). Recorders were deployed intermittently between 2012 and 2016 at the seven different locations.

Table 3*:* Soundscape code data set information

Data set (Site abbreviation)	Location	Latitude (° North)	Longitude (° East)	Depth (meters)	Sample Rate (kHz)	Duration (min)	Duty cycle (min)

Melville Bay (MB)	Baffin Bay (Greenland)	75.3	-58.6	370	64	240	continuous
Biogully East (BGE)	Nova Scotian Shelf	43.8	-58.9	2000	250	250	continuous
Grand Banks (GB4v0)	Nova Scotian Shelf	45.4	-48.8	112	32	204	continuous
Grand Banks (GB4v35)	Nova Scotian Shelf	45.4	-48.8	112	32	354	continuous
Grand Banks (GB5)	Nova Scotian Shelf	44.9	-49.3	119	16	360	continuous
Great Barrier Reef (GBR)	Wheeler Reef (Great Barrier Reef)	-18.8	147.5	18	64	112	7/14
Orsted (OR)	Block Island (RI, USA)	41.2	-71.6	42	64	270	continuous

Recordings from these sites were chosen for specific acoustic events captured in the recordings. While the sites may not all be unique in their location, the acoustic content of their recordings was unique; GB5 is about 70 km from GB4v35 and GB4v0, and while the latter two share the same site location designation, the datasets were recorded weeks apart. The seven data sets contain a variety of human-generated, natural biologic, and natural abiotic sounds including sounds from a seismic survey, impact pile driving, vessel passages, ice calving and icebergs, fin (*Balaenoptera physalus*) and humpback whale (*Megaptera novaeangliae)* vocalizations, northern bottlenose whale (*Hyperoodon ampullatus*) and common dolphin (*Delphinus delphis*) whistles and echolocation clicks, and shallow-water reef sounds including snapping shrimp, and fish grunts (*Figure 4)*. The biological sounds present in the data sets are representative of the diversity of marine life and sounds produced ocean wide.

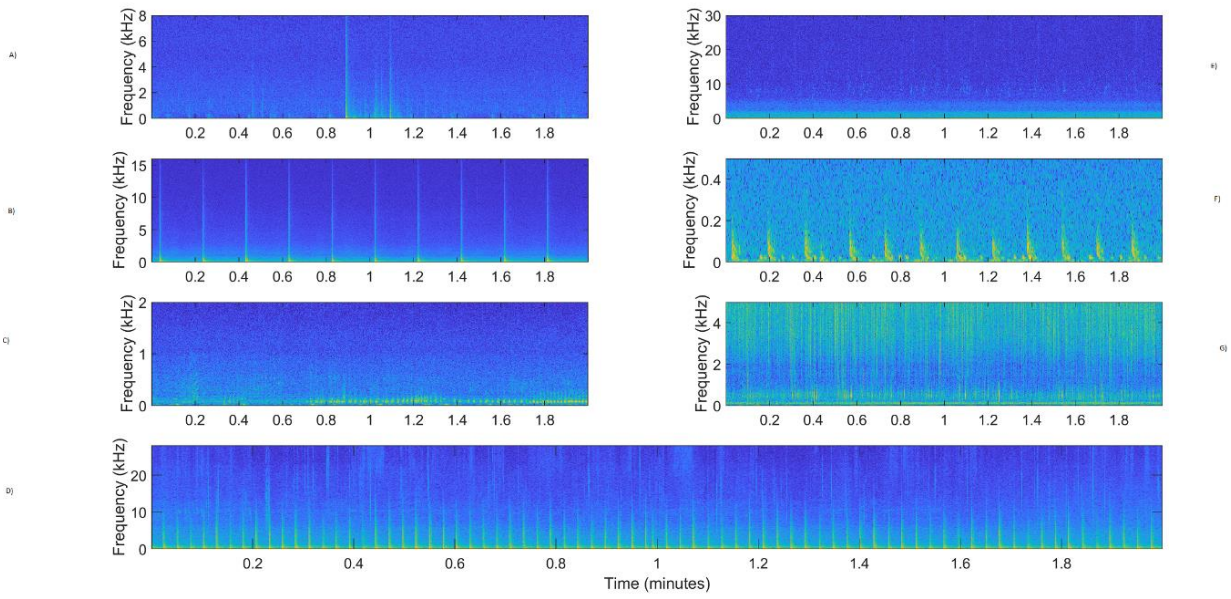

Figure 4 Signals detected at designated soundscape code dataset sites A) Ice sounds, B) seismic survey, C) humpback and fin whale vocalization, D) impact pile driving, E) northern bottlenose whale and common dolphin vocalizations in quiet soundscape, F) fin whale vocalizations, G) reef sounds.

Data processing

Five frequency bands were selected for soundscape code analysis: 1) 10–100 Hz (Low), 2) 100–1000 Hz (Mid), 3) 1–10 kHz (High), 4) 10 kHz and above (Ultra-High), and 5) 10 Hz and above (broadband; BB). Data was filtered using a custom digital filter that operates like a gate function and makes all values outside of the pass bands 0. These frequency bands were chosen because the dominant frequencies of many signals can be isolated into a single soundscape code frequency band. Data from Biogull East (BGE) was low pass filtered with a passband out to 32 kHz to provide a uniform analysis in the Ultra-High band across Melville Bay (MB), Great Barrier Reef (GBR), Orsted (OR), and BGE. Sample rate restrictions precluded analysis of the Ultra-High band at the Grand Banks sites (GB4v0, GB4v35, GB5). The high band at GB5 was included, even though the data could only be resolved up to 8 kHz due to the sample rate at this site (16 kHz) (Table *2)*.

The metrics assessed for the soundscape code were calculated over one-minute time windows. The one-minute time window is a standard time length in soundscape analysis and corresponds with the human auditory experience (Ainslie et al., 2018). All FFTs performed in calculating soundscape code metrics used 1-second time windows. Acorr2, acorr3, SPL_{rms}, SPL_{pk}, kurtosis, crest factor, D-index, and H-index were calculated using custom code written in MATLAB (The Mathworks Inc, Natick MA). The median and central 95^{th} percentage (C95) of each metric were analyzed and reported for each site. The 95% confidence interval was initially proposed as the measure of variability, but because the metric values are not all normally distributed, the size of the interval between the 2.5 and 97.5 percentile is more accurately referred to as the C95. A color coding scheme was adopted to aid in visual interpretation of the soundscape code results whereby the metric range across all sites of individual metric medians and C95s was divided into four quarters, and the cells of the soundscape code were colored based on quarter. For example, the range of the broadband kurtosis medians across all sites (3 - 215) was divided into four quarters, and then the individual cells kurtosis category of the soundscape code were colored accordingly. The current color-coding scheme is weighted to the specific soundscapes analyzed in this particular study and standard soundscape code metric levels need to be developed for color coding of soundscape codes universally. The color coding process was applied to all medians and C95s for all frequency bands.

Cepstrum was calculated over averaged pressure time series using a built-in MATLAB function *rceps*. However, the output of cepstrum needed to be further quantified for use in the soundscape code. To do this, a threshold set at $c(n) = 0.1$ was chosen, and any peaks above this threshold were used as proxies for periodicities with the number of peaks per 1-minute cepstrum counted and reported in the soundscape code. A similar method was adopted for the autocorrelation

metrics (acorr2 and acorr3): minimum peak prominence of $\rho_{yy}(t, t+\tau) = 0.5$ was set in the MATLAB function *findpeaks*, and any autocorrelation coefficient peaks in the 1-minute time window above this threshold were counted (ppm). The threshold for the autocorrelation functions was identified after rigorous analysis of outputs showed it filtered out false peaks from noise but correctly characterized periodicities. Due to the increased variability at extreme lags, only 45 (75%) lags were considered for acorr2, and 420 lags (70%) for acorr3.

Metric response analysis

The SPL_{pk} and SPL_{rms} metrics have been well-studied as quantitative metrics of amplitude (Madsen, 2005; Merchant et al., 2015; Thompson et al., 2013) and further comparison was not deemed necessary. A qualitative analysis was performed to determine the optimal representative metric for the remaining three soundscape properties in the soundscape code. Visual analysis of spectrograms and waveforms, coupled with knowledge of the sound sources present at each site, helped to form *a priori* expectations for the candidate soundscape metrics (*Figure 5*). Metric statistics were compared against *a priori* expectations, identifying which metrics produced the strongest agreement across soundscape code properties.

Site name	Acoustic characteristics	Amplitude					Impulsiveness					Periodicity					Uniformity				
		BB	L	M	H	UH	BB	L	M	H	UH	BB	L	M	H	UH	BB	L	M	H	UH
Melville Bay	Random impulsive events																				
Biogully East	Quiet environment with intermittent vocalizing biology																				
Grand Banks 4v0	Periodic and impulsive seismic survey sounds																				
Grand Banks 4v35	LF pulsed biological sounds (fin whale), ships passage, elevated sound levels from high wind																				
Grand Banks 5	LF pulsed biological sounds (fin and minke whale), ships passage, elevated sound levels from high wind																				
Great Barrier Reef	Impulsive in higher frequency bands from snapping shrimp; urchin sounds, LF fish grunts, highly uniform																				
Orsted (Block Island)	High sound level, chaotic, and dynamic environment																				

Figure 5 A priori metric response expectations for each data set. Expectations formed criteria to compare metrics and inform the metric selection. Green-Yellow-Red coloration represents relative expected metric response level where green indicates a low property level, yellow indicates a mid-level, and red indicates high-level responses. Low-level responses for the uniformity category indicate a highly uniform acoustic environment, and high level responses indicate a lack of uniformity. Corresponding soundscape code frequency band is indicated by BB, L, M, H, UH.

A series of qualitative comparisons (*Table 4*) were used to inform the determination of which metric was optimal for each property. The qualitative comparisons shown in *Table 4* do not represent an exhaustive review of the analysis completed using the soundscape code datasets, but rather represent the comparisons that produced definitive results in the analysis. Because amplitude metrics were already chosen, they are not featured among the list of comparisons.

Table 4 Qualitative comparisons of soundscape code property metrics and summary of results.

Qualitative Comparison I.D.	Site	Data represented	Test basis	Expectations	Summary of Results
Impulsiveness 1 (I1)	Melville Bay (MB)	Iceberg noise	The entirety of the recording was considered in this test.	Intermittent levels of impulsiveness in frequency bands associated with the ice noise (Low, Mid, decaying in High)	Kurtosis outperformed crest factor by indicating frequency of dominant signals of ice sounds more appropriately
Impulsiveness 2 (I2)	Grand Banks Station 4 (GB4v35)	Fin whale	Two consecutive 10-minute time windows were considered. 1) contains two full and one partial fin whale pulse train. 2) contains no pulse trains.	High levels of impulsiveness in the low band in the first 10-min time windows.	Kurtosis outperformed crest factor by indicating frequency of dominant signals of fin whale vocalizations more appropriately
Impulsiveness 3 (I3)	Grand Banks Station 4 (GB4v0)	Seismic survey	Two 10-minute time windows were considered: 1) sounds from distant seismic, 2) sounds from close proximity seismic.	High levels of impulsiveness in only the low, mid and high bands. Clear increases in metric value in second time window.	Kurtosis outperformed crest factor. Kurtosis results indicated frequency of dominant signals of seismic survey signals and highlighted the difference in strength of seismic signals more accurately.
Periodicity 1 (P1)	Grand Banks Station 4 (GB4v0)	Seismic survey	Identical subsets used in I3	Indication of weaker periodicities in time windows 1 and stronger periodicities in the time window 2.	Cepstrum and acorr3 outperformed acorr2 and accurately reported decreased periodicity of signals contained in second time window.
Periodicity 2 (P2)	Grand Banks Station 4 (GB4v35)	Fin whale	Identical subsets used in I1	More peaks in time window 1 than in the time window 2.	All three periodicity metrics performed similarly and accurately report increased periodicity of signals in time window 1.
Periodicity 3 (P3)	Orsted (OR; Block Island)	Pile Driving	Two 10 minute time window were considered: 1) periods of intense and repetitive pile driving sounds, 2) no pile driving	Expectations Identical to those in P2.	All three periodicity metrics performed similarly and accurately report decreased periodicity of signals in time window 2.
Uniformity 1 (U1)	Melville Bay/Biogully East	Ice sounds, quiet environment	Two full recordings. Metrics must reflect acoustic uniformity within site and between sites.	Reflect sporadic nature of ice sounds and consistent nature of BGE	D-index outperformed H-index and accurately contrasted acoustic uniformity at MB and BGE.
Uniformity 2 (U2)	Orsted/Great Barrier Reef	Pile driving, ship noise, reef sounds	Two entire recordings were considered for U2. Methods utilized in U2 identical to U1.	Indicate different “phases” of acoustic activity at OR.	Range measure of the D-index provided an accurate assessment of the different sites.

To add statistical rigor to the metric analyses and further explore how metric values could be used to distinguish or draw comparisons among sites, multiple comparisons tests (MCTs) using the Dunn method for Joint ranking (Dunn, 1964) were carried out using JMP Pro^{TM} 14.0.0 for every soundscape code (SSC) frequency band. The MCTs identified groupings among the SSC metrics that were then connected back to the respective sites and were used to create connected letters plots which highlighted the resultant groupings. The groupings were compared to *a priori* metric expectations formed by an understanding of the characteristics of the sounds contained in the soundscapes. Comparing the groupings to the expectations allowed us to see if the metrics from soundscapes with different characteristics came from statistically different populations. Impulsiveness metrics, for example, were expected to have different distributions among sites that had substantially different impulsiveness characteristics.

Soundscape Code results

Results from a series of comparisons that led to the final choice of metrics are presented on a property-by-property basis. Results from several of the qualitative comparisons outlined in *Table 4* are presented to highlight the responses that guided the metric selection. Metric comparisons were conducted for impulsiveness, periodicity, and uniformity properties. Calculated metric time series were compared to spectrograms, pressure waveforms, and *a priori* expectations to guide final metric selection.

Impulsiveness

Both kurtosis and crest factor were generally found to accurately report the presence of impulsive signals. The superiority of kurtosis in indicating the presence of impulsive signals was suggested in qualitative comparison I1, which featured sound from only one dominant sound source: ice. Spectrograms showed that ice cracks, groans, and rumbling acoustic activity dominated the lower frequencies of the soundscape, but several instances of more broadband ice

cracks exist in the dataset (*Figure 4 A*). Impulsive metrics were expected to reflect the presence of impulsive signals in mostly BB, Low, or Mid soundscape code bands. Kurtosis reported many values exceeding the impulsive threshold in the BB, Low, and Mid soundscape code frequency bands indicating considerable impulsive acoustic activity in the expected frequency bands (*Figure 6).* Crest factor values, on the other hand, indicated little difference among the values corresponding to the different frequency bands.

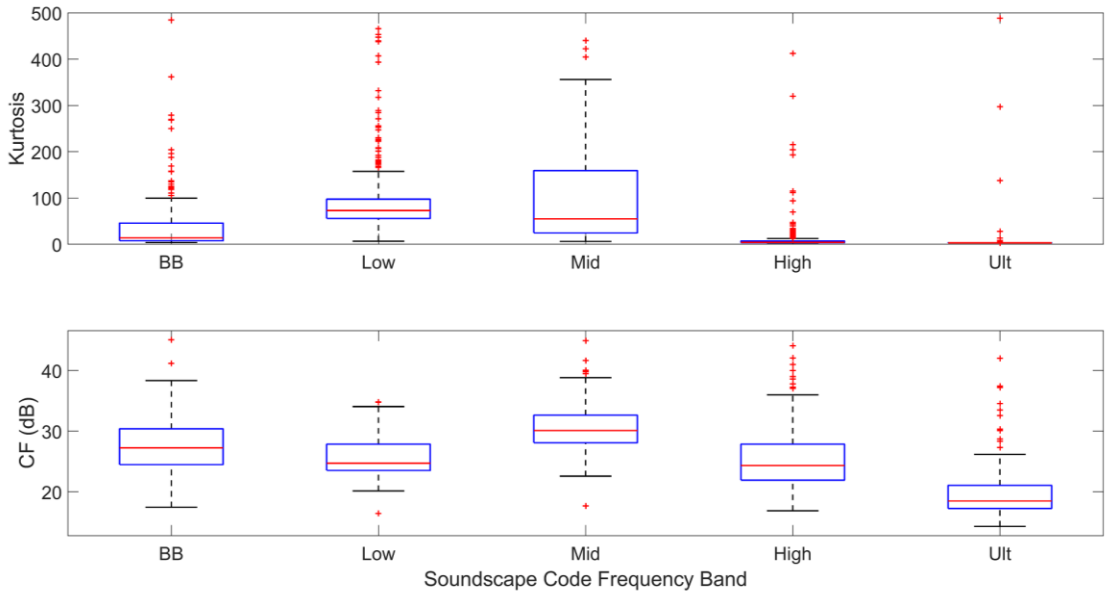

Figure 6 Impulsiveness comparison 1 (I1) results. Wherein the boxplots red horizontal line indicates median value, outer edges of boxes represent 25th and 75th percentiles, whiskers mark the boundary that contains approximately 99% of data values, and the red points are outliers.

Based on spectrogram analysis and an analysis of the sound pressure levels at MB, it was understood that while potentially impulsive events occurred frequently throughout the recording, a handful of high intensity events dominated the soundscape. It was expected that the impulse metrics would reflect the sporadic and intermittent nature of the ice cracks in boxplots of impulsiveness metric values through greater variability (*Figure 6*). Kurtosis performed as expected

by indicating a wide range of kurtosis values that accurately captured the sporadic nature of the ice sounds. While crest factor reflected the presence of impulsive signals, it reported very little distinction between the soundscape code frequency bands, and indicated an abundance of impulsive signals in the High and Ultra-High bands when only sporadic impulsive signals were understood to occur in these bands.

At GB4v35, where the 20 Hz pulsed vocalizations formed the basis for the second qualitative comparison I2, kurtosis values indicated the presence of impulsive signals in the Low band for minutes 1, 2, 3, 5, 6, 7, 9, 10, 11 which corresponded closely to the minutes containing pulsed fin whale vocalizations. Mid and High band kurtosis maintained values of 3 for the duration of qualitative comparison I2. Crest factor peaks also aligned with the pulse trains, but unlike kurtosis, crest factor impulse detections were identified in all soundscape code frequency bands, and for every minute but the 8^{th}. The crest factor values in the Mid, High, and Ultra-High soundscape code bands did not align with content visualized in the spectrograms or *a priori* expectations made based on the knowledge that the dominant sound source at this site was fin whales. However, 3-10 dB re 1 µPa fluctuations in the 1-second SPL_{pk} in the Ultra-High band were detected, which could indicate the presence of an impulsive sound and justify the higher than expected crest factor values (*Figure 7*).

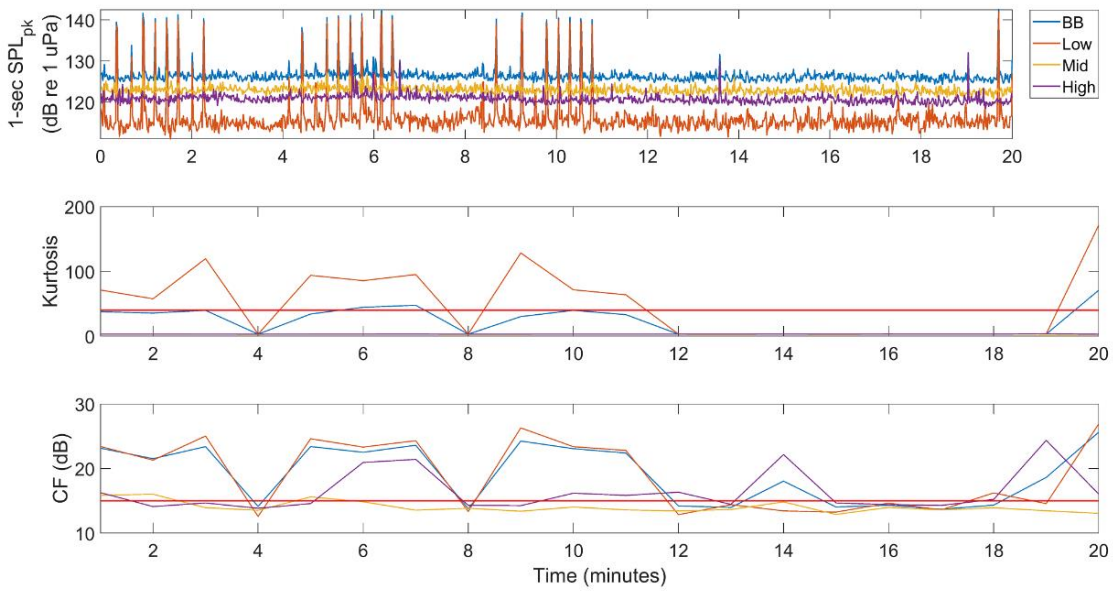

Figure 7 Impulsiveness comparison I2 results. 1-second SPL_{pk} plot shows pulsed nature of the fin whale vocalizations and the 1-minute metric time series report the response of kurtosis and crest factor metrics. Horizontal red line shows the impulsiveness threshold for each impulse metric. Values above this threshold indicate the presence of impulsive signals.

Ten-minute boxplots were used to explore how the metric values changed over time at GB4v35 (*Figure 8*). Crest factor (*Figure 8 right)* remained high during the period of ship noise (box 10-11), so it was difficult to deduce from the crest factor values that a ship had contributed significantly to the soundscape by masking the pulsed fin whale signals. In contrast, kurtosis values (*Figure 8 left*) dropped quickly after the introduction of vessel noise to the soundscape (box 10-11), and values only increased after the vessel noise had subsided and the soundscape returned to being dominated by the pulsed signals of the fin whales (boxes 14-21). Kurtosis also only showed a slightly elevated response to a different fin whale chorus that corresponds roughly to boxes 22-3. Crest factor indicated little difference between the impulsiveness of the two different fin whale choruses.

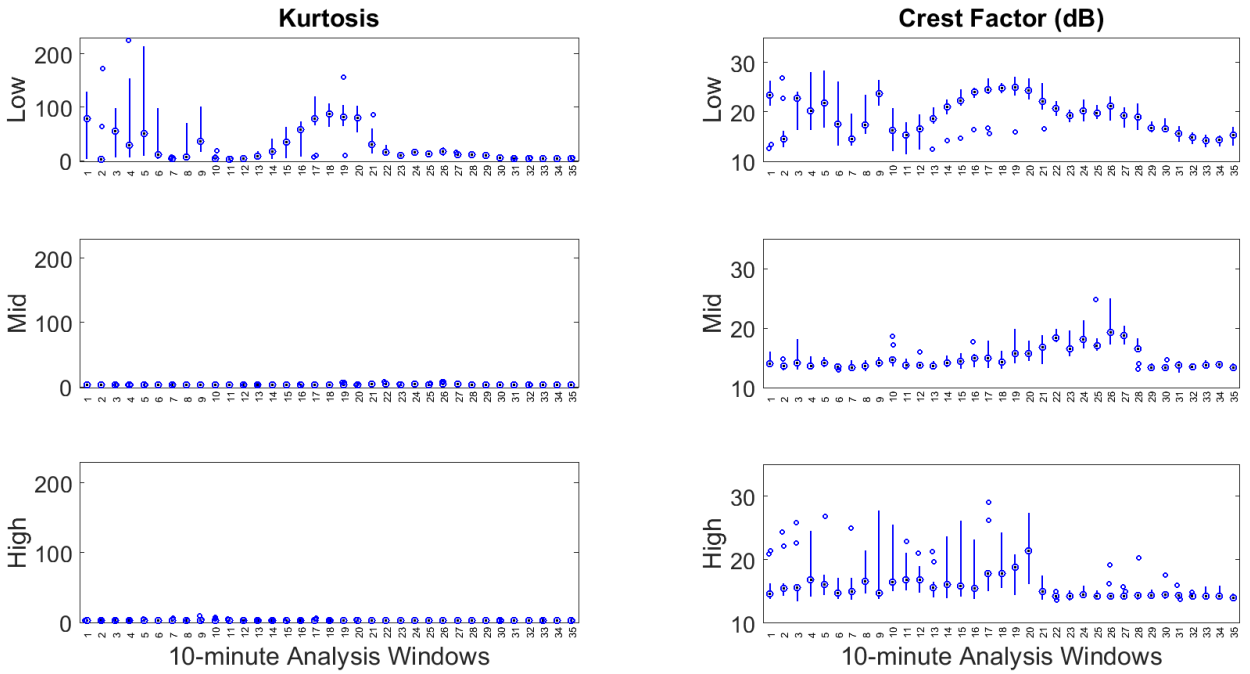

Figure 8 Boxplots of kurtosis (left) and crest factor (right) values at GB4v35. Each box represents the range of metric values in a 10-minute time window comprised of metrics calculated over 1-minute time windows (each boxplot contains 10 metrics values). Circled dots intersecting boxes indicate median values, thick boxes indicate 25th and 75th percentile range, skinny lines indicate range of 99% of data, and blue circles indicate outliers.

Qualitative comparison I3 which contained signals from a seismic survey (*Figure 4 C*) yielded similar results in terms of the performance of the two impulsiveness metrics. Ultimately, both metrics adequately reported the nature of the impulsive seismic survey signals, but kurtosis again aligned more with the salient signals in the relevant frequency bands (*Figure 9*).

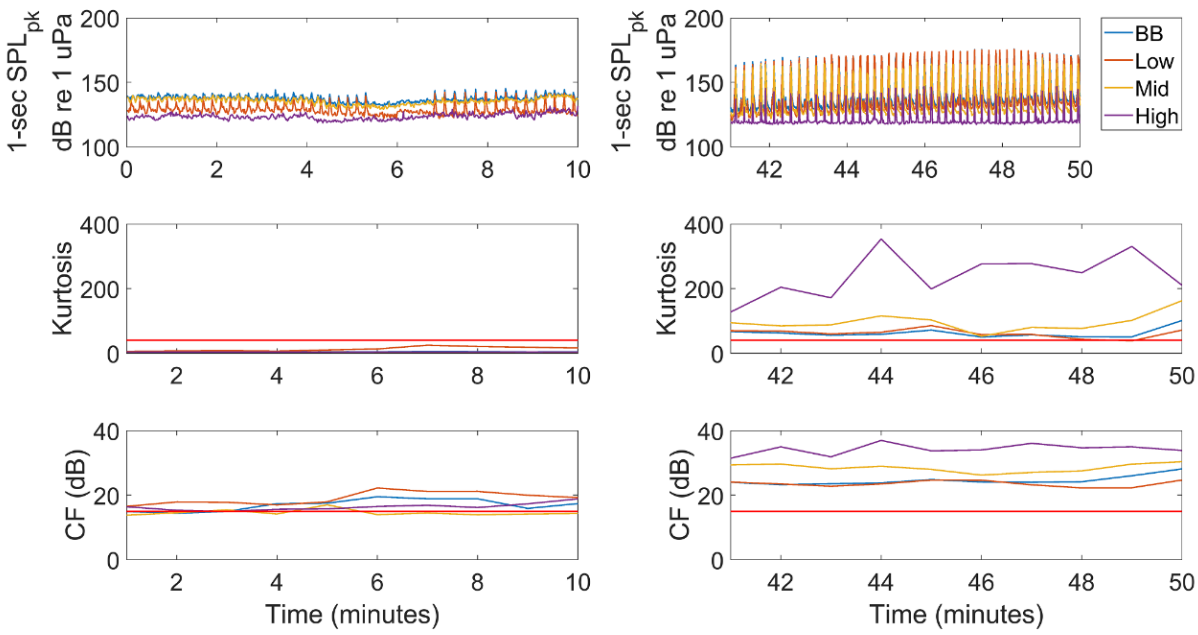

Figure 9 Impulsiveness comparison 3 (I3) results. 1-second SPL_{pk} plot shows pulsed acoustic signature of the seismic survey and the 1-minute metric time series report the response of kurtosis and crest factor metrics. Horizontal red line shows the impulsiveness threshold for each impulse metric. Values above this threshold indicate the presence of impulsive signals.

10-minute boxplots of both crest factor and kurtosis values adequately reflected the nature of the impulsive signals in the GB4v0 soundscape (*Figure 10*). However, kurtosis boxplots at GB4v0 highlighted the difference in seismic survey signals as the survey vessel approached, passed over the hydrophone, and departed. Crest factor, on the other hand, indicated little difference among the phases of the survey.

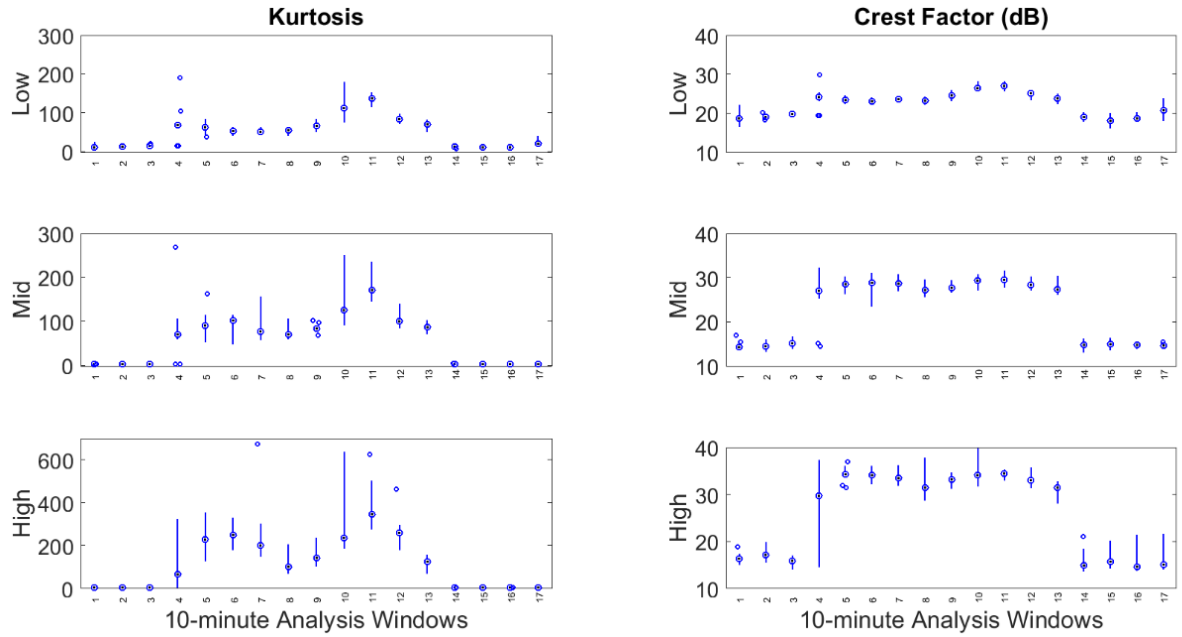

Figure 10 Boxplots of kurtosis (left) and crest factor (right) values at GB4v0. Each box represents the range of metric values in a 10-minute time window comprised of metrics calculated over 1-minute time windows (each boxplot contains 10 metrics values). Circled dots intersecting boxes indicate median values, thick boxes indicate 25th and 75th percentile range, skinny lines indicate range of 99% of data, and blue circles indicate outliers.

Periodicity

Periodicity metrics all reflected aspects of the periodic nature of each of the soundscapes, and differences in metric responses were typically nuanced (*Figure 11*). Acorr3 results suggested it was more closely linked to the periodic nature of the soundscapes, and also that it was more robust to mischaracterizations of the soundscapes which were observed with acorr2 and cepstrum.

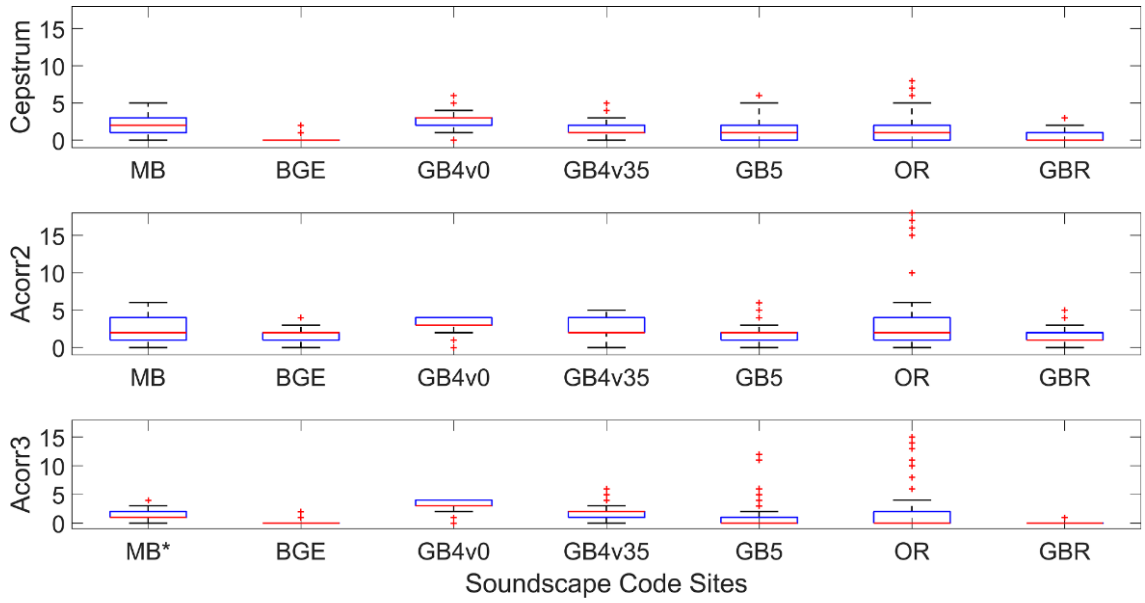

Figure 11 Broadband periodicity metric candidate results for all soundscape code datasets. Values represent peaks-per-minute as reported by periodicity metrics. Red horizontal line indicates median value, outer edges of boxes represent 25th and 75th percentiles, whiskers mark the boundary that contains approximately 99% of data values, and the red points are outliers.

In comparison P1, subsets of the GB4v35 dataset contained unequal numbers of fin whale pulsed vocalizations, and this disparity was used to compare the responses of the periodicity measures. Metrics were expected to report more peaks in time window 1, which contained far more of the 20 Hz periodic fin whale vocalizations (*Figure 12*). Cepstrum reported 27 fewer peaks across frequency bands in time window 2 compared to window 1, while acorr3 reported 11 fewer peaks. In a deviation from expectations, acorr2 reported six more peaks for time window 2.

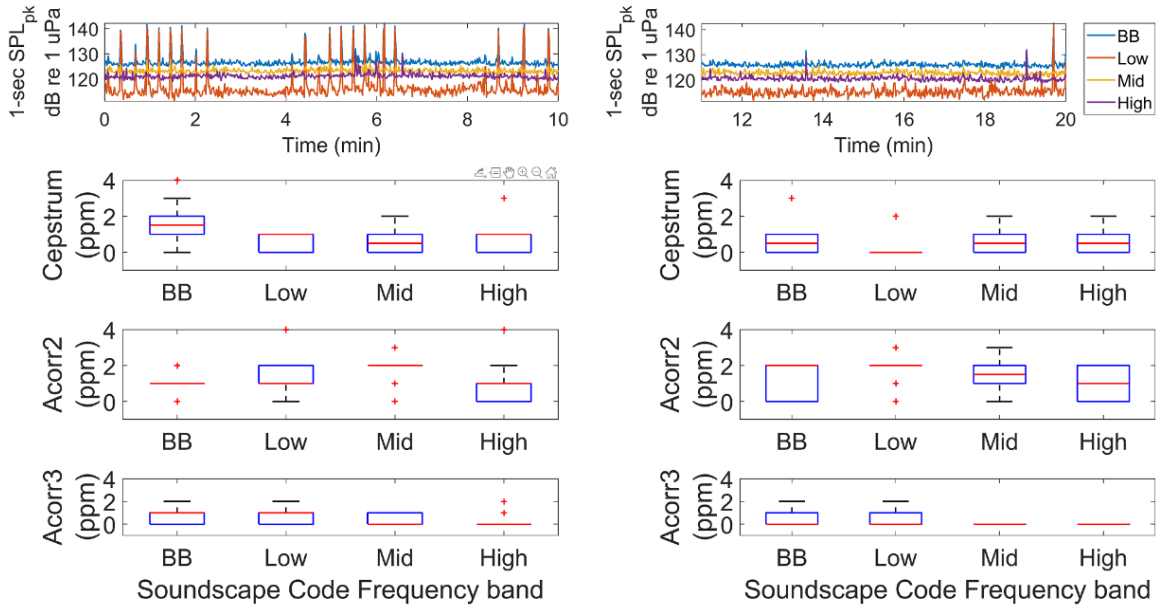

Figure 12 Qualitative comparison (P1) results. Frequency filtered 1-second SPL_{pk} for time window 1 (left) and time window 2 (right). Range of periodicity candidate metric values (ppm) corresponding to the two time windows for cepstrum, acorr2, and acorr3. Red horizontal line indicates median value, outer edges of boxes represent 25th and 75th percentiles, whiskers mark the boundary that contains approximately 99% of data values, and the red points are outliers.

Time series analysis using 10-minute boxplots over the entirety of the GB4v35 dataset similar to the analysis presented in *Figure 8* showed two main differences: 1) Acorr2 reported more peaks per minute than acorr3 in the High band for 69% of the minutes analyzed (n = 353). 2) Both acorr2 and acorr3 were highly consistent during the second period of fin whale vocalizations while cepstrum varied more (*Figure 13*).

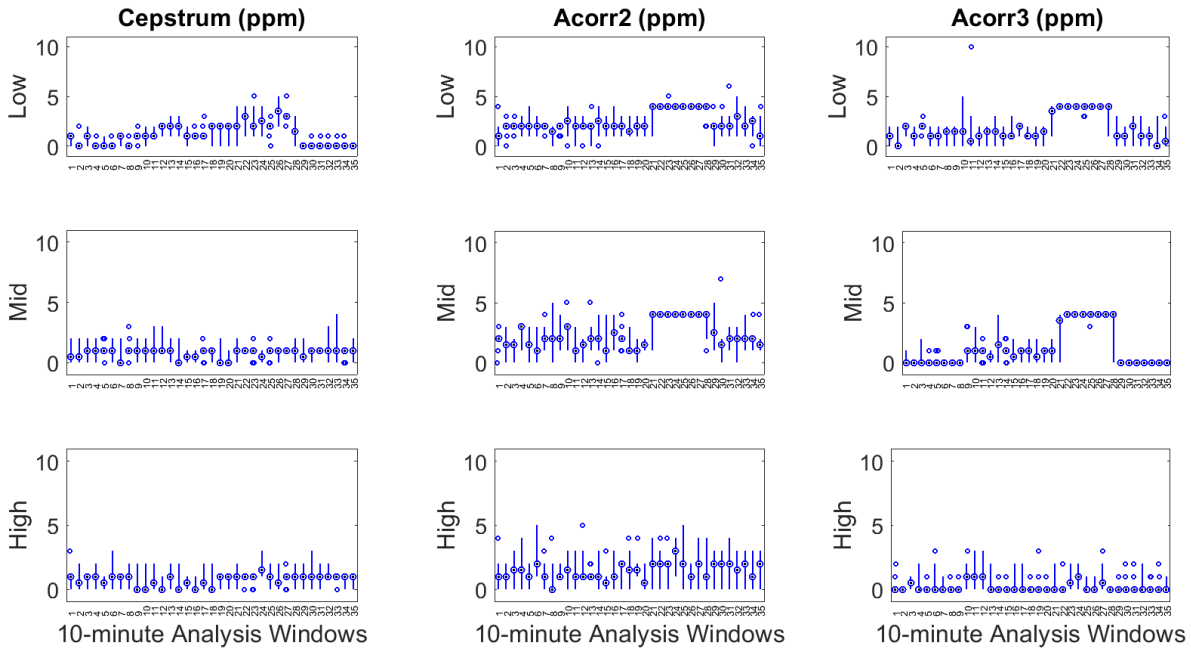

Figure 13 Boxplots of cepstrum (left), acorr2 (middle), and acorr3 (right) values at GB4v35. Each box represents the range of metric values in a 10-minute time window comprised of metrics calculated over 1-minute time windows (each boxplot contains 10 metrics values). Circled dots intersecting boxes indicate median values, thick boxes indicate 25th and 75th percentile range, skinny lines indicate range of 99% of data, and the blue circles indicate outliers.

Qualitative comparisons (P2) and (P3) yielded results that were less conclusive than (P1). Comparison P2 utilized sounds from a seismic survey (*Figure 4 C*), and metrics were expected to report an increase in peaks-per-minute from time window 1 to time window 2. Time window 1 captured distant seismic survey signals, while time window 2 captured close proximity signals that were louder and had more consistent repetition. All metrics reported more peaks-per-minute across soundscape code frequency bands for time window 2 of the GB4v0 dataset (*Figure 14)*.

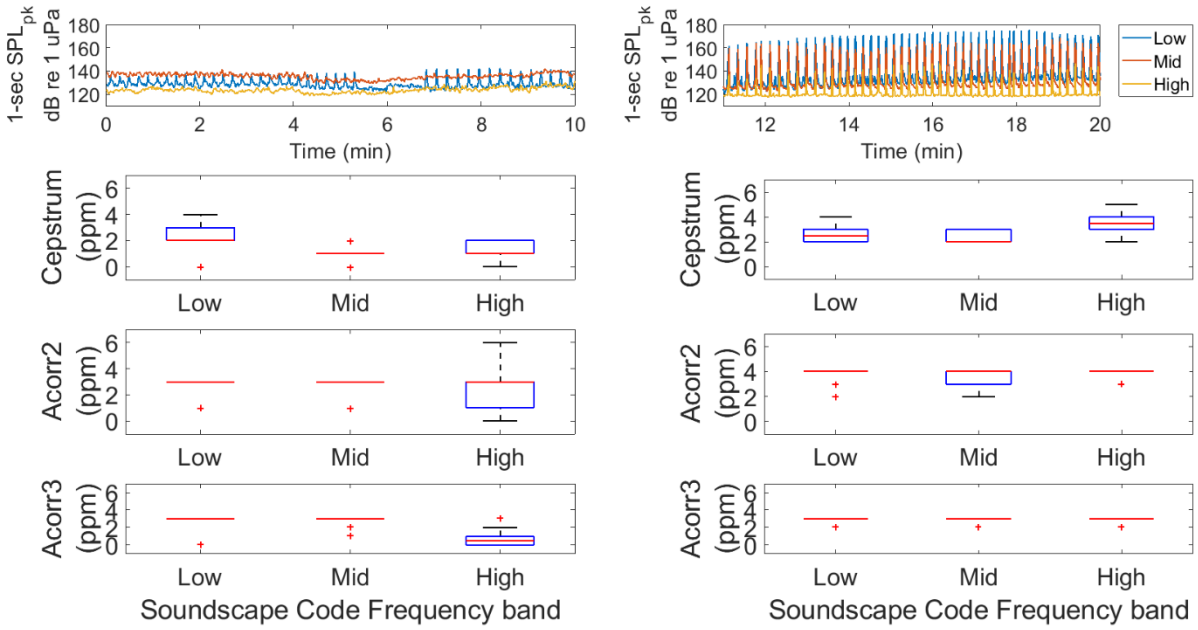

Figure 14 Qualitative comparison P2 Frequency filtered 1-second SPL_{pk} for time window 1 (left) and time window 2 (right). Range of periodicity candidate metric values (ppm) corresponding to the two time windows for cepstrum, acorr2, and acorr3. Red horizontal line indicates median value, outer edges of boxes represent 25th and 75th percentiles, whiskers mark the boundary that contains approximately 99% of data values, and the red points are outliers.

Comparison P3 utilized the sounds from an impact pile driving operation (*Figure 4 G)* and metrics were expected to report a decrease in peaks-per-minute from time window 1 to time window 2. Time window 1 featured intense pile driving sounds and time window 2 did not. The periodicity metrics in P3 reported a substantial decrease in peaks-per-minute across the two time windows (*Figure 15*).

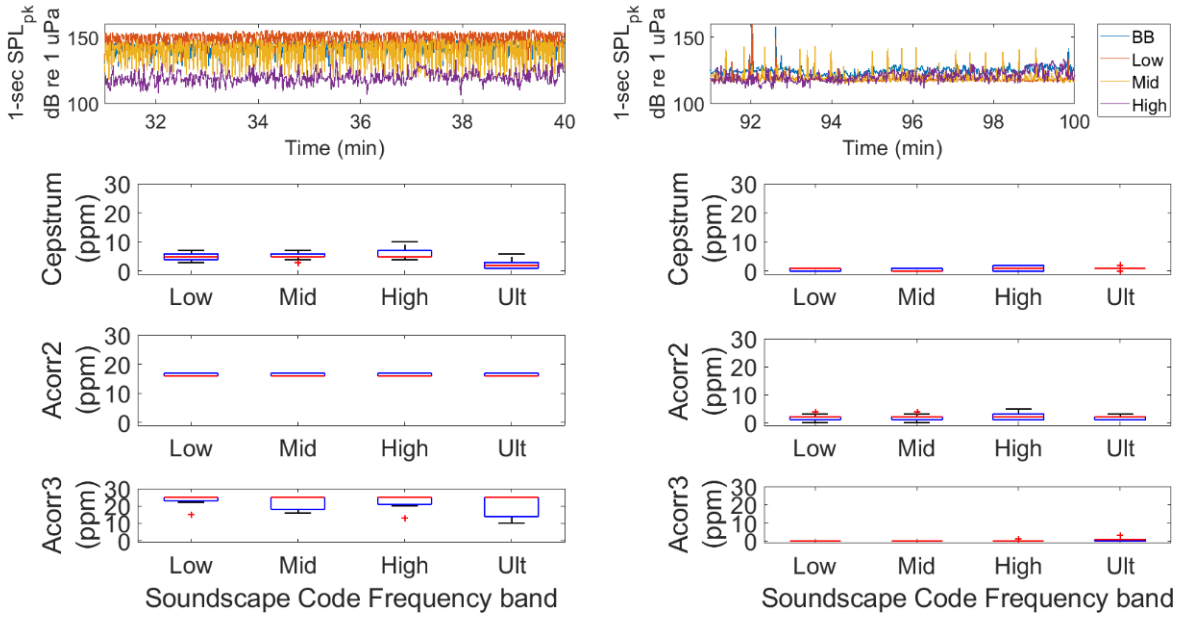

Figure 15 Qualitative comparison (P3) results. Frequency filtered 1-second SPL_{pk} for time window 1 (left) and time window 2 (right). Range of periodicity candidate metric values (ppm) corresponding to the two time windows for cepstrum, acorr2, and acorr3. Red horizontal line indicates median value, outer edges of boxes represent 25th and 75th percentiles, whiskers mark the boundary that contains approximately 99% of data values, and the red points are outliers.

10-minute boxplots of periodicity metrics plotted over the duration of the datasets used in qualitative comparisons P2 and P3 did not indicate conclusive differences and all metrics responded appropriately to the different acoustic activity featured in the two datasets.

Uniformity

D-index values aligned with *a priori* expectations and outperformed the H-index in every qualitative analysis conducted using the soundscape code datasets. D-index values accurately captured the acoustic uniformity at all soundscape code datasets by indicating consistently high values at GB4v0 and OR, and the presence of high values in sites where dramatic changes in the acoustic environment occurred (*Figure 16*).

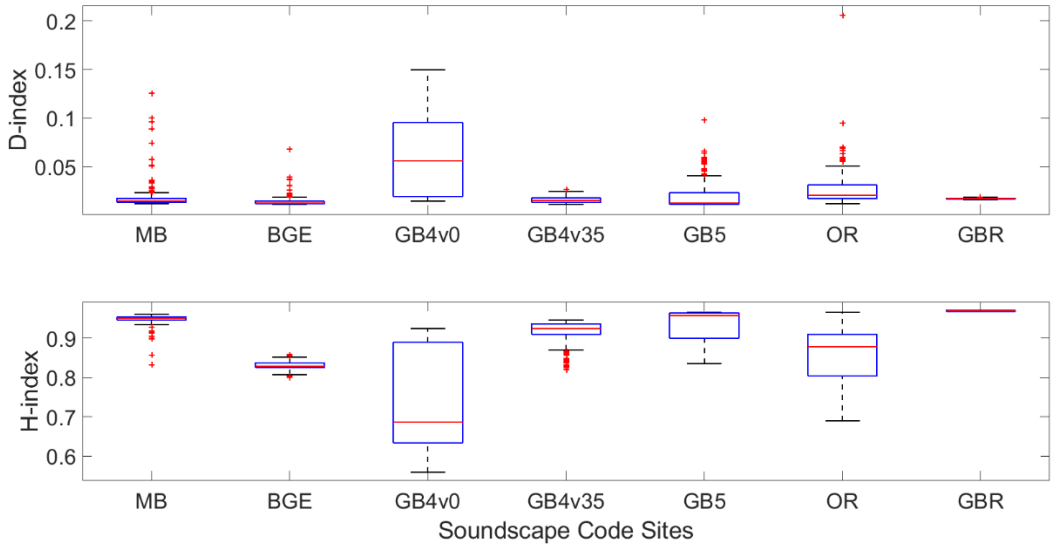

Figure 16 Broadband uniformity metric values. Red horizontal line indicates median value, outer edges of boxes represent 25th and 75th percentiles, whiskers mark the boundary that contains approximately 99% of data values, and the red points are outliers.

Comparisons of uniformity metric results drew on ice sounds from MB (Figure 4 *A*), pile driving and boat noise from OR (*Figure* 4 *G*), reef sounds from GBR (Figure 4 *F*), and sporadic echolocation and whistling activity from BGE (*Figure 4 B*) to determine which metric would represent soundscape uniformity in the soundscape code (*Table 2*). In qualitative comparison U1, uniformity candidate metrics were expected to reflect differences in acoustic uniformity across BGE and MB. Ice noise in lower frequency bands at MB produced a soundscape that was less acoustically uniform in frequencies under 1 kHz, while the vocalizations of the bottlenose whales at BGE decreased uniformity in the higher frequencies. At MB, the D-index values in the Low and Mid bands reflected the sporadic and random ice noise (*Figure 17*). Compared to BGE, D-index values accurately characterized MB as more variable in these bands. In the High and Ultra-High bands, BGE D-index values were greater than MB, which again was an accurate representation of

the acoustic activity of northern bottlenose. Disruption of acoustic uniformity from the northern bottlenose whales at BGE was reflected in time series analyses of D-index values and in the slightly increased range of BGE D-index values relative to MB D-index values. H-index also reflected the decreased uniformity at MB, but the dependence of this metric on a number of frequency bands made interpretation and comparison difficult, as H-index values increased from the Low to Ultra-High soundscape code band regardless of acoustic uniformity. D-index soundscape code values in *Figure 17* reflect the substantial disparity in acoustic uniformity between the two sites in both magnitude and variability of the index. In contrast, the slightly larger range of the H-index values corresponding to the MB Low band suggested only a slight disparity in acoustic uniformity between the two sites, and the magnitude of the index was not representative of the recording content.

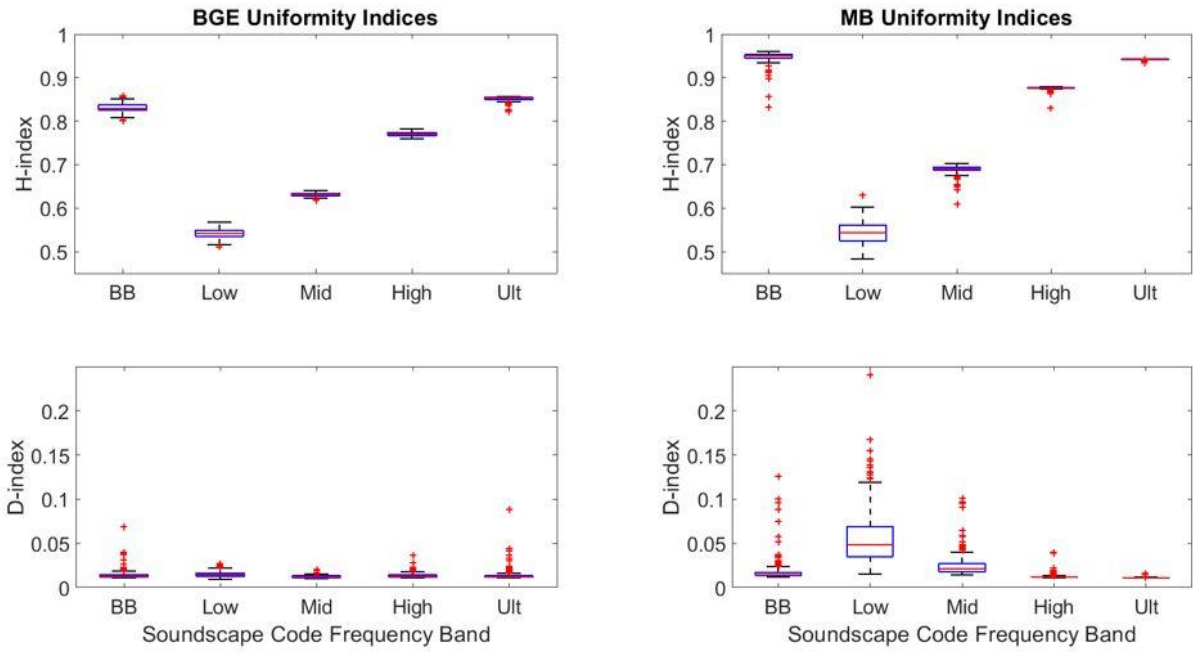

Figure 17 Qualitative comparison (U1) results showing the H-index values for BGE and MB sites and D-index values for BGE and MB sites wherein the boxplots' red horizontal line indicates median value, outer edges of boxes represent 25th and 75th percentiles, whiskers mark the boundary that contains approximately 99% of data values, and the red points are outliers.

Similar analysis carried out on data from the OR and GBR sites yielded slightly different results. In qualitative comparison U2, comparisons of respective uniformity metrics across the sites highlighted differences in acoustic uniformity. D-index values more clearly captured the disparity in acoustic uniformity between OR and GBR especially in the increased size of the boxplots of values at OR in the High and Ultra-High bands (*Figure 18*). H-index values used to compare the acoustically distinct OR and GBR sites failed to reflect the acoustic disparity by producing almost identical soundscape code medians, with only slightly more variability of the 1-minute H-index values reported at OR. Similar to the H-index, the magnitudes of the D-index values at both OR and GBR were only slightly different. The variability measure of the D-index however did reflect the disparity in acoustic uniformity across OR and GBR.

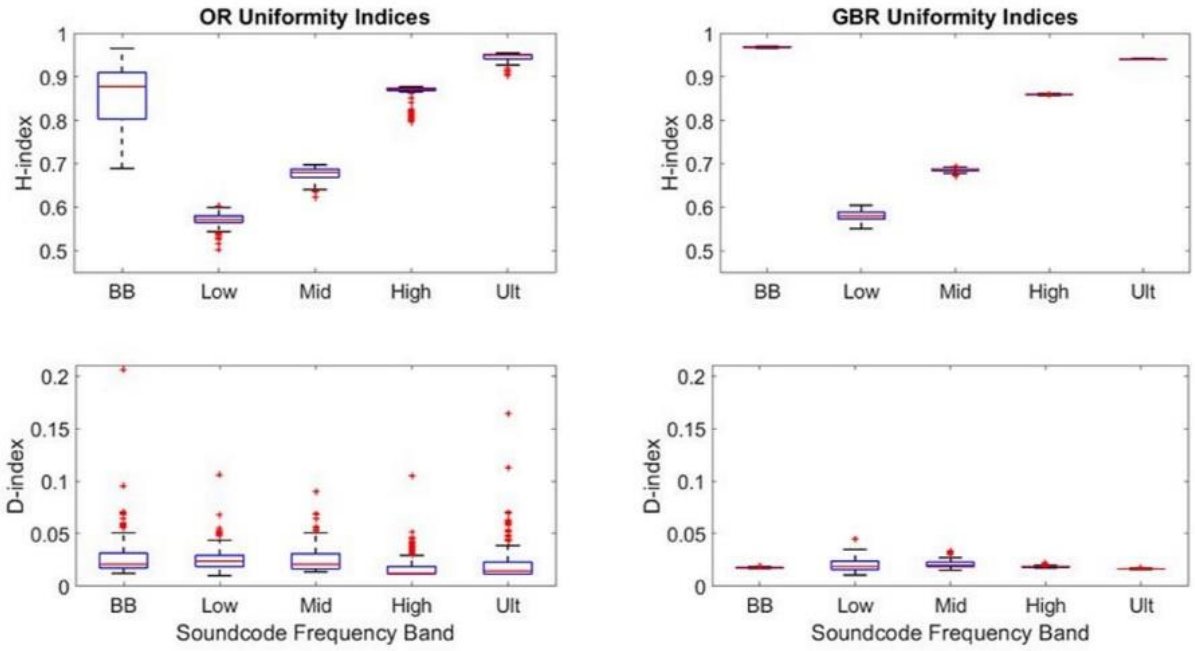

Figure 18 Uniformity comparison (U2) results showing the H-index and D-index values for OR and GBR sites wherein the boxplots' red horizontal line indicates median value, outer edges of boxes represent 25th and 75th percentiles, whiskers mark the boundary that contains approximately 99% of data values, and the red points are outliers.

When metric values were analyzed using 10-minute boxplots over the full OR recording, the increased range of the D-index (indicated by the increased size of the boxplots) suggests the D-index more effectively captured the dynamic nature of the soundscape, while the relatively consistent H-index values suggest little change in acoustic activity (*Figure 19*). The intuitive nature of the D-index, and much closer alignment to salient acoustic activity in the soundscapes of the soundscape code datasets than H-index, suggested D-index was the optimal metric to represent acoustic uniformity in the soundscape code.

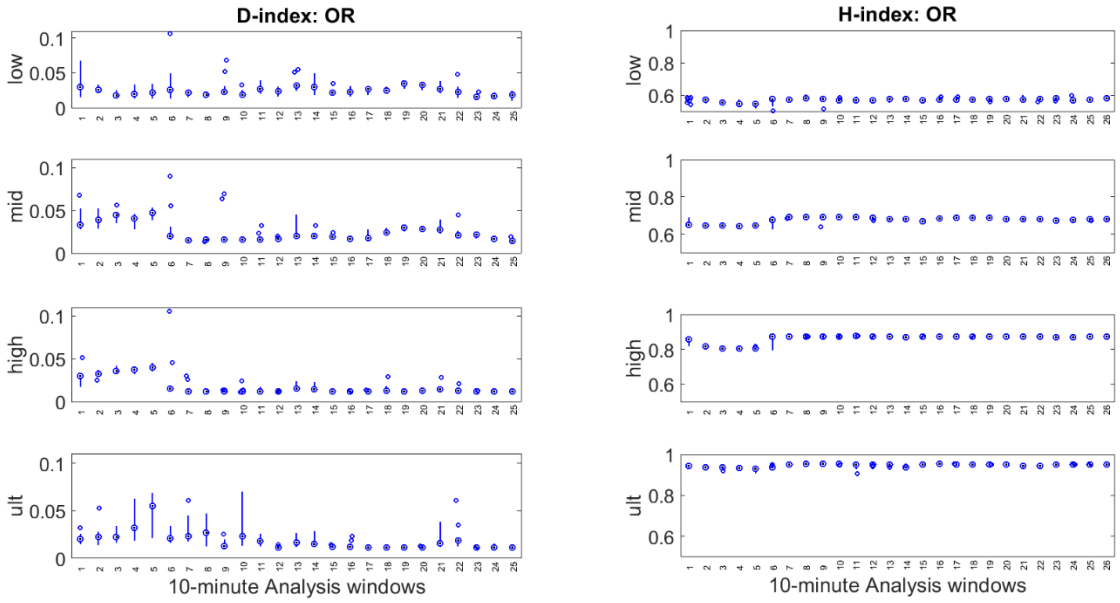

Figure 19 Boxplots of D-index (left) and H-index (right) values at OR. Each box represents the range of metric values in a 10-minute time window comprised of metrics calculated over 1-minute time windows (each boxplot contains 10 metrics values). Circled dots intersecting boxes indicate median values, thick boxes indicate 25th and 75th percentile range, skinny lines indicate range of 99% of data, and blue circles indicate outliers.

Statistical Groupings of Metric Values

MCTs using the rank sum method determined which SSC metrics came from different populations (sites), and results from the tests are presented in the form of connected letters plots. Connected letters plots effectively summarize the MCTs, and show on a SSC frequency band-by-

band basis which sites produce statistically different metrics. Respective to each site, metric values that are not significantly different are connected by identical letters.

In key frequency bands, the uniquely impulsive soundscapes of MB, GBR, and GB4v0 were all found to have kurtosis values that were significantly different than the sites where impulsive signals were either rare or only faint (*Figure 20*).

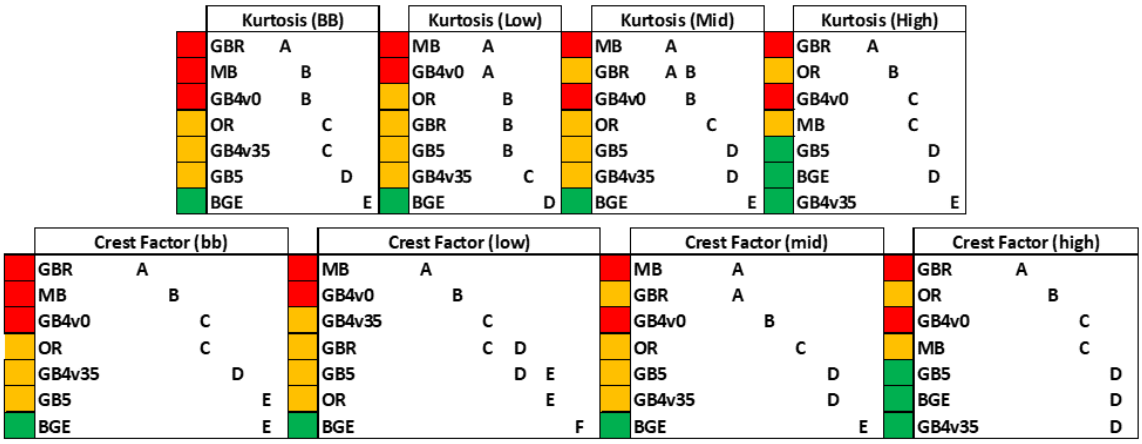

Figure 20 MCT results for (top) kurtosis and (bottom) crest factor. Site designations appear in a column on the left of each panel. Identical letters indicate corresponding sites have metric values that are not significantly different. MCTs were performed on 1-minute metric values observing the soundscape code frequency bands. Color bars represent *a priori* expectations for metric levels where red represents a high-level, yellow represents a mid-level, and green represents a low-level response.

Kurtosis was observed to outperform crest factor in the qualitative comparisons, and MCT results were slightly more favorable for kurtosis than crest factor. Kurtosis values distinguished between OR and the other mostly impulsive sites (GBR, MB, GB4v0), and between BGE and the other sites in key frequency bands, which led to the selection of kurtosis to represent impulsiveness in the soundscape code. Periodicity metrics failed to produce intuitive groupings of the sites in terms of periodic content, but acorr3 was the only metric that produced significantly different values between the highly periodic sites and the moderate-low periodic sites (*Figure 21*).

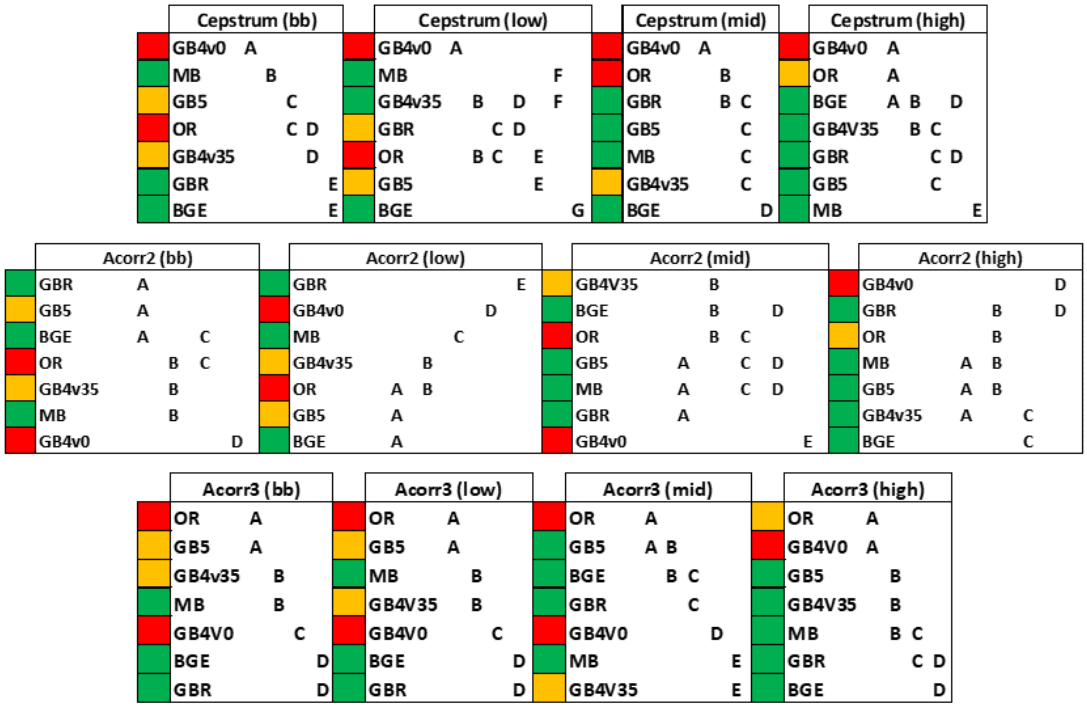

Figure 21 MCT results for (top) cepstrum, (middle) acorr2, and (bottom) acorr3. Site designations appear in a column on the left of each panel. Identical letters indicate corresponding sites have metric values that are not significantly different. MCTs were performed on 1-minute metric values observing the soundscape code frequency bands. Color bars represent *a priori* expectations for metric levels where red represents a high-level, yellow represents a mid-level, and green represents a low-level response.

The characterization of MB as highly periodic by acorr3 is not an ideal response and indicates a problem with either the metric or the definition of periodicity in the project. In spite of less-than-ideal MCT results for acorr3, optimal performance in qualitative comparisons and other analyses made it the only viable choice, and acorr3 was selected as the metric to represent soundscape periodicity. MCT results for the D-index were both adequate and less than ideal, depending on which frequency band was being considered (*Figure 22*).

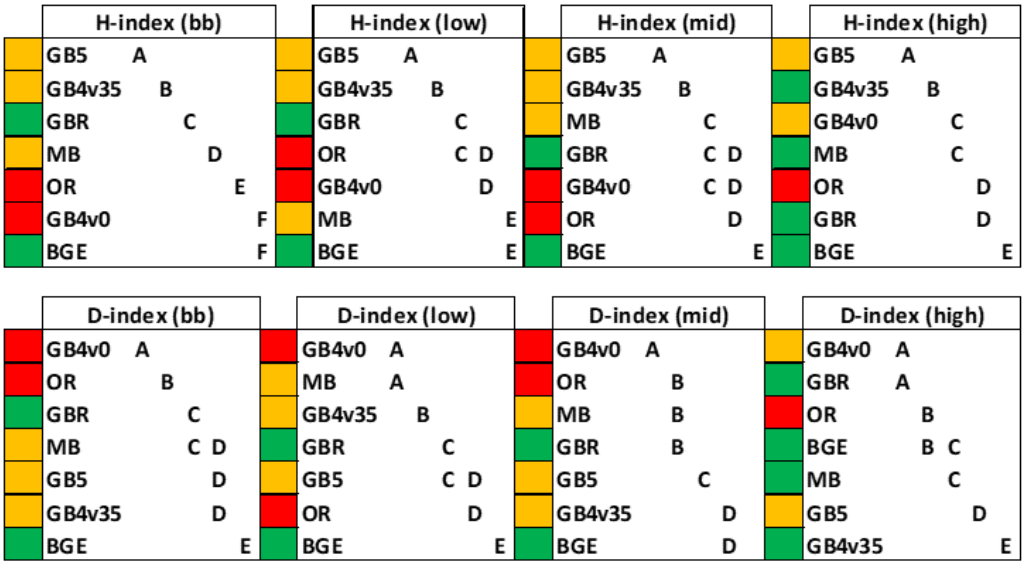

Figure 22 MCT results for (top) H-index and (bottom) D-index. Site designations appear in a column on the left of each panel. Identical letters indicate corresponding sites have metric values that are not significantly different. MCTs were performed on 1-minute metric values observing the soundscape code frequency bands. Color bars represent *a priori* expectations for metric levels where red represents a high-level, yellow represents a mid-level, and green represents a low-level response.

Considering the far more intuitive nature of the D-index and consistently better performance relative to the H-index, D-index was chosen to represent acoustic uniformity in the soundscape code.

Soundscape Code Discussion

A collection of metrics was applied to a series of unique soundscapes to identify the optimal suite of metrics for capturing the salient soundscape characteristics, which ultimately enables quick and simple quantitative comparisons of soundscapes. The final determination considered both the metric efficacy in quantifying the corresponding soundscape property, and how well the metric fit into the infrastructure of the soundscape code. SPL_{rms} and SPL_{pk} (amplitude), kurtosis (impulsiveness), D-index (uniformity), and acorr3 (periodicity) were determined to be the best metrics out of the candidate metrics for comparing soundscapes. Soundscape codes comprised of the optimal metrics indicated dominant signal frequencies and salient differences in acoustic

environments (*Figure 23*). *Figure 23* represents what an initial soundscape assessment using the soundscape code methodology might look like; tabulated soundscape information across frequency bands and metrics offers an initial "glimpse" into a marine acoustic environment and highlights areas of interest for further targeted analysis. The soundscape code is proposed here as a first step in the direction of a standardized soundscape analysis methodology that will ultimately facilitate quantitative comparison and assessment of soundscapes and guide subsequent analysis.

A)

MB	BB		Low		Mid		High		Ult-High	
	med	C95	med	C95	med	C95	med	C95	med	C95
Amplitude	116	10	108	22	110	13	113	2	105	4
	143	21	133	27	140	23	137	21	124	16
Impulsiveness	14	534	72	428	54	1344	4	264	3	5
Uniformity	0.015	0.044	0.048	0.116	0.021	0.047	0.012	0.006	0.011	0.001
Periodicity	1	4	2	4	1	2	0	1	0	0

E)

GB4v35	BB		Low		Mid		High		Ult-High	
	med	C95	med	C95	med	C95	med	C95	med	C95
Amplitude	118	17	116	23	112	21	108	9		
	139	17	137	24	126	21	123	13		
Impulsiveness	6	75	11	112	3	3	3	2		
Uniformity	0.015	0.011	0.028	0.067	0.012	0.01	0.011	0.002		
Periodicity	2	4	2	4	0	4	0	2		

B)

OR	BB		Low		Mid		High		Ult-High	
	med	C95	med	C95	med	C95	med	C95	med	C95
Amplitude	124	29	122	32	113	30	104	26	97	25
	144	28	138	38	129	37	141	28	129	33
Impulsiveness	4	95	4	38	3	39	47	486	12	1249
Uniformity	0.02	0.048	0.023	0.038	0.02	0.04	0.012	0.03	0.014	0.05
Periodicity	0	27	0	27	0	27	1	27	0	41

F)

GB4v0	BB		Low		Mid		High		Ult-High	
	med	C95	med	C95	med	C95	med	C95	med	C95
Amplitude	149	51	149	51	139	52	113	27		
	173	61	172	60	167	65	145	48		
Impulsiveness	51	197	51	140	65	229	105	482		
Uniformity	0.056	0.115	0.073	0.141	0.05	0.116	0.021	0.046		
Periodicity	3	2	3	2	3	4	3	4		

C)

BGE	BB		Low		Mid		High		Ult-High	
	med	C95	med	C95	med	C95	med	C95	med	C95
Amplitude	101	4	98	5	94	5	95	9	84	10
	117	10	111	6	108	7	111	12	109	19
Impulsiveness	3	1	3	2	3	0	3	1	6	51
Uniformity	0.013	0.015	0.014	0.013	0.012	0.005	0.012	0.009	0.012	0.019
Periodicity	0	2	0	2	0	2	0	1	0	1

G)

GB5	BB		Low		Mid		High		Ult-High	
	med	C95	med	C95	med	C95	med	C95	med	C95
Amplitude	113	20	105	20	110	24	107	19		
	127	18	121	22	124	23	122	23		
Impulsiveness	3	32	4	31	3	5	3	4		
Uniformity	0.013	0.045	0.021	0.081	0.013	0.026	0.011	0.009		
Periodicity	0	3	1	6	0	3	0	3		

D)

GBR	BB		Low		Mid		High		Ult-High	
	med	C95	med	C95	med	C95	med	C95	med	C95
Amplitude	116	1	95	10	103	5	113	2	112	1
	156	6	112	19	132	9	153	10	152	7
Impulsiveness	215	420	3	68	33	221	321	1161	195	764
Uniformity	0.017	0.002	0.019	0.022	0.02	0.015	0.018	0.002	0.016	0.001
Periodicity	0	1	0	1	0	1	0	1	0	1

H)

RANGE	BB		Low		Mid		High		Ult-High	
	min	max	min	max	min	max	min	max	min	max
Amplitude	101	149	95	149	94	139	95	113	84	112
	117	173	111	172	108	167	111	153	109	152
Impulsiveness	3	215	3	51	3	65	3	321	3	195
Uniformity	0.013	0.115	0.014	0.073	0.01	0.163	0.011	0.021	0.011	0.016
Periodicity	0	3	0	3	0	3	0	3	0	0

Figure 23 Soundscape code results for the seven soundscape code datasets: (A) MB, (B) OR, (C) BGE, (D) GBR, (E) GB4v35, (F) GB4v0, (G) GB5. Columns indicate the frequency band, and for each band the median (med) and 95% confidence intervals (C95) are reported. Panel (H) reports the minimum and maximum soundscape code median values observed across all sites in corresponding frequency bands. Metrics represented in each row of the soundscape codes are from top to bottom: SPL_{rms}, SPL_{pk}, kurtosis, D-index Index, acorr3. The total range of the soundscape code medians and C95s presented in panel H was divided into quartiles (respectively), and the cell colors correspond to which quartile the value falls into from low (1/4) to high (4/4): blue (1/4), green (2/4), yellow (3/4), red (4/4).

Traditionally, underwater soundscape studies focus mostly on quantifying fluctuations, central tendencies, or minimum/maximum observed levels of amplitude typically represented by sound pressure, intensity, or acoustic energy (*Table 1*). If metrics that quantify aspects of other soundscape properties are included in soundscape analysis, a more thorough assessment of soundscapes is possible. The soundscape properties outlined in (*Table 2*) were quantified by the selected metrics, which allowed comparisons of the soundscape code datasets to be made in terms

of sound amplitude, impulsiveness and transient events, content of repetitive signals, and spectral and temporal variability. For example, in a comparison of the impulsiveness of the soundscape code datasets BGE, GB4v35, and GB5, impulsiveness metric values indicate they are the least impulsive sites of the seven (*Figure 23* C, E, and G respectively*)*. This observation was made quickly and demonstrates the ease with which one can compare and contrast different soundscapes when identical metrics are being compared. This assessment of across site impulsiveness can be taken a step further: The elevated C95 value in the Ultra-High (relative to BB, Low, Mid, and High) band at BGE indicates the presence of acoustically active northern bottlenose whales. At the same time, the median and C95 in the Low bands at GB4v35 and GB5 respectively indicate the presence of chorusing fin whales. Martin *et al.,* (2020) showed that 1-min kurtosis values increased as the amplitude of simulated impulses increased, so the slightly elevated impulsiveness metric values at GB4v35 relative to GB5 could be a manifestation of the higher amplitude of the fin whale chorus at GB4v35, and this coincides with increased SPL_{pk} values at this site. This example highlights how a combination of multidimensional metrics can be used congruently to understand a soundscape and how nuanced differences in the metrics can indicate significant differences in soundscape composition.

The selection of acorr3 as the periodicity metric is a prime candidate for additional assessment and development within the soundscape code structure. It was noticed that acorr3 produced false positives due to noise in the autocorrelation outputs. This was found with all of the candidate periodicity metrics, but in acorr3 it occurred at a much reduced and more manageable manner. In spite of the potential to falsely indicate the presence of periodicities, acorr3 best characterized the soundscape datasets in terms of periodicity, with the exception of MB where the repeated cracking of ice led to a mischaracterization of this site being more periodic than expected.

The candidate metric for uniformity, the H-index, exhibited a strong dependence on the bandwidth of the signal being analyzed, which made within-site comparisons of the H-index across soundscape code frequency bands futile and would severely limit the utility of the uniformity metric in the soundscape code. Furthermore, the observed behavior of the H-index in response to anthropogenic activity is similar to findings in Parks et al. (2014): anthropogenic sounds confounded the metric. At OR and GB4v0, the chaotic and variable sounds of a seismic survey and pile driving drove the H-index down, while the opposite was observed for the D-index. Ship noise at GB4v35 and GB5 had little effect on the H-index but drove D-index values down as biological signals from fin whales were masked. The D-index was found to more closely align with the real-world signals in the soundscape code datasets and consistently reflected the acoustic uniformity of known sound sources in proper frequency bands. D-index demonstrated a sensitivity that allowed it to highlight subtle differences in soundscape composition, and ultimately it was chosen as the metric to represent acoustic uniformity.

Both impulsiveness metrics were closely tied to the content of impulsive signals in the soundscape, but kurtosis outperformed crest factor in meeting *a priori* expectations and produced values that made assessments of impulsiveness easier and quicker. The constrained range of possible crest factor values means the variability it produced when characterizing sites in terms of impulsiveness can be narrow and hard to interpret. The larger range of possible kurtosis values meant it could more dramatically reflect differences in transient or impulsive acoustic activity between sites, which makes rapid assessments more feasible and informative. Analysis of kurtosis time series to explain soundscape code metric values across properties led to a realization that time series analysis of the soundscape code metrics is also an informative method for exploring and assessing acoustic environments with implications for future applications.

CHAPTER 3: Soundscape comparison using the proposed methodology

The second phase of this project focused on quantifying and comparing the marine soundscapes of five recording locations spanning three different ecosystem types related to live hard bottom coral.

Introduction

Five long-term data sets were analyzed to demonstrate the utility of the soundscape code (SSC) and compare acoustic environments. SSCs were generated to compare the soundscapes of a shallow coral reef, two deep cold-water reefs, and two deep sandy-bottom marine environments. Comparing the five soundscapes using the SSC methodology provides a rapid assessment of the soundscapes and guides subsequent analysis by highlighting salient differences in acoustic properties, which are connected to both the function of the environments and transient sound sources.

Deep sea coral habitats are common in the Outer Continental Shelf (OCS) region off the southeastern U.S. within the Exclusive Economic Zone, but few have been mapped or characterized in terms of benthic biology (Reed et al., 2006). Wilmington (WIL), Savannah Deep (SAV), Blake Escarpment (BLE), and Richardson Hills (RH) are sites along the OCS currently being studied by researchers involved with the Atlantic Deep Sea Ecosystem Observatory Network (ADEON) and DEEP Sea Exploration to Advance Research on Coral/Canyon/Cold Seep Habitats (DEEP SEARCH) projects. GBR is the designation for Wheeler Reef, a shallow tropical reef that is part of the Great Barrier Reef chain. The Great Barrier Reef as a whole is one of the largest reef systems of the world, supports billions of dollars of annual revenue for Australia, and provides a range of ecosystem goods and services (McCook et al., 2010; Stoeckl et al., 2011). The five selected sites differ in habitat type, depth, and proximity to the mid-Atlantic coast of the United States.

WIL is located in a region dominated by a single deep-sea coral bioherm. This mound is steep, rugged, and rises 100m above the sea floor and is made up of living and dead coral (Ross, 2006); high abundances of orange cup corals and anemones were observed on the deep submergence vehicle (DSV) Alvin during a DEEP SEARCH cruise aboard the R/V Atlantis (AT41). However, the ADEON lander from which the WIL data was recorded was located on a sandy bottom environment with no sign of coral at least 250 m in all directions.

SAV is a site along a large ridge that makes up part of a larger study area called Stetson Banks, which is made up of complex ledges and slopes (Ross, 2006). This rugged and varied habitat ranges in depth from 550 m-850 m, and the ADEON lander is located at a depth of 790 m. A variety of stony corals, as well as cup corals, soft corals, octocorals, brittle stars, and urchins were found and sampled at SAV on the DEEP SEARCH DSV Alvin dive (AT41) to the region where the lander was deployed, although the lander itself could not be located by the ROV. The sessile invertebrate fauna is more diverse in the Stetson Banks region than the communities observed at several North Carolina bioherms, and an abundance of sponges with 18 different taxa have also been observed here (Reed et al., 2006).

RH is a site located in the Richardson Hills Complex, which overlaps with the region described previously in literature as Stetson Banks. The RH lander was located within 20 nautical miles of the SAV lander, but recordings were made during different time periods. The RH habitat features an abundance of living and dead coral species, urchins, fish, and sponges, which were all observed during a recent DEEPSEARCH dive to this site (RB1903).

BLE is the deepest site, located furthest offshore, and is primarily a sandy bottom habitat (*Figure 24*).

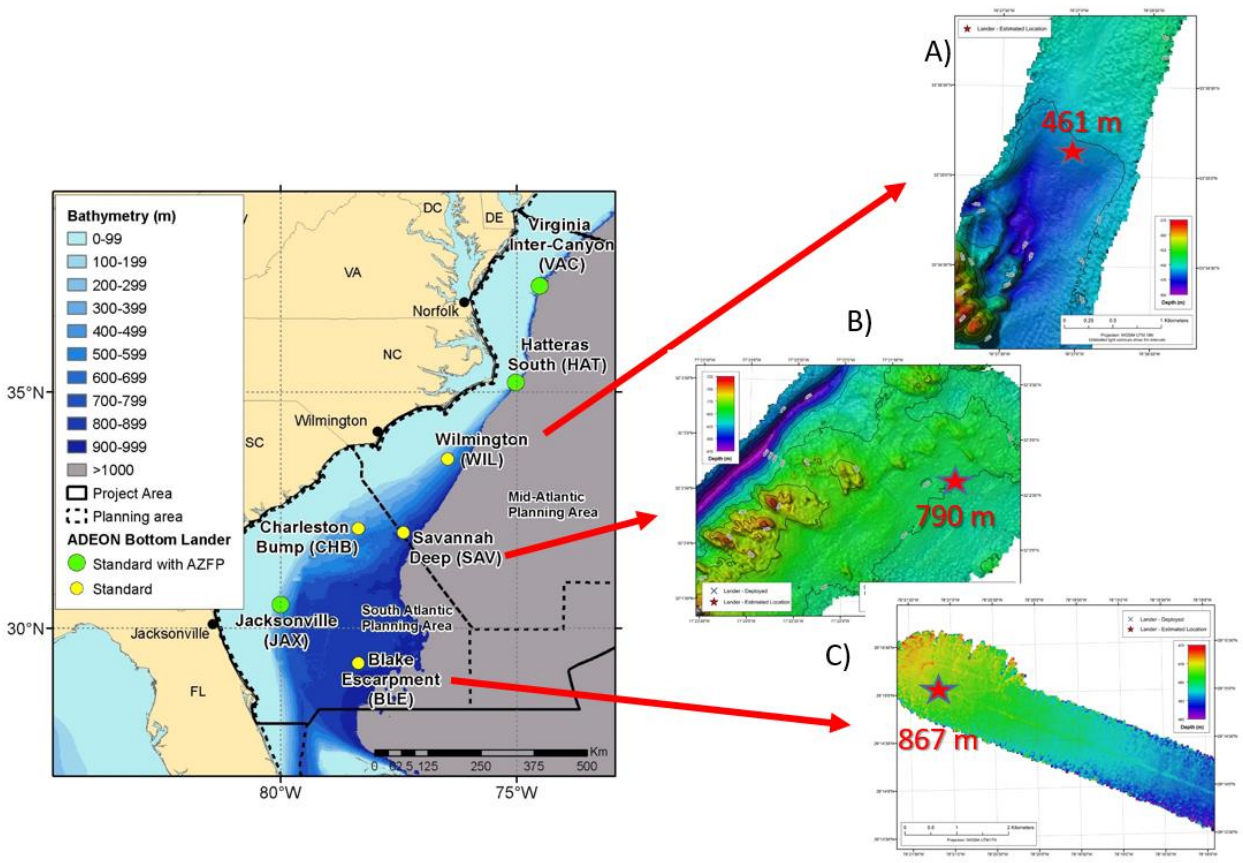

Figure 24 ADEON lander locations and bathymetry for (A) WIL, (B) SAV and (C) BLE. RH lander location in close proximity to the SAV lander, but is not indicated on this figure.

A specific coral community located in the Great Barrier Reef (GBR) region was chosen as a type of control for the thesis as it has been well-studied in this past. At this particular coral community, an abundance and diversity of corals, fish, and invertebrates have been observed (Graham *et al*. 2014). Unlike SAV, RH, and GBR, BLE and WIL do not feature any coral and are soft sediment habitats (*Figure 25*).

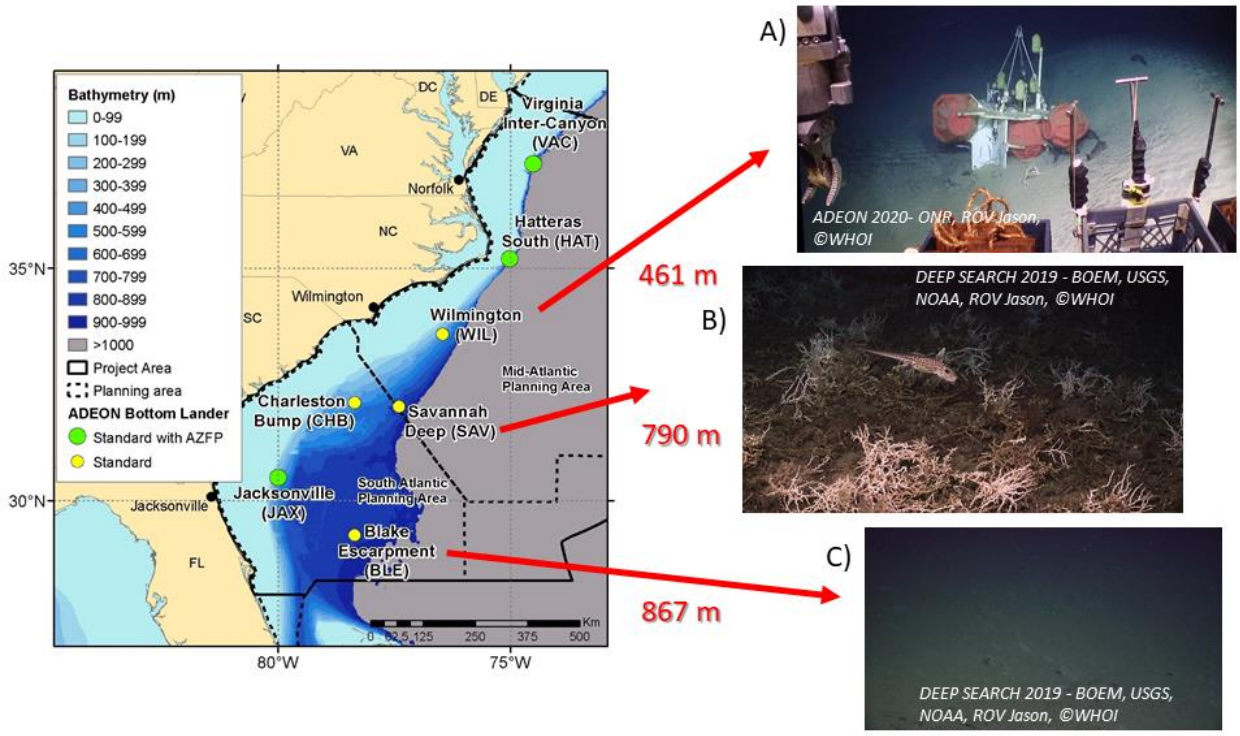

Figure 25 ADEON lander locations and site images captured by ROVs on research dives to (A) Wilmington, (B) Savannah Deep and (C) Blake Escarpment.

These sites were expected to offer interesting comparisons as disparities in depth and bottom type, specifically coral and soft sediment, were hypothesized to have an impact on the respective soundscapes.

Methodologies

A winter period consisting of the months December through February 2017 was chosen for analysis of the WIL, SAV, and BLE sites. This three-month period consists of about 6170 minutes of passive acoustic data per site sampled at 375 kHz. Data from the Richardson Hills site was recorded on an icListen Smart Hydrophone (Ocean Sonics, Truro Heights, NS, Canada) between April 14th, 2019 and June 20th, 2019 and consist of about 3220 minutes of passive acoustic data sampled at 126 kHz. Data from the Great Barrier Reef site was recorded on an AMAR G3 recorder (JASCO Applied Sciences, Dartmouth, NS, Canada) between April 27th, 2013 and May 31st, 2013 and consist of about 6480 minutes of passive acoustic data. (*Table 5*).

Table 5 Long-term dataset information and data collection parameters

Data set	Ecosystem Type	Latitude (° North)	Longitude (° East)	Depth (meters)	Sample Rate (kHz)	Duration (min)	Duty cycle (min)
Wilmington (WIL)	Deep, Sandy	33.6	-76.4	461	375	6171	1/20
Savannah Deep (SAV)	Deep, Coral	32	-77.3	790	375	6171	1/20
Blake Escarpment (BLE)	Deep, Sandy	29.2	-78.3	872	375	6170	1/20
Richardson Hills (RH)	Deep, Coral	31.89	-77.35	700	128	3222	1/30
Great Barrier Reef (GBR)	Shallow, Coral	147.52	-18.8	18	375	6486	1/20

One-minute SSC metrics were calculated over the acoustic recordings that had been converted into pressure time series. SSCs calculated by reporting the median (med) and central 95th percentage (C95) of the 1-minute SSC metrics were used to compare the SSC properties for each soundscape to highlight potential differences in the acoustic environments. To explore how different time periods of analysis might impact SSC values and interpretation as more and more data are factored into integration and averaging, SSCs were generated over several different durations of data: monthly, weekly, daily. The variability and medians of values generated by calculating the SSC over different analysis windows were considered to understand how different durations of data might impact a comparison of soundscapes using the SSC methodology. To condense and numerically present the results from the assessment of how analysis window impacted the comparative soundscape assessment of the five sites, the SSC color coding scheme was quantified. The color coding employed by the SSC shows which quartile the corresponding metric value (median or C95) falls into. The first quartile was assigned a value of 1, the second quartile a value of 2, the third a value of 3, and the fourth a value of 4. This was done to form a difference table from the changes in quartile of the metrics that occurred over different time windows. Differences were calculated over the three analysis periods (week, month, day), and

summed across SSC frequency bands to produce a total metric difference value and compare how consistent SSC interpretations were in a process highlighted in (*Figure 26*).

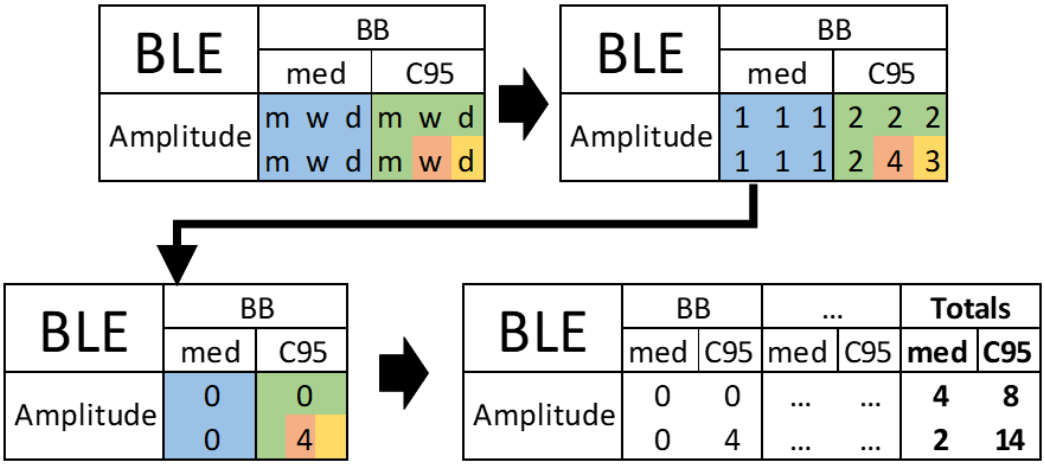

Figure 26 Example of process by which change in SSC interpretation was quantified shown for BLE BB amplitude metrics only. Black arrows indicate the flow of the procedure. Upper left box shows condensed SSC color code information where m, w, and d represent the month, week, and day SSCs and the color shows which quartile the corresponding metric fell into. Upper right box shows how the quartiles were quantified. Lower left shows the difference value found by summing the differences between the month and week, month and day, and week and day quartile values. Lower left shows the BB difference values and totals for BLE amplitude metrics. Totals calculated by summing differences across frequency bands for each metric.

In response to the disparity in volume of data across sites, the 1-month SSC is the focus of the assessment, although as previously stated, the other analysis periods are considered to better understand how different analysis periods might impact interpretation. The SSC methodology was applied to the five soundscapes to quickly assess salient differences in acoustic environments and highlight avenues for subsequent analysis.

Results

Results from the application of the SSC methodology to the soundscapes of BLE, SAV, WIL, RH, and GBR are accompanied by corresponding assessments and comparisons. The SSC methodology is something that was proposed for use in a variety of situations including use over variable analysis periods. To demonstrate how interpretation of the SSC might change over different analysis periods, SSC metrics were calculated over a monthly, weekly, and daily time

window. The differences in metric quartiles across analysis periods represents an aspect of the soundscape variability and shows which sites are most likely to have a SSC that changes over analysis period (*Figure 27*).

BLE	BB		Low		Mid		High		Ult		**Totals**	
	med	C95	med	C95	med	C95	med	C95	med	C95	**med**	**C95**
Amplitude	0	0	0	0	2	2	2	6	0	0	**4**	**8**
	0	4	0	6	2	0	0	4	0	0	**2**	**14**
Impulsiveness	0	0	0	0	0	0	0	0	0	4	**0**	**4**
Uniformity	2	2	0	0	6	0	0	2	2	4	**10**	**8**
Periodicity	0	0	0	0	0	2	0	0	0	2	**0**	**4**

RH	BB		Low		Mid		High		Ult		**Totals**	
	med	C95	med	C95	med	C95	med	C95	med	C95	**med**	**C95**
Amplitude	4	6	2	4	2	6	4	6	0	4	**12**	**26**
	0	6	2	4	4	6	2	6	0	2	**8**	**24**
Impulsiveness	0	6	0	4	0	6	0	2	0	6	**0**	**24**
Uniformity	0	6	4	0	0	6	0	2	0	6	**4**	**20**
Periodicity	0	0	0	0	0	4	0	6	0	4	**0**	**14**

SAV	BB		Low		Mid		High		Ult		**Totals**	
	med	C95	med	C95	med	C95	med	C95	med	C95	**med**	**C95**
Amplitude	0	2	4	4	6	0	0	0	0	6	**10**	**12**
	0	4	4	6	2	4	0	4	0	2	**6**	**20**
Impulsiveness	0	0	0	0	0	0	0	0	0	0	**0**	**0**
Uniformity	6	0	2	4	2	0	2	0	2	2	**14**	**6**
Periodicity	0	0	0	0	0	2	0	2	0	0	**0**	**4**

GBR	BB		Low		Mid		High		Ult		**Totals**	
	med	C95	med	C95	med	C95	med	C95	med	C95	**med**	**C95**
Amplitude	0	0	0	0	0	0	0	0	0	4	**0**	**4**
	0	0	0	0	0	0	0	0	0	0	**0**	**0**
Impulsiveness	0	4	0	0	0	0	0	0	0	6	**0**	**10**
Uniformity	0	0	4	0	0	0	0	0	0	0	**4**	**0**
Periodicity	0	0	0	0	0	0	0	2	0	0	**0**	**2**

WIL	BB		Low		Mid		High		Ult		**Totals**	
	med	C95	med	C95	med	C95	med	C95	med	C95	**med**	**C95**
Amplitude	0	2	0	2	4	4	2	2	0	6	**6**	**16**
	0	4	6	4	2	6	0	4	0	2	**8**	**20**
Impulsiveness	0	0	0	0	0	0	0	0	0	0	**0**	**0**
Uniformity	6	0	0	0	2	2	0	4	2	2	**10**	**8**
Periodicity	0	0	0	2	0	2	0	4	0	0	**0**	**8**

Figure 27 Numerical differences in SSC metric quartiles across month, week, and day analysis periods. Metric differences are calculated for the median and C95s, and then summed across frequency bands. Total difference values are shown in far right column of each box.

The values in the totals column in Figure 27 align closely with the variability of the SSC metrics observed in the 1-month SSCs for the 5 sites. GBR is the most consistent site and metric quartiles change very little across analysis periods at GBR. Following GBR in order of consistency are BLE, WIL, SAV and RH. Most change in quartiles is observed in the C95. More changes were observed in metric quartiles for uniformity medians at BLE, SAV, and WIL, while at RH more changes in median quartiles were observed in amplitude metrics. The C95 quartiles changed far more at RH than at the other sites. The analysis of how a comparative assessment might change at the sites across analysis periods helps to understand one aspect of the SSC methodology and the soundscapes. The SSCs themselves, especially the 1-month SSC (*Figure 28*), provide a wealth of information about the soundscapes and produce results that set the stage for subsequent analysis.

BLE	BB		Low		Mid		High		Ult-High	
	med	C95	med	C95	med	C95	med	C95	med	C95
Amplitude	103	16	101	17	92	18	93	23	89	7
	118	26	114	18	107	21	108	27	106	34
Impulsiveness	3	14	3	3	3	6	3	17	3	875
Uniformity	0.015	0.045	0.023	0.03	0.018	0.046	0.012	0.016	0.013	0.038
Periodicity	0	3	0	3	0	12	0	1	0	2

RH	BB		Low		Mid		High		Ult-High	
	med	C95	med	C95	med	C95	med	C95	med	C95
Amplitude	100	32	94	34	94	26	94	27	87	14
	118	39	110	41	111	36	111	36	108	38
Impulsiveness	3	964	3	153	3	188	3	506	3	1546
Uniformity	0.015	0.078	0.025	0.091	0.015	0.095	0.011	0.034	0.012	0.044
Periodicity	0	5	0	5	0	11	0	3	0	2

SAV	BB		Low		Mid		High		Ult-High	
	med	C95	med	C95	med	C95	med	C95	med	C95
Amplitude	102	24	94	30	97	24	97	23	90	6
	118	26	109	34	111	27	112	23	108	21
Impulsiveness	3	17	3	20	3	25	3	1	3	5
Uniformity	0.016	0.055	0.028	0.078	0.017	0.094	0.012	0.018	0.012	0.029
Periodicity	0	16	0	15	0	21	0	0	0	1

GBR	BB		Low		Mid		High		Ult-High	
	med	C95	med	C95	med	C95	med	C95	med	C95
Amplitude	116	6	73	6	84	5	107	6	115	7
	160	12	98	16	118	16	146	9	159	13
Impulsiveness	585	2532	21	217	102	1307	334	1168	585	2532
Uniformity	0.017	0.003	0.015	0.018	0.014	0.005	0.017	0.003	0.016	0.003
Periodicity	0	1	0	2	0	2	0	1	0	1

WIL	BB		Low		Mid		High		Ult-High	
	med	C95	med	C95	med	C95	med	C95	med	C95
Amplitude	103	18	98	23	96	20	98	19	92	8
	120	25	112	24	110	21	113	19	113	30
Impulsiveness	3	10	3	4	3	4	3	2	3	366
Uniformity	0.015	0.046	0.03	0.053	0.014	0.054	0.012	0.012	0.013	0.028
Periodicity	0	9	0	9	0	7	0	0	0	1

RANGE	BB		Low		Mid		High		Ult-High	
	min	max	min	max	min	max	min	max	min	max
Amplitude	100	116	73	101	84	97	93	107	87	115
	118	160	98	114	107	118	108	146	106	159
Impulsiveness	3	585	3	21	3	102	3	334	3	585
Uniformity	0.015	0.017	0.015	0.03	0.014	0.018	0.011	0.017	0.012	0.016
Periodicity	0	0	0	0	0	0	0	0	0	0

Figure 28 One-month soundscape codes for the deep/shallow, coral/sandy bottom sites analyzed. The ranges reported in the lower right panel indicate the range of 1-month SSC medians. The total range of the SSC medians and C95s was divided into quartiles, and the cell colors correspond to which quartile the value falls into from low to high: blue, green, yellow, red.

GBR amplitude metrics are much larger in frequencies over 1 kHz than in frequencies under 1 kHz. The GBR amplitude metrics are also much larger in the BB, High, and Ultra-High bands than the OCS sites, which suggests GBR is driven by acoustic activity in the High and Ultra-High bands. This differs from what was observed in the OCS sites, which appear to be driven by acoustic activity in the Low, Mid, and High bands. All OCS site BB amplitude metric medians are within 3 dB of each other (across site), but nuanced differences in the amplitude metric medians across frequency bands (within site) suggest fundamental soundscape differences. At SAV, WIL, and RH the respective 1-month SSC SPL_{rms} medians in the Low, Mid, and High bands are within 3 dB of each other and are between 4 dB and 7 dB larger than median SPL_{rms} values in the Ultra-High band. This trend of amplitude metric dominance in the Low, Mid, and High bands varies slightly across analysis periods at SAV with the weekly SSC reporting SPL_{rms} medians of 90 dB for both Low and Ultra-High bands (*Figure 29*).

BLE	BB		Low		Mid		High		Ult-High	
	med	C95	med	C95	med	C95	med	C95	med	C95
Amplitude	102	14	100	15	90	17	92	17	89	5
	117	25	113	15	105	18	107	19	105	32
Impulsiveness	3	18	3	0	3	7	3	14	3	1108
Uniformity	0.015	0.045	0.022	0.024	0.018	0.048	0.012	0.015	0.013	0.048
Periodicity	0	2	0	1	0	6	0	1	0	2

RH	BB		Low		Mid		High		Ult-High	
	med	C95	med	C95	med	C95	med	C95	med	C95
Amplitude	101	19	94	19	96	26	97	27	89	12
	119	24	111	25	113	29	113	30	108	28
Impulsiveness	3	90	3	102	3	239	3	463	3	149
Uniformity	0.013	0.07	0.024	0.081	0.013	0.12	0.011	0.066	0.011	0.023
Periodicity	0	5	0	5	0	25	0	6	0	1

SAV	BB		Low		Mid		High		Ult-High	
	med	C95	med	C95	med	C95	med	C95	med	C95
Amplitude	100	23	90	26	95	26	95	26	90	14
	116	26	105	29	109	28	110	27	108	24
Impulsiveness	3	24	3	18	3	27	3	1	3	50
Uniformity	0.016	0.084	0.03	0.091	0.018	0.112	0.012	0.027	0.013	0.091
Periodicity	0	18	0	16	0	21	0	1	0	1

GBR	BB		Low		Mid		High		Ult-High	
	med	C95	med	C95	med	C95	med	C95	med	C95
Amplitude	117	6	73	5	84	4	108	6	116	6
	160	10	99	15	118	15	147	8	159	10
Impulsiveness	562	1794	22	208	111	1265	326	1118	562	1794
Uniformity	0.017	0.002	0.015	0.019	0.014	0.005	0.017	0.003	0.016	0.002
Periodicity	0	1	0	2	0	2	0	1	0	1

WIL	BB		Low		Mid		High		Ult-High	
	med	C95	med	C95	med	C95	med	C95	med	C95
Amplitude	104	19	100	21	95	20	97	20	92	13
	120	24	114	23	110	25	113	26	112	29
Impulsiveness	3	25	3	6	3	26	3	11	3	367
Uniformity	0.017	0.06	0.035	0.05	0.015	0.074	0.012	0.026	0.013	0.045
Periodicity	0	5	0	6	0	6	0	1	0	1

RANGE	BB		Low		Mid		High		Ult-High	
	min	max	min	max	min	max	min	max	min	max
Amplitude	100	117	73	100	84	96	92	108	89	116
	116	160	99	114	105	118	107	147	105	159
Impulsiveness	3	562	3	22	3	111	3	326	3	562
Uniformity	0.013	0.017	0.015	0.035	0.013	0.018	0.011	0.017	0.011	0.016
Periodicity	0	0	0	0	0	0	0	0	0	0

Figure 29 One-week soundscape codes for the deep/shallow, coral/sandy bottom sites analyzed. The ranges reported in the lower right panel indicate the range of 1-month SSC medians. The total range of the SSC medians and C95s was divided into quadrants, and the cell colors correspond to which quadrant the value falls into from low to high: blue, green, yellow, red.

At BLE, the 1-month SSC Low band amplitude metrics (both SPL_{rms} and SPL_{pk}) are substantially larger than the Mid, High, and Ultra-High bands, which are all within 4 dB of each other (*Figure 28*). The dominance of the Low band amplitude metrics at BLE is consistent across SSC analysis windows, and draws a contrast to the other OCS sites, which vary slightly across analysis windows, and in terms of SPL_{pk} do not exhibit any clear frequency-related amplitude metric trends like BLE does.

The 1-month GBR SSC reports the smallest variability of amplitude metrics in almost all frequency bands, and RH reports the largest variability of amplitude metrics in all frequency bands. Variability of BLE, SAV, and WIL amplitude metrics was considerably different across frequency band, site, and SSC analysis period, although the 1-month SSC reported an interesting similarity between GBR and BLE, SAV, and WIL. In the Ultra-High band, 1-month SSCs corresponding to GBR, BLE, SAV, and WIL all report SPL_{rms} variability within 2 dB of each other (across site), although the variability of the SPL_{pk} metric indicates there are substantial differences in the maximum sound levels that occur among these sites, especially in the Ultra-High band.

GBR is also the most impulsive site, which is identified by the largest impulsiveness metric medians and variability, and are consistent across the SSC analysis periods. The remaining sites all report identical impulsiveness metric medians, so the variability was used to assess soundscape impulsiveness. RH is the only site to report a larger kurtosis range than GBR, and this occurs only on the randomly selected 1-day SSC analysis period in the Ultra-High band (*Figure 30).*

BLE	BB		Low		Mid		High		Ult-High	
	med	C95	med	C95	med	C95	med	C95	med	C95
Amplitude	101	14	99	15	90	11	92	4	89	2
	117	21	112	16	105	16	107	6	105	31
Impulsiveness	3	9	3	0	3	0	3	0	3	845
Uniformity	0.014	0.036	0.023	0.019	0.016	0.034	0.012	0.009	0.013	0.032
Periodicity	0	0	0	0	0	1	0	0	0	2

RH	BB		Low		Mid		High		Ult-High	
	med	C95	med	C95	med	C95	med	C95	med	C95
AMP	105	8	95	14	100	8	102	8	92	4
	120	19	112	20	114	13	116	8	108	28
IMP	3	3325	3	41	3	2	3	0	3	15786
UNI	0.012	0.007	0.022	0.092	0.012	0.053	0.011	0.025	0.011	0.051
PER	0	2	0	2	0	36	0	0	0	1

SAV	BB		Low		Mid		High		Ult-High	
	med	C95	med	C95	med	C95	med	C95	med	C95
Amplitude	91	13	86	16	81	18	83	16	88	6
	112	26	100	16	98	19	100	22	108	27
Impulsiveness	3	10	3	13	3	28	3	1	3	46
Uniformity	0.017	0.067	0.028	0.042	0.03	0.079	0.014	0.021	0.012	0.077
Periodicity	0	18	0	16	0	22	0	1	0	1

GBR	BB		Low		Mid		High		Ult-High	
	med	C95	med	C95	med	C95	med	C95	med	C95
AMP	116	5	73	5	84	4	108	5	116	5
	160	10	98	15	118	15	146	8	159	10
IMP	571	1603	27	236	116	1303	321	1060	571	1603
UNI	0.017	0.004	0.016	0.023	0.014	0.005	0.017	0.004	0.016	0.004
PER	0	1	0	2	0	2	0	1	0	1

WIL	BB		Low		Mid		High		Ult-High	
	med	C95	med	C95	med	C95	med	C95	med	C95
Amplitude	99	22	98	26	87	21	89	16	89	3
	122	29	113	25	107	26	108	31	109	34
Impulsiveness	3	43	3	7	3	31	3	67	3	725
Uniformity	0.018	0.049	0.038	0.051	0.021	0.084	0.012	0.038	0.013	0.038
Periodicity	0	5	0	5	0	11	0	2	0	1

RANGE	BB		Low		Mid		High		Ult-High	
	min	max	min	max	min	max	min	max	min	max
Amplitude	91	116	73	99	81	100	83	108	88	116
	112	160	98	113	98	118	100	146	105	159
Impulsiveness	3	571	3	27	3	116	3	321	3	571
Uniformity	0.012	0.018	0.016	0.038	0.012	0.03	0.011	0.017	0.011	0.016
Periodicity	0	0	0	0	0	0	0	0	0	0

Figure 30 One-day soundscape codes for the deep/shallow, coral/sandy bottom sites analyzed. The ranges reported in the lower right panel indicate the range of 1-month SSC medians. The total range of the SSC medians and C95s was divided into quadrants, and the cell colors correspond to which quadrant the value falls into from low to high: blue, green, yellow, red.

For the monthly analysis period, RH remains the second most impulsive site and does not surpass GBR. WIL and BLE report large (kurtosis > 350) impulsiveness values in the Ultra-High band consistently across SSC analysis periods, while the largest variability measure for 1-minute kurtosis at SAV is 50 and occurs in the Ultra-High band for the weekly SSC analysis period (*Figure 29*). This suggests that BLE and WIL were being influenced by some impulsive acoustic activity in the Ultra-High bands while SAV appears to be influenced by broadband transient acoustic activity. The 1-month analysis period BB kurtosis variability at SAV is the largest of these three sites, followed by BLE.

The dominant acoustic activity at GBR is not periodic in nature, as the periodicity values for GBR are the lowest of all the sites, even across analysis periods. Periodic signals appear to be well-represented in the OCS sites, as all the sites report considerable variability in periodicity metric values in a variety of frequency bands. At SAV, this trend is most obvious, and the variability of periodicity metric values in the Broadband, Low, and Mid bands is the highest out of all the sites, even across analysis periods. 1-month periodicity metric ranges suggest some periodic sound component is present and influential at SAV and WIL, and that in general that periodic signals influence the soundscapes of the OCS sites. The SSCs also suggest that among the OCS sites, there is a disparity in the content of periodic signals. Based on SSCs corresponding to the 1-month analysis period, SAV is the most periodic of the five sites, followed by RH, WIL, BLE, and GBR.

Assessments of uniformity based on the D-index values need to consider both the median D-index value and the C95 which quantifies the variability of the metric over the analysis period. The median values of the D-index at GBR report that out of all the sites, the minute-to-minute changes in acoustic activity are greatest at this location in the Broadband, High, and Ultra-High frequency bands. However, the C95 of the D-index values at GBR are substantially lower than the other sites. Instead of a conflicting assessment, the reality is that the median and the C95 of the D-index are capturing and reporting different aspects of what has been defined in this project as acoustic uniformity. The relatively miniscule C95 of almost all metrics at GBR describes the low variability of the soundscape, while the median D-index values appear to describe the chaotic nature of the acoustic activity in frequencies above 1 kHz. While the minute-to-minute changes at GBR are greater than at the other sites in the Broadband, High, and Ultra-High bands, the consistency with which these changes occur makes the site acoustically uniform. RH reports the

largest ranges in the D-index but also mostly the smallest medians. This suggests that at RH there are more transient events that shift the D-index to values higher than the other sites, but not enough to result in a larger median. SAV D-index ranges are mostly the second largest behind RH, and while the median D-index values at SAV are never the largest among the sites, they come close (within D = 0.002) and no other site produces a combination of high D-index medians and C95s like SAV does in the Broadband, Low, and Mid bands. The broadband D-index medians and ranges suggest WIL and BLE are the most uniform behind GBR. However, WIL reports the highest median of the five sites in the Low band along with low-moderate variability (0.056), and BLE reports the highest median in the Mid band also accompanied by low-moderate variability (0.046). BLE also reports the second highest D-index C95 in the Ultra-High band (0.038). D-index results for BLE, SAV, and WIL are similar, but there are nuanced differences in where the dynamic acoustic activity occurs in frequency space, which suggests differences in respective soundscapes. D-index medians were mostly consistent across analysis windows, but in some cases, considerable differences were observed. The C95s of the D-index varied dramatically across analysis windows, which was expected.

In summary, the tropical, shallow GBR soundscape generated a SSC remarkably different from the other sites in terms of all soundscape code properties. The GBR soundscape is far more consistent than the OCS sites, which is most clearly reflected in the narrow range of the SSC metrics calculated over the 1-month analysis period. The high median amplitude, impulsiveness, and uniformity metric values in the High and Ultra-High bands suggest that GBR is dominated by acoustic activity in the higher frequencies (>1 kHz). In comparison, SSCs corresponding to SAV, WIL, and BLE suggest that dominant acoustic activity is in the mostly lower frequencies (Low, Mid, and High bands), with a nuanced OCS SSC comparison suggesting BLE is dominated by

activity in the Low band. RH is intermediate in its characteristics between GBR and the other OCS sites. Large impulsiveness ranges in all frequency bands, and large amplitude ranges in frequencies over 1 kHz suggest RH is more similar to GBR, but large periodicity and uniformity metric ranges, and large amplitude metric medians in frequencies under 1 kHz suggest RH is more like the OCS soundscapes. Periodicity appears to be a distinguishing feature of the OCS sites, and a disparity among the OCS sites in terms of periodicity suggests some fundamental difference in the respective soundscapes.

Soundscape Code comparison discussion

The five sites were chosen to see if the soundscape code metrics would distinguish between the respective soundscapes knowing that disparities in depth and presence of coral could manifest acoustically. The SSC showed clear distinctions between the shallow coral environment of GBR, and the deeper OCS sites, and nuanced differences among the OCS SSCs suggest potentially fundamental soundscape differences among the deep ocean soundscapes. The results from the comparison of the five sites using the soundscape code assessment methodology provide many avenues for subsequent analysis. SSC results for the OCS sites also provide a cursory soundscape assessment of the deep ocean sites, which helps to establish a baseline for the acoustic environments.

In general, the shallow reef soundscape of GBR was louder in frequencies over 1 kHz, while the deep-water OCS sites were louder in frequencies under 1 kHz, with some overlap occurring between several of the OCS sites and GBR in the High band. The comparison of amplitude properties of GBR and the OCS sites appears to distinguish between the deep and shallow soundscapes. This is probably due to attenuation of low frequency sound in shallow water, which acts as a sort of high-pass filter and would explain why the deeper OCS sites report larger

amplitude medians in the Low and Mid bands relative to the shallow GBR site (Hermannsen et al., 2015; Urick, 1983). Nuanced differences in amplitude metrics among the deep ocean sites could represent a connection between the deep and shallow coral environments, and also suggest the soundscapes of the OCS sites are unique. SAV and RH both have the largest broadband amplitude metric ranges, which are influenced at SAV by acoustic activity in the Low, Mid, and High bands, and at RH by acoustic activity in the Low, Mid, High, and Ultra-High bands. Healthier reefs in shallow water were found to be significantly louder than degraded environments (Piercy et al., 2014), and if the increased amplitude of SAV and RH is connected to the content of coral at these sites, it represents a significant finding that can be explored in future work. BLE also exhibited slightly different amplitude properties than the other OCS sites, and this could be connected to a fundamental soundscape difference.

Soundscape impulsiveness drew stark contrasts between the deep and shallow ocean soundscapes. GBR reported high medians and variability, while the deep ocean sites all reported medians of 3, and considerable variability among sites and frequency bands. While impulsive acoustic activity at all OCS sites was so infrequent that the kurtosis medians in the SSCs were all 3, the variability of kurtosis at the deep ocean sites indicated differences in soundscape impulsiveness. The greatly increased range in impulsiveness metric values at RH sets it apart from the other OCS sites, but does not necessarily suggest it is similar to GBR, but rather that it is intermediate in its characteristics. All OCS SSCs reported varying levels of impulsiveness, and due to the connection between increased transient events and coral reef health in shallow water (Piercy et al., 2014), the sound sources responsible for the increased kurtosis values at the OCS sites should be explored. The OCS sites exhibit unique impulsiveness characteristics and

determining the nature of the signals that are responsible could illuminate important soundscape and habitat relationships in deep ocean environments.

The disparity in amplitude and impulsiveness metrics between the deep and shallow soundscapes was most obvious, but influence by periodic signals also appears to suggest a difference in the soundscapes. Periodicity metrics report substantial values in different frequency bands at the OCS sites, which could be a result of acoustically active marine life that inhabit or are transient to these deep ocean environments. A concentration of marine life could indicate the presence of a healthy deep ocean OCS community. The periodicity values of the OCS sites provide an interesting comparison between the soundscapes, and two of the OCS sites (SAV and WIL) produce SSCs that indicate substantial influence by periodic signals, which could be a distinguishing soundscape feature. To understand the nature of the increased periodicity of the OCS sites and nuanced differences among them, the sound sources responsible for the periodicity values would have to be determined.

The median D-index values at the OCS sites are similar in magnitude, which suggests the minute-to-minute changes in acoustic activity at these sites are typically similar. However, the disparity in D-index ranges at these sites suggest a difference in soundscape. SAV and RH both have the largest broadband uniformity index ranges, but the magnitude of the D-index ranges for WIL and BLE are so high that without knowing more about the responsible sound sources, it is difficult to understand what this disparity in uniformity metric value represents. If D-index values are directly related to biologic acoustic activity, then increased D-index ranges at RH and SAV might suggest that these sites are more biologically active than WIL and BLE, although how this translates to bottom type, habitat, or presence of coral is unknown.

In summary, the most obvious differences in respective SSCs group all the deep ocean soundscapes in one group and the shallow, tropical reef soundscape in another. The SSC features that distinguish these two groups are the range of all SSC metrics, impulsiveness values, periodicity values, and which SSC frequency bands the largest amplitude metric median and range occur in. The consistent rhythm of the biological signals of GBR produced SSC metric ranges that are miniscule compared to the OCS sites, with kurtosis the only exception. The impulsiveness of the shallow, tropical coral reef environment, most likely driven by snapping shrimp, was the highest of all the sites, especially during the 1-month analysis period. RH also exhibited impulsive tendencies, but in a much reduced manner relative to GBR. The other OCS soundscapes (BLE, SAV, and WIL) also indicated some influence by impulsive signals, but in mostly solitary frequency bands (WIL & BLE), or in a magnitude so small that it suggests only transient acoustic activity (SAV). The SSCs of the OCS sites suggest the soundscapes may have unique acoustic signatures or properties. Periodic signals appeared well-represented in the OCS sites, with SAV reporting the most substantial presence of these types of signals. The SSC frequency band in which these metrics peaked also indicated a nuanced difference between the shallow and OCS sites, especially in terms of sound amplitude. At the shallow coral environment the maximum sound amplitude occurred in frequencies above 1 kHz, while at the OCS sites the maximum amplitudes occurred in frequencies below 1 kHz. Uniformity as indicated by the D-index was difficult to interpret and appeared well correlated with other metric values.

SSC results both provide valuable soundscape information and highlight areas that subsequent analysis should explore to better understand the soundscape dynamics of the five sites. Determining the sound sources that are responsible for the elevated periodicity metrics in the OCS sites would help to understand the deep-sea environments, and could illuminate connections

among the OCS sites across bottom type. It would also be beneficial to explore what is driving the RH impulsiveness values, as a distinguishing feature of the GBR soundscape is also the large impulsiveness values. Determining what is driving sound levels in all frequency bands at the deep ocean sites would also help to understand if dominant acoustic activity of the deep ocean sites is different across bottom types, or if there is a connection between increased sound amplitude and habitat quality/bottom type. The uniformity metric suggested a clear distinction between GBR and the OCS sites, and exploring the driving sources for the uniformity metric would help to understand what has significant impacts on the variability of the OCS soundscapes across bottom type. The connection between amplitude, periodicity, and uniformity metrics should also be explored.

CHAPTER 4: Discussion

The proposed SSC provides a valuable framework to simply convey complex ocean characteristics and is a first step in the direction of a standardized soundscape analysis and reporting structure. The SSCs in Chapter 2 highlighted salient differences in acoustic properties of generally short duration soundscape recordings featuring a diversity of known sounds. In Chapter 3, soundscapes were analyzed using the methodology, and while some site information like location, depth, and bottom type/general ecology were known, the signals present in the environments were not assessed prior to the application of the soundscape code.

The results of the application of the SSC in Chapter 3 demonstrated the effectiveness of the methodology in doing two things: 1) reporting salient soundscape information in a way that allows comparison of important soundscape properties, and 2) highlighting specific avenues for subsequent analysis. Concise soundscape information provided by the SSCs produced rankings among the sites in terms of sound amplitude, impulsiveness, and periodicity of the respective soundscapes. The uniform metrics allowed for a direct comparison of soundscape properties across

sites to be made quickly and accurately. The SSCs also highlighted important frequency information, which provided interesting comparisons of the distribution of acoustic energy in the respective soundscapes. The SSC assessments are by no means exhaustive, but clearly highlight the salient differences among the respective soundscapes. Subsequent analysis targeting fluctuations in SSC properties (as quantified by the SSC metrics) and frequency information highlighted by the SSC will allow for a further understanding of the environments that ultimately produced the soundscapes assessed in Chapter 3.

The future use and potential improvement of the soundscape code will benefit from more thorough assessment of duty cycling, bandwidth definitions, and dataset durations, as only data sets of multiple hours and a majority of continuous sampling regimes were used to select the proposed soundscape code metrics. The selected frequency bandwidths worked for the purposes of this project, but other frequency banding should be explored to better represent evolving regulations and knowledge of marine life hearing. Similar to duty cycle concerns, dataset duration being represented in the soundscape code should be explored to understand how a comparison of soundscape code results from a small duration dataset (minutes to hours) compares to results from larger duration datasets (days to months). The color coding scheme adopted in this project provides a relative comparison among the sites analyzed, but needs to be standardized to make the color coding scheme universal. Some thresholds for the soundscape code amplitude and impulsiveness metrics already exist and could be used in a standard color coding scheme. Testing of the metric responses to synthetic soundscapes could be used to develop a standard color coding scheme for the periodicity and uniformity metrics.

All soundscape code metrics were based on 1-minute time windowing protocol to align with what few soundscape analysis method guidelines exist (Ainslie et al., 2018). Averaging of

sound pressure for the periodicity metrics was done with 0.1-second and 1.0 second windows. Other window sizes should be explored to assess performance and use of the SSC. Exhaustive analysis of the impact that different analysis parameters have on the SSC metrics would have added to the value of this research, but it did not fit into the scope of the project. Further work assessing the impact and performance of different analysis windows (larger time scales), datasets with unique acoustic features not captured in this work, datasets with significant overlapping of source signals, and threshold selections is required to ensure the development of an effective, rapid, and robust quantitative soundscape framework.

Targeted analysis of large acoustic datasets could be made easier by analyzing the tabulated and color-coded SSC products, but also by analyzing time series data of the SSC metrics. In Chapter 2, D-index time series consistently indicated time periods of dynamic acoustic activity. Peaks in acorr3 metric time series regularly highlighted the presence of echolocation signals and transient periodic acoustic signatures. Time series analysis of kurtosis values demonstrated an impressive utility in the assessment of a variety of aspects of underwater sound by indicating the presence of transient acoustic activity and shifts in acoustic activity in general. Time series analysis of kurtosis suggests the metric could be used in a variety of applications beyond the scope of soundscape comparison using the SSC.

The relationship between kurtosis and impulsive sounds, and resultant relevance in impact studies indicates it could be used in assessments of noise impacts and mitigation. While the soundscape code proposed here focusses on simple assessment of soundscape properties, this methodology could be more directly applied in impact assessments by focusing on the sound amplitude and impulsiveness properties. This could be done by simply reporting only amplitude and impulsiveness metrics, or by utilizing different amplitude metrics like the sound exposure

level; the inclusion of kurtosis is important to report whether the sounds are impulsive. Cumulative impacts to a soundscape from disparate sound sources could easily be assessed with the soundscape code methodology by comparing soundscape code metrics over time and isolating soundscape contributions from different sound sources. The SSC methodology would distill complex and dynamic sound source contributions to concise SSC metrics, which would allow for easy interpretation of how a multitude of acoustic impacts accumulate in a soundscape. More specific impact related assessments could also benefit from the concision of the soundscape code methodology. For example, bubble curtains are used to mitigate sound impacts by inhibiting sound transmission through the water (Würsig et al., 2000), and bubble curtain efficacy could potentially be assessed using the SSC or spatial/time series analysis of SSC metrics. The change in signal impact manifested within the soundscape on either side of a bubble curtain would assuredly be captured by impulsiveness and amplitude metrics, if not uniformity and periodicity metrics as well. Noise studies sometimes analyze sound at different ranges from a sound source (Hermannsen et al., 2015; Martin & Barclay, 2019), and the SSC metrics could easily be applied to this type of assessment and would quickly and clearly highlight salient spatial differences in multidimensional soundscape properties.

The SSC methodology provides a structure for quick and easy quantitative comparisons meant to capture salient soundscape characteristics for directed assessments of sources, patterns, and trends. The value of this project is the demonstration that multidimensional soundscape properties can be easily and directly compared when a relatively simple but uniform quantitative framework is utilized. Ambiguity in reporting of metric calculation parameters makes interpretation of results time-consuming and can result in erroneous conclusions; the uniform integration times and frequency bands of the SSC allows for accurate direct comparisons with

immediate understanding of exactly what is being calculated. The utility of the SSC structure lies in succinct, consistent, and transparent reporting of acoustic soundscape properties. Using direct comparisons made possible by the SSC, soundscapes corresponding to environments that varied in depth and bottom type were assessed in Chapter 3 with relative ease and rapidity. Frequency information was immensely informative in the Chapter 3 assessment and helped to understand nuanced differences among the soundscapes; if only broadband metrics were considered in Chapter 3, the interpretation of the results would have been much different. Furthermore, the multidimensional nature of the SSC helped to highlight similarities and differences in periodicity, impulsiveness, and uniformity/variability of the deep sea and coral reef soundscapes, which would have been overlooked in traditional soundscape analyses, and could be tied to important ecosystem functions of the respective environments. The cursory assessment carried out in Chapter 3 provides some important information about poorly understood deep-ocean soundscapes. Increased interest in deep seabed mineral deposits (Hannington et al., 2011; Hein et al., 2013; Petersen et al., 2016) will most likely result in an expansion of deep sea mining operations and it will be critical to establish baseline soundscape information to monitor impacts to these environments which to date are not thoroughly understood (Washburn et al., 2019). The methodology highlighted in this study is by no means exhaustive and was never meant to be. It is a starting point and demonstrates the utility of a succinct and consistent reporting methodology that provides a cursory first glance into deep ocean soundscapes. It is my hope that researchers in the future make efforts to implement a similar methodology so that people interested in soundscapes can assess the acoustic environments of our oceans more effectively, efficiently, and accurately.

List of References

Ainslie, M. A., Miksis-Olds, J., Martin, S. B., Heaney, K., de Jong, C. A. F., von Benda-Beckmann, A. M., & Lyons, A. P. (2018). *ADEON underwater soundscape and modeling metadata standard, version 1.0*. Technical report by JASCO Applied Sciences for ADEON Prime Contract No. M16PC00003 (JASCO, Halifax, Canada).

Anonymous. (2007). *Final Supplemental Environmental Impact Statement for Surveillance Towed Array Sensor System Low Frequency Active (SURTASS LFA) Sonar*.

Au, W. W. L. (1993). *The Sonar of Dolphins*. Springer-Verlag. https://doi.org/10.1007/978-1-4612-4356-4

Bass, A. H., & McKibben, J. R. (2003). Neural mechanisms and behaviors for acoustic communication in teleost fish. *Progress in Neurobiology*, *69*(1), 1–26. https://doi.org/10.1016/S0301-0082(03)00004-2

Bertucci, F., Parmentier, E., Berten, L., Brooker, R. M., & Lecchini, D. (2015). Temporal and Spatial Comparisons of Underwater Sound Signatures of Different Reef Habitats in Moorea Island, French Polynesia. *PLOS ONE*, *10*(9), e0135733. https://doi.org/10.1371/journal.pone.0135733

Bogert, B. P., Healy, M. J. R., & Tukey, J. W. (1963). Quefrency alanysis of time series for echoes: cepstrum, pseudo-autocovariance, cross-cepstrum, and saphe-cracking. *Time Series Analysis*, ch. 15, pp 209-243.

Bohnenstiehl, D. R., Lyon, R. P., Caretti, O. N., Ricci, S. W., & Eggleston, D. B. (2018). Investigating the utility of ecoacoustic metrics in marine soundscapes. *Journal of Ecoacoustics*, *2*(2), 1–1. https://doi.org/10.22261/JEA.R1156L

Bolgan, M., Amorim, M. C. P., Fonseca, P. J., Di Iorio, L., & Parmentier, E. (2018). Acoustic Complexity of vocal fish communities: A field and controlled validation. *Scientific Reports*, *8*(1), 10559. https://doi.org/10.1038/s41598-018-28771-6

Bradley, D. L., & Nichols, S. M. (2015). Worldwide low-frequency ambient noise. *Acoustics Today*, *11*(1), 20–26.

Brockett, P. L., Hinich, M., & Wilson, G. R. (1987). Nonlinear and non-Gaussian ocean noise. *The Journal of the Acoustical Society of America*, *82*(4), 10.

Buscaino, G., Ceraulo, M., Pieretti, N., Corrias, V., Farina, A., Filiciotto, F., Maccarrone, V., Grammauta, R., Caruso, F., Giuseppe, A., & Mazzola, S. (2016). Temporal patterns in the soundscape of the shallow waters of a Mediterranean marine protected area. *Scientific Reports*, *6*(1), 34230. https://doi.org/10.1038/srep34230

Casper, B. M., Halvorsen, M. B., Matthews, F., Carlson, T. J., & Popper, A. N. (2013). Recovery of Barotrauma Injuries Resulting from Exposure to Pile Driving Sound in Two Sizes of Hybrid Striped Bass. *PLoS ONE*, *8*(9), e73844. https://doi.org/10.1371/journal.pone.0073844

Casper, B. M., Smith, M. E., Halvorsen, M. B., Sun, H., Carlson, T. J., & Popper, A. N. (2013). Effects of exposure to pile driving sounds on fish inner ear tissues. *Comparative Biochemistry and Physiology Part A: Molecular & Integrative Physiology*, *166*(2), 352–360. https://doi.org/10.1016/j.cbpa.2013.07.008

Clarke, E., Feyrer, L. J., Moors-Murphy, H., & Stanistreet, J. (2019). Click characteristics of northern bottlenose whales (*Hyperoodon ampullatus*) and Sowerby's beaked whales (*Mesoplodon bidens*) off eastern Canada. *The Journal of the Acoustical Society of America*, *146*(1), 307–315. https://doi.org/10.1121/1.5111336

Coles, R. R. A., Garinther, G. R., Hodge, D. C., & Rice, C. G. (1968). Hazardous exposure to impulse noise. *The Journal of the Acoustical Society of America*, *43*(2), 336-343.

Dunn, O. J. (1964). Multiple Comparisons Using Rank Sums. *Technometrics*, *6*(3), 241–252. https://doi.org/10.2307/1266041

Erbe, C. (2002). Underwater noise of whale-watching boats and potential effects on killer whales (*Orcinus Orca*) based on an acoustic impact model. *Marine Mammal Science*, *18*(2), 394–418. https://doi.org/10.1111/j.1748-7692.2002.tb01045.x

Erdreich, J. (1986). A distribution based definition of impulse noise. *The Journal of the Acoustical Society of America*, *79*(4), 990–998. https://doi.org/10.1121/1.393698

Graham, N. A. J., Chong-Seng, K. M., Huchery, C., Januchowski-Hartley, F. A., & Nash, K. L. (2014). Coral Reef Community Composition in the Context of Disturbance History on the Great Barrier Reef, Australia. *PLoS ONE*, *9*(7), e101204. https://doi.org/10.1371/journal.pone.0101204

Greene, C. R. (1987). Characteristics of oil industry dredge and drilling sounds in the Beaufort Sea. *The Journal of the Acoustical Society of America*, *82*(4), 1315–1324. https://doi.org/10.1121/1.395265

Greene, C. R., & Richardson, W. J. (1988). Characteristics of marine seismic survey sounds in the Beaufort Sea. *The Journal of the Acoustical Society of America*, *83*(6), 2246–2254. https://doi.org/10.1121/1.396354

Halvorsen, M. B., Casper, B. M., Matthews, F., Carlson, T. J., & Popper, A. N. (2012). Effects of exposure to pile-driving sounds on the lake sturgeon, Nile tilapia and hogchoker. *Proceedings of the Royal Society B: Biological Sciences*, *279*(1748), 4705–4714. https://doi.org/10.1098/rspb.2012.1544

Halvorsen, M. B., Casper, B. M., Woodley, C. M., Carlson, T. J., & Popper, A. N. (2012). Threshold for Onset of Injury in Chinook Salmon from Exposure to Impulsive Pile Driving Sounds. *PLoS ONE*, *7*(6), e38968. https://doi.org/10.1371/journal.pone.0038968

Hannington, M., Jamieson, J., Monecke, T., Petersen, S., & Beaulieu, S. (2011a). The abundance of seafloor massive sulfide deposits. *Geology*, *39*(12), 1155–1158. https://doi.org/10.1130/G32468.1

Hannington, M., Jamieson, J., Monecke, T., Petersen, S., & Beaulieu, S. (2011b). The abundance of seafloor massive sulfide deposits. *Geology*, *39*(12), 1155–1158. https://doi.org/10.1130/G32468.1

Harris, S. A., Shears, N. T., & Radford, C. A. (2016). Ecoacoustic indices as proxies for biodiversity on temperate reefs. *Methods in Ecology and Evolution*, *7*(6), 713–724. https://doi.org/10.1111/2041-210X.12527

Haver, S. M., Klinck, H., Nieukirk, S. L., Matsumoto, H., Dziak, R. P., & Miksis-Olds, J. L. (2017). The not-so-silent world: Measuring Arctic, Equatorial, and Antarctic soundscapes in the Atlantic Ocean. *Deep Sea Research Part I: Oceanographic Research Papers*, *122*, 95–104. https://doi.org/10.1016/j.dsr.2017.03.002

Hawkins, R. S., Miksis-Olds, J. L., & Smith, C. M. (2014). Variation in low-frequency estimates of sound levels based on different units of analysis. *The Journal of the Acoustical Society of America*, *135*(2), 705–711. https://doi.org/10.1121/1.4861252

Hein, J. R., Mizell, K., Koschinsky, A., & Conrad, T. A. (2013). Deep-ocean mineral deposits as a source of critical metals for high- and green-technology applications: Comparison with land-based resources. *Ore Geology Reviews*, *51*, 1–14. https://doi.org/10.1016/j.oregeorev.2012.12.001

Hermannsen, L., Tougaard, J., Beedholm, K., Nabe-Nielsen, J., & Madsen, P. T. (2015). Characteristics and propagation of airgun pulses in shallow water with implications for effects on small marine mammals. *PLOS ONE*, *10*(7), e0133436. https://doi.org/10.1371/journal.pone.0133436

Hildebrand, J. (2009). Anthropogenic and natural sources of ambient noise in the ocean. *Marine Ecology Progress Series*, *395*, 5–20. https://doi.org/10.3354/meps08353

JCOMM Expert Team on Sea Ice. (2004). WMO Sea Ice Nomenclature. *WMO*.

JCOMM Expert Team on Sea Ice. (2014). Ice chart colour code standard. *WMO*.

Kastelein, R. A., Gransier, R., Marijt, M. A. T., & Hoek, L. (2015). Hearing frequency thresholds of harbor porpoises (*Phocoena phocoena*) temporarily affected by played back offshore pile driving sounds. *The Journal of the Acoustical Society of America*, *137*(2), 556–564. https://doi.org/10.1121/1.4906261

Kastelein, R. A., Helder-Hoek, L., Van de Voorde, S., von Benda-Beckmann, A. M., Lam, F.-P. A., Jansen, E., de Jong, C. A. F., & Ainslie, M. A. (2017). Temporary hearing threshold shift in a harbor porpoise (*Phocoena phocoena*) after exposure to multiple airgun sounds. *The Journal of the Acoustical Society of America*, *142*(4), 2430–2442. https://doi.org/10.1121/1.5007720

Kibblewhite, A. C., & Wu, C. Y. (1989). The generation of infrasonic ambient noise in the ocean by nonlinear interactions of ocean surface waves. *The Journal of the Acoustical Society of America*, *85*(5), 1935–1945. https://doi.org/10.1121/1.397847

Kinsler, L. E., Frey, A. R., Coppens, A. B., & Sanders, J. V. (1999). *Fundamentals of Acoustics*. John wiley & sons.

Kipple, B., & Gabriele, C. (2004). Underwater noise from skiffs to ships. *Proceedings of Glacier Bay Science Symposium*, 172–175.

Kyhn, L. A., Wisniewska, D. M., Beedholm, K., Tougaard, J., Simon, M., Mosbech, A., & Madsen, P. T. (2019). Basin-wide contributions to the underwater soundscape by multiple seismic surveys with implications for marine mammals in Baffin Bay, Greenland. *Marine Pollution Bulletin*, *138*, 474–490. https://doi.org/10.1016/j.marpolbul.2018.11.038

Lin, T.-H., Yang, H.-T., Huang, J.-M., Yao, C.-J., Lien, Y.-S., Wang, P.-J., & Hu, F.-Y. (2019). Evaluating Changes in the Marine Soundscape of an Offshore Wind Farm via the Machine Learning-Based Source Separation. *2019 IEEE Underwater Technology (UT)*, 1–6. https://doi.org/10.1109/UT.2019.8734295

Lucke, K., Siebert, U., Lepper, P. A., & Blanchet, M.-A. (2009). Temporary shift in masked hearing thresholds in a harbor porpoise (*Phocoena phocoena*) after exposure to seismic airgun stimuli. *The Journal of the Acoustical Society of America*, *125*(6), 4060–4070. https://doi.org/10.1121/1.3117443

Madsen, P. T. (2005). Marine mammals and noise: Problems with root mean square sound pressure levels for transients. *The Journal of the Acoustical Society of America*, *117*(6), 3952–3957. https://doi.org/10.1121/1.1921508

Madsen, P. T., Johnson, M., Miller, P. J. O., Aguilar Soto, N., Lynch, J., & Tyack, P. (2006). Quantitative measures of air-gun pulses recorded on sperm whales (Physeter macrocephalus) using acoustic tags during controlled exposure experiments. *The Journal of the Acoustical Society of America*, *120*(4), 2366–2379. https://doi.org/10.1121/1.2229287

Martin, S. B., & Barclay, D. R. (2019). Determining the dependence of marine pile driving sound levels on strike energy, pile penetration, and propagation effects using a linear mixed model based on damped cylindrical spreading. *The Journal of the Acoustical Society of America*, *146*(1), 109–121. https://doi.org/10.1121/1.5114797

Martin, S. B., Lucke, K., & Barclay, D. R. (2020). Techniques for distinguishing between impulsive and non-impulsive sound in the context of regulating sound exposure for marine mammals. *The Journal of the Acoustical Society of America*, *147*(4), 2159–2176. https://doi.org/10.1121/10.0000971

Martin, S. B., Matthews, M.-N. R., MacDonnell, J. T., & Bröker, K. (2017). Characteristics of seismic survey pulses and the ambient soundscape in Baffin Bay and Melville Bay, West Greenland. *The Journal of the Acoustical Society of America*, 142(6), 3331-3346

Martin, S. B., Morris, C., Bröker, K., & O'Neill, C. (2019). Sound exposure level as a metric for analyzing and managing underwater soundscapes. *The Journal of the Acoustical Society of America*, *146*(1), 135–149. https://doi.org/10.1121/1.5113578

McCook, L. J., Ayling, T., Cappo, M., Choat, J. H., Evans, R. D., De Freitas, D. M., Heupel, M., Hughes, T. P., Jones, G. P., Mapstone, B., Marsh, H., Mills, M., Molloy, F. J., Pitcher, C. R., Pressey, R. L., Russ, G. R., Sutton, S., Sweatman, H., Tobin, R., Wachenfeld, D.R., & Williamson, D. H. (2010). Adaptive management of the Great Barrier Reef: A globally significant demonstration of the benefits of networks of marine reserves. *Proceedings of the National Academy of Sciences*, *107*(43), 18278–18285. https://doi.org/10.1073/pnas.0909335107

McDonald, M. A., Hildebrand, J. A., & Wiggins, S. M. (2006). Increases in deep ocean ambient noise in the Northeast Pacific west of San Nicolas Island, California. *The Journal of the Acoustical Society of America*, *120*(2), 711–718. https://doi.org/10.1121/1.2216565

McWilliam, J. N., & Hawkins, A. D. (2013). A comparison of inshore marine soundscapes. *Journal of Experimental Marine Biology and Ecology*, *446*, 166–176. https://doi.org/10.1016/j.jembe.2013.05.012

Medwin, H., & Beaky, M. M. (1989). Bubble sources of the Knudsen sea noise spectra. *The Journal of the Acoustical Society of America*, *86*(3), 1124–1130. https://doi.org/10.1121/1.398104

Merchant, N. D., Blondel, P., Dakin, D. T., & Dorocicz, J. (2012). Averaging underwater noise levels for environmental assessment of shipping. *The Journal of the Acoustical Society of America*, *132*(4), EL343–EL349. https://doi.org/10.1121/1.4754429

Merchant, N. D., Fristrup, K. M., Johnson, M. P., Tyack, P. L., Witt, M. J., Blondel, P., & Parks, S. E. (2015). Measuring acoustic habitats. *Methods in Ecology and Evolution*, *6*(3), 257–265. https://doi.org/10.1111/2041-210X.12330

Miksis-Olds, J. L., Stabeno, P. J., Napp, J. M., Pinchuk, A. I., Nystuen, J. A., Warren, J. D., & Denes, S. L. (2013). Ecosystem response to a temporary sea ice retreat in the Bering Sea: Winter 2009. *Progress in Oceanography*, *111*, 38–51. https://doi.org/10.1016/j.pocean.2012.10.010

National Research Council (NRC). (2003). *Ocean noise and marine mammals*. National Academies Press, Washington, DC.

Nichols, R. H. (1987). Infrasonic ocean noise sources: Wind versus waves. *The Journal of the Acoustical Society of America*, *82*(4), 1395–1402. https://doi.org/10.1121/1.395830

NIOSH. (1998). Criteria for a Recommended Standard: Occupational Noise Exposure. Revised Criteria. *US Department of Health and Human Services*, 126.

NMFS. (2018). *2018 Revisions to: Technical Guidance for Assessing the Effects of Anthropogenic Sound on Marine Mammal Hearing (Version 2.0)*. 178.

Nystuen, J. A. (1986). Rainfall measurements using underwater ambient noise. *The Journal of the Acoustical Society of America*, *79*(4), 972–982. https://doi.org/10.1121/1.393695

Oppenheim, A. V., & Schafer, R. W. (2004). DSP history - From frequency to quefrency: A history of the cepstrum. *IEEE Signal Processing Magazine*, *21*(5), 95–106. https://doi.org/10.1109/MSP.2004.1328092

Parks, S. E., Miksis-Olds, J. L., & Denes, S. L. (2014). Assessing marine ecosystem acoustic diversity across ocean basins. *Ecological Informatics*, *21*, 81–88. https://doi.org/10.1016/j.ecoinf.2013.11.003

Parmentier, E., Berten, L., Rigo, P., Aubrun, F., Nedelec, S. L., Simpson, S. D., & Lecchini, D. (2015). The influence of various reef sounds on coral-fish larvae behaviour: Reef-sound influence on fish larvae behaviour. *Journal of Fish Biology*, *86*(5), 1507–1518. https://doi.org/10.1111/jfb.12651

Patek, S. N., Shipp, L. E., & Staaterman, E. R. (2009). The acoustics and acoustic behavior of the California spiny lobster (*Panulirus interruptus*). *The Journal of the Acoustical Society of America*, *125*(5), 3434–3443. https://doi.org/10.1121/1.3097760

Peet, R. K. (1974). The Measurement of Species Diversity. *Annual review of ecology and systematics* 5.1 (1974): 285-307.

Petersen, S., Krätschell, A., Augustin, N., Jamieson, J., Hein, J. R., & Hannington, M. D. (2016). News from the seabed – Geological characteristics and resource potential of deep-sea mineral resources. *Marine Policy*, *70*, 175–187. https://doi.org/10.1016/j.marpol.2016.03.012

Pettit, E. C. (2012). Passive underwater acoustic evolution of a calving event. *Annals of Glaciology*, *53*(60), 113–122. https://doi.org/10.3189/2012AoG60A137

Piercy, J., Codling, E., Hill, A., Smith, D., & Simpson, S. (2014). Habitat quality affects sound production and likely distance of detection on coral reefs. *Marine Ecology Progress Series*, *516*, 35–47. https://doi.org/10.3354/meps10986

Pieretti, N., Farina, A., & Morri, D. (2011). A new methodology to infer the singing activity of an avian community: The Acoustic Complexity Index (ACI). *Ecological Indicators*, *11*(3), 868–873. https://doi.org/10.1016/j.ecolind.2010.11.005

Pieretti, N., Lo Martire, M., Farina, A., & Danovaro, R. (2017). Marine soundscape as an additional biodiversity monitoring tool: A case study from the Adriatic Sea (Mediterranean Sea). *Ecological Indicators*, *83*, 13–20. https://doi.org/10.1016/j.ecolind.2017.07.011

Pijanowski, B. C., Villanueva-Rivera, L. J., Dumyahn, S. L., Farina, A., Krause, B. L., Napoletano, B. M., Gage, S. H., & Pieretti, N. (2011). Soundscape Ecology: The Science of Sound in the Landscape. *BioScience*, *61*(3), 203–216. https://doi.org/10.1525/bio.2011.61.3.6

Pimm, S. L., & Lawton, J. H. (1998). Planning for Biodiversity. *Science*, *279*(5359), 2068–2069. https://doi.org/10.1126/science.279.5359.2068

Qiu, W., Hamernik, R. P., & Davis, R. I. (2013). The value of a kurtosis metric in estimating the hazard to hearing of complex industrial noise exposures. *The Journal of the Acoustical Society of America*, *133*(5), 2856–2866. https://doi.org/10.1121/1.4799813

Radford, C., Stanley, J., & Jeffs, A. (2014). Adjacent coral reef habitats produce different underwater sound signatures. *Marine Ecology Progress Series*, *505*, 19–28. https://doi.org/10.3354/meps10782

Radford, C., Stanley, J., Tindle, C., Montgomery, J., & Jeffs, A. (2010). Localised coastal habitats have distinct underwater sound signatures. *Marine Ecology Progress Series*, *401*, 21–29. https://doi.org/10.3354/meps08451

Randall, R. B. (2017). A history of cepstrum analysis and its application to mechanical problems. *Mechanical Systems and Signal Processing*, *97*, 3–19. https://doi.org/10.1016/j.ymssp.2016.12.026

Reed, J. K., Weaver, D. C., & Pomponi, S. A. (2006). Habitat and fauna of deep-water *Lophelia pertusa* coral reefs off the southeastern US: Blake Plateau, Straits of Florida, and Gulf of Mexico. *Bulletin of Marine Science*, *78*(2), 343–375.

Richardson, W. J., Greene Jr, C. R., Malme, C. I., & Thomson, D. H. (2013). *Marine mammals and noise*. Academic press.

Ross, D. (1976). *Mechanics of Underwater Noise*. Peninsula Pub.

Ross, S. W. (2006). Review of distribution, habitats, and associated fauna of deep water coral reefs on the southeastern United States continental slope (North Carolina to Cape Canaveral, Fl). *South Atlantic Fishery Management Council Report*, *1*, 1–36.

Schevill, W., Watkins, W., & Backus, R. (1964). The 20-cycle signals and *Balaenoptera* (fin whales). *Marine Bio-Acoustics*, *45*, 147–152.

Schmidt, V. (2004). Seismic contractors realign equipment for industry's needs. *Offshore (Conroe, Tex.)*, *64*(3).

Southall, B. L., Bowles, A. E., Ellison, W. T., Finneran, J. J., Gentry, R. L., Greene, C. R., Jr., Kastak, D., Ketten, D. R., Miller, J. H., Nachtigall, P. E., Richardson, W. J., Thomas, J. A., and Tyack, P.L. (2007). Marine mammal noise exposure criteria: Initial scientific recommendations. Aquatic Mammals 33, 411–521.

Southall, B. L., Finneran, J. J., Reichmuth, C., Nachtigall, P. E., Ketten, D. R., Bowles, A. E., Ellison, W. T., Nowacek, D. P., & Tyack, P. L. (2019). Marine Mammal Noise Exposure Criteria: Updated Scientific Recommendations for Residual Hearing Effects. *Aquatic Mammals*, *45*(2), 125–232. https://doi.org/10.1578/AM.45.2.2019.125

Staaterman, E., Ogburn, M., Altieri, A., Brandl, S., Whippo, R., Seemann, J., Goodison, M., & Duffy, J. (2017). Bioacoustic measurements complement visual biodiversity surveys: Preliminary evidence from four shallow marine habitats. *Marine Ecology Progress Series*, *575*, 207–215. https://doi.org/10.3354/meps12188

Staaterman, E., Paris, C., DeFerrari, H., Mann, D., Rice, A., & D'Alessandro, E. (2014). Celestial patterns in marine soundscapes. *Marine Ecology Progress Series*, *508*, 17–32. https://doi.org/10.3354/meps10911

Staaterman, E., Rice, A. N., Mann, D. A., & Paris, C. B. (2013). Soundscapes from a Tropical Eastern Pacific reef and a Caribbean Sea reef. *Coral Reefs*, *32*(2), 553–557. https://doi.org/10.1007/s00338-012-1007-8

Starck, J., & Pekkarinen, J. (1987). Industrial impulse noise: Crest factor as an additional parameter in exposure measurements. *Applied Acoustics*, *20*(4), 263–274. https://doi.org/10.1016/0003-682X(87)90063-6

Stoeckl, N., Hicks, C., Mills, M., Fabricius, K., Esparon, M., Kroon, F., Sangha, K., & Costanza, R. (2011). The economic value of ecosystem services in the Great Barrier Reef: Our state of knowledge. *Annals of the New York Academy of Sciences*, *1219*, 113–133. https://doi.org/10.1111/j.1749-6632.2010.05892.x

Sueur, J., Pavoine, S., Hamerlynck, O., & Duvail, S. (2008). Rapid Acoustic Survey for Biodiversity Appraisal. *PLoS ONE*, *3*(12), e4065. https://doi.org/10.1371/journal.pone.0004065

Thompson, P. M., Brookes, K. L., Graham, I. M., Barton, T. R., Needham, K., Bradbury, G., & Merchant, N. D. (2013). Short-term disturbance by a commercial two-dimensional seismic survey does not lead to long-term displacement of harbour porpoises (*Phocoena phocoena)*. *Proceedings of the Royal Society B: Biological Sciences*, *280*(1771), 20132001. https://doi.org/10.1098/rspb.2013.2001

Tolstoy, M., Diebold, J. B., Webb, S. C., Bohnenstiehl, D. R., Chapp, E., Holmes, R. C., & Rawson, M. (2004). Broadband calibration of R/V Ewing seismic sources. *Geophysical Research Letters*, *31*(14).

Traverso, F., Vernazza, G., & Trucco, A. (2012). Simulation of non-White and non-Gaussian underwater ambient noise. *2012 Oceans - Yeosu*, 1–10. https://doi.org/10.1109/OCEANS-Yeosu.2012.6263385

Tyack, P. (2018). Essential Ocean Variables (EOV) for Biology and Ecosystems: Ocean Sound. *GOOS*.

Tyack, P. L. (1998). Acoustic communication under the sea. *Animal acoustic communication* (pp. 163–220). Springer.

Urick, R. (1983). *Principles of Underwater Sound* (3rd ed.). Peninsula Publishing.

Urick, R. J. (1984). *Ambient Noise in the Sea*. Undersea Warfare Technology Office, Naval Sea Systems Command, Department of the Navy.

Wartzok, D., & Ketten, D. R. (1999). Marine Mammal Sensory Systems. *Biology of Marine Mammals*, 117–175.

Washburn, T. W., Turner, P. J., Durden, J. M., Jones, D. O. B., Weaver, P., & Van Dover, C. L. (2019). Ecological risk assessment for deep-sea mining. *Ocean & Coastal Management*, *176*, 24–39. https://doi.org/10.1016/j.ocecoaman.2019.04.014

Watts, A. J. (1996). *Jane's Underwater Warfare Systems, 1996-97*. Jane's Information Group.

Wenz, G. M. (1962). Acoustic ambient noise in the ocean: Spectra and sources. *The Journal of the Acoustical Society of America*, *34*(12), 1936–1956.

Wilford, D. C., Miksis-Olds, J. L., Martin, B. S., Howard, D. R., Lowell, K., Lyons, A. P., & Smith, M. J. (2021). Quantitative Soundscape Analysis to Understand Multidimensional Features. *Frontiers in Marine Science*, *8*, 949.

Würsig, B., Greene, C. R., & Jefferson, T. A. (2000). Development of an air bubble curtain to reduce underwater noise of percussive piling. *Marine Environmental Research*, *49*(1), 79–93. https://doi.org/10.1016/S0141-1136(99)00050-1